

2006

Development of Electroanalytical Methods for the Determination of Sialic Acid as a Biomarker for Cancer

Khawla Ali Rashid Al-Tayyari

Follow this and additional works at: https://scholarworks.uaeu.ac.ae/all_theses

Part of the [Environmental Sciences Commons](#)

Recommended Citation

Rashid Al-Tayyari, Khawla Ali, "Development of Electroanalytical Methods for the Determination of Sialic Acid as a Biomarker for Cancer" (2006). *Theses*. 412.

https://scholarworks.uaeu.ac.ae/all_theses/412

This Thesis is brought to you for free and open access by the Electronic Theses and Dissertations at Scholarworks@UAEU. It has been accepted for inclusion in Theses by an authorized administrator of Scholarworks@UAEU. For more information, please contact fadl.musa@uaeu.ac.ae.



**United Arab Emirates University
Deanship of Graduate Studies
M.Sc. Program in Environmental Sciences**

**DEVELOPMENT OF ELECTROANALYTICAL METHODS
FOR THE DETERMINATION OF SIALIC ACID
AS A BIOMARKER FOR CANCER**

By

Khawla Ali Rashid Al-Tayyari

**A thesis
Submitted to**

**United Arab Emirates University
In partial fulfillment of the requirements
For the Degree of M.Sc. in Environmental Sciences**

2005 -2006



United Arab Emirates University
Deanship of Graduate Studies
M.Sc. Program in Environmental Sciences

**DEVELOPMENT OF ELECTROANALYTICAL METHODS
FOR THE DETERMINATION OF SIALIC ACID
AS A BIOMARKER FOR CANCER**

By

Khawla Ali Rashid Al-Tayyari

A thesis
Submitted to

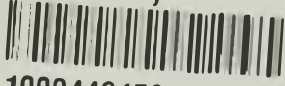
United Arab Emirates University
In partial fulfillment of the requirements
For the Degree of M.Sc. in Environmental Sciences

Supervisors

| | |
|---|--|
| Dr. Sayed A. M. Marzouk Associate Professor of Analytical Chemistry Department of Chemistry Faculty of Science United Arab Emirates University | Dr. Salman Ashraf Assistant Professor of Biochemistry Department of Chemistry Faculty of Science United Arab Emirates University |
|---|--|

2005 -2006

JAEU Library

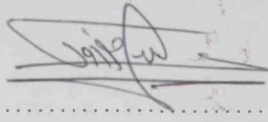


1000442479



مكتبة زايد المركزية
ZAYED CENTRAL LIB.

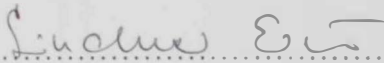
The Thesis of Khawla Ali Al Tayyari for the Degree of Master of Science in Environmental is approved.



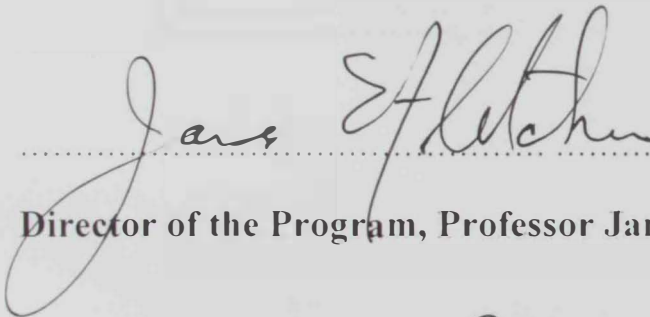
Examining Committee Member, Dr. Sayed A. M. Marzouk



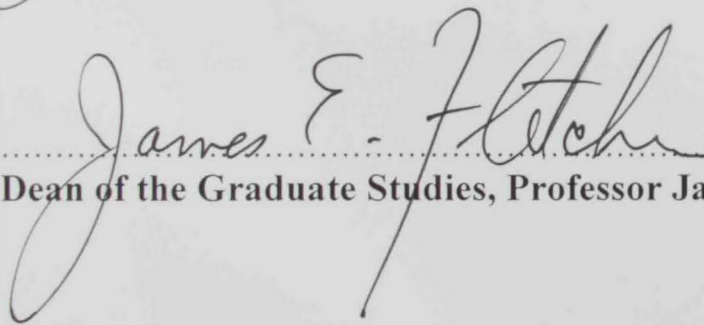
Examining Committee Member, Dr. Ahmed Almehti



Examining Committee Member, Dr. Erno Lindner



Director of the Program, Professor James E. Fletcher



Dean of the Graduate Studies, Professor James E. Fletcher



*"To research means to see what all people
have seen and to think what no body has thought"*

*Dedicated to my Beloved Parents
And
Dr. Hazem Kataya Soul*

Acknowledgement

All praises to Allah. All loves for the holy prophet Mohammad "peace be upon him", all devotions to Islam. It is a dept of honour for me to express my deep sense of gratitude to my supervisor Dr. Sayed A. M. Marzouk, Associate Professor of Analytical Chemistry, for providing me inexhaustible inspiration and enthusiastic guidance throughout my research work. I want also to thank him for allotment of this thesis and providing facilities of all kinds.

I offer my heartfelt thanks to Dr. Salman Ashraf, Assistant Professor of Biochemistry for his help and support.

I'm highly indebted and to Mr. Abdul Razzaq Gulf Company for Pharmaceutical Industries "Julphar", for his kindness, inspiring attitude, unlimited assistance and patronage.

I'm also grateful to Mr. Aqeel Ahmed Khan, Quality Control Officer, Julphar, for his helpful attitude and providing me with initial tangible encouragement.

Also I would like to pay tribute to all my family members, specially my parents as they have been a constant source of encouragement and inspiration. I thank them for providing me with support, faith, confidence and patience. I would also like to thank my precious sister Wafa and my beloved brothers Mohammad and Rashid and devotion.

Finally I have to express my thanks and appreciation to all my friends, specially my best friends Deema Khalil Al-Jayousi and Habiba Saleh Al-Yafei for their help, understanding and encouragement and being such real friends.

Abstract

Sialic acid (SA) is a general term for a family composed of 43 derivatives of neuraminic acid. Whereas *N*-acetylneuraminic acid (NANA) is the most commonly occurring sialic acid in human. There has been a great interest in the determination of SA in humans because variations in SA level was linked to different medical conditions and diseases. In particular, serum SA are elevated in several types of cancers. SA also exists in Erythropoietin (EPO), a hormone, which induces the production of red blood cells and hence used in the treatment of anemia.

Although of the great physiological significance of SA and the attractive merits offered by the electrochemical techniques, there was a notable absence of literature describing electrochemical methods for the determination of SA. This surprising observation triggered this project to develop and to evaluate the first flow injection analysis (FIA) system as well as the first biosensor - based on amperometric transduction - for simple, fast, direct, and reliable determination of SA for clinical applications.

The principle of the present work is based on a sequence of two enzymes, i.e., *N*-acetylneuraminic acid aldolase (NANA-aldolase) and pyruvate oxidase (PO) which catalyze a two-step conversion of SA into H_2O_2 , which could be detected by anodic amperometry using platinum electrode polarized 0.6 V vs Ag/AgCl.

The first phase of the current project was to investigate the effect of different experimental variables on the generation of hydrogen peroxide by the sequence action of the two enzymes. This initial study is carried out using the two enzymes in the soluble form (i.e., homogenous enzyme catalysis). The obtained optimum experimental conditions for hydrogen peroxide generation and detection are 0.1 M phosphate buffer pH

6.3 at 37 °C, using NANA-aldolase/PO activity ratio of 1.5 and a thiamine pyrophosphate (TPP) cofactor concentration of 0.5-2 mM.

The second phase aimed to construct an FIA system based on an immobilized enzyme reactor (IER) and an amperometric detector for the generated hydrogen peroxide. The IER is prepared by co-immobilization of the two enzymes on controlled pore glass beads activated with glutaraldehyde and packed in a glass tube (3-5 cm in length). A tubular platinum detector of large surface area is suggested in this work and proved efficient to enhance the sensitivity of SA determination by the proposed FIA system. The entire FIA system is evaluated under the optimum conditions obtained from the initial investigation. The obtained linear range, analysis time, and sensitivity could be easily tuned to meet the required performance characteristics by controlling the carrier buffer flow rate, and the injected sample volume. The determination of SA in real samples using the proposed FIA system is presented as well.

The third phase is devoted to the most challenging task in this project, i.e., to construct a prototype SA biosensor which necessitated co-immobilization of the two enzymes as well as their integration in a close proximity of platinum electrode surface. Although, three methods are tested for enzyme immobilization, the method based on glutaraldehyde crosslinking with BSA proved the most efficient. A novel microporous polyester membrane is used as a substrate for the enzyme layer, which provided high adhesion and reproducible fabrication of the enzyme layer. The optimum pH of the crosslinked enzyme system is ~ 1 pH higher (~ pH 7.3) than that obtained with homogenous catalysis. Careful optimization of enzyme layer composition and thickness allowed stable and fast response with detection limit of less than 10 μ M SA.. Protection of the platinum surface with an inner electropolymeric layer enhanced the selectivity of

the SA biosensor in the presence of interfering oxidizable species such as ascorbic and uric acids and acetaminophen. The favorable performance characteristics of the developed SA biosensor allowed its successful application in the determination of SA in simulated serum sample and real biological samples.

The obtained performance characteristics of the newly developed electrochemical methods suggest their wide use in the numerous clinical applications and in particular as a non-specific tumor marker and to monitor tumor therapy.

Key Words: Sialic acid; Tumor markers; Erythropoietin, Electroanalytical methods, Amperometric biosensors; Immobilized enzyme reactors; Flow injection analysis.

Table of Content

| | Page |
|---|------|
| DEDICATION | i |
| ACKNOWLEDGEMENT | ii |
| ABSTRACT | iii |
| TABLE OF CONTENTS | vi |
| LIST OF FIGURES | ix |
| LIST OF ABBREVIATIONS | xii |
| CHAPTER I: INTRODUCTION | |
| 1.1 Introduction | 1 |
| 1.2 Physiological roles of sialic acid | 3 |
| 1.3 Sialic acid as a biomarker | 4 |
| 1.3.1 Sialic acid as a cancer biomarker | 5 |
| 1.3.2 Sialic acid as a marker for other diseases | 7 |
| 1.3.3 Sialic acid and Erythropoietin | 9 |
| 1.4 Analytical methods for the determination of sialic acid | 10 |
| 1.4.1 Colorimetric assays | 10 |
| 1.4.1.1 Orcinol method | 10 |
| 1.4.1.2 Resorcinol method | 10 |
| 1.4.1.3 Periodic/thiobarbiturate method | 11 |
| 1.4.1.4 Other colorimetric methods | 11 |
| 1.4.2 Fluorometric assays | 12 |
| 1.4.3 Enzymatic assays | 12 |
| 1.4.4 Chromatographic methods | 15 |
| 1.5 Determination of sialic acid by chemical sensors and biosensors | 17 |
| 1.6 Biosensors | 18 |
| 1.6.1 Enzyme immobilization | 20 |
| 1.6.1.1 Adsorption | 20 |
| 1.6.1.2 Gel entrapment | 20 |
| 1.6.1.3 Covalent attachment | 21 |
| 1.6.1.4 Crosslinking | 21 |
| 1.6.2 Interference to a biosensor response | 22 |

| | |
|---|----|
| 1.7 Objectives | 23 |
| CHAPTER II : MATERIALS AND METHODS | |
| 2. Materials and Methods | 24 |
| 2.1 Materials and Reagents | 24 |
| 2.2 Apparatus | 25 |
| 2.3 Investigation of the dual enzyme system by homogeneous catalysis | 25 |
| 2.3.1 Effect of buffer type | 26 |
| 2.3.2 Effect of the TPP cofactor concentration | 26 |
| 2.3.3 Effect of temperature | 26 |
| 2.3.4 Optimization of pH | 27 |
| 2.3.5 Effect of NANA-aldolase/PO activity ratio | 27 |
| 2.3.6 Effect of the freshness of TPP cofactor | 27 |
| 2.3.7 Effect of SA freshness | 28 |
| 2.3.8 Effect of enzymes freshness | 28 |
| 2.4 Flow injection analysis | 28 |
| 2.4.1 Preparation of the immobilized enzyme reactors (IER) | 31 |
| 2.4.2 Preparation of the flow-through amperometric detector for FIA setup | 31 |
| 2.4.3 FIA determination of bound SA | 33 |
| 2.5 Construction of SA biosensor | 34 |
| 2.5.1 Electrochemical Polymerization of <i>m</i> -PDA | 34 |
| 2.5.2 Enzyme immobilization | 34 |
| 2.5.3 Optimization of Enzyme layer | 36 |
| 2.5.3.1 Effect of Glutaraldehyde (GA) | 36 |
| 2.5.3.2 Optimization of the total enzymes ratio | 36 |
| 2.5.3.3 Optimization of enzyme layer thickness | 36 |
| 2.5.4 Effect of temperature and pH on the response of SA biosensor ... | 37 |
| 2.5.5 Stability and Selectivity of SA biosensor | 37 |
| 2.5.6 Amperometric measurements | 38 |
| 2.5.7 SA measurements in protein solution and biological samples | 38 |
| 2.5.8 Immobilization of the two enzymes using chitosan and ultra-bind membrane | 38 |

CHAPTER III: RESULTS AND DISCUSSION

| | |
|---|-----|
| 3. Results and Discussion | 40 |
| 3.1 The dual enzyme system | 40 |
| 3.2 Investigation of the optimization of the condition | 41 |
| 3.2.1 Effect of buffer type on the generated current signal | 42 |
| 3.2.2 Effect of temperature on the generated current signal | 44 |
| 3.2.3 Effect of TPP cofactor concentration | 44 |
| 3.2.4 Effect of pH on the generated current signal | 47 |
| 3.2.5 Effect of NANA-aldolase/PO ratio | 47 |
| 3.2.6 Evaluation of the NANA-aldolase and PO stability | 51 |
| 3.3 Flow injection analysis of SA | 53 |
| 3.3.1 Optimization of the platinum detector | 53 |
| 3.3.2 Optiization of the experimental conditions and the IER | 54 |
| 3.3.3 Bound SA IER | 67 |
| 3.4 Preparation, characterization and application of SA amperometric Biosensor | 70 |
| 3.4.1 Effect of pH of the SA biosensor response | 71 |
| 3.4.2 Effect of temperature of the SA biosensor response | 75 |
| 3.4.3 Optimization of the immobilization conditions | 75 |
| 3.4.4 SA biosensor response, stability and reproducibility | 79 |
| 3.4.5 SA biosensor selectivity | 84 |
| 3.4.6 Application of SA biosensor to real biological samples | 93 |
| 3.4.7 Additional approaches used for enzyme immobilization | 99 |
| CHAPTER IV : CONCLUSIONS | |
| 4. Conclusions | 100 |
| REFERENCES | 101 |

List of Figures

| | | Page |
|--------------------|--|------|
| Figure 1.1 | The chemical structure of Sialic acid | 2 |
| Figure 1.2 | Enzymatic based methods scheme | 14 |
| Figure 2.1 | Schematic diagram of FIA experimental setup for SA determination | 30 |
| Figure 2.2 | Construction of tubular Pt detector and electrochemical cell | 32 |
| Figure 2.3 | Construction of SA biosensor | 35 |
| Figure 3.1 | Effect of buffer type in homogenous catalysis | 43 |
| Figure 3.2 | Effect of temperature in homogenous catalysis | 45 |
| Figure 3.3 | Effect of TTP concentration in homogenous catalysis | 46 |
| Figure 3.4 | Effect of pH of PB in homogenous catalysis at 28° C | 48 |
| Figure 3.5 | Effect of pH of PB in homogenous catalysis at 37° C | 49 |
| Figure 3.6 | Effect of NANA-aldolase/PO activity in homogenous catalysis .. | 50 |
| Figure 3.7 | Stability of NANA-aldolase and PO enzymes | 52 |
| Figure 3.8 | Comparison between Pt disc and Pt tube as FIA detectors | 56 |
| Figure 3.9 | Effect of carrier flow rate on FIA peak current | 57 |
| Figure 3.10 | FIA peaks and calibration curve using 1.5-cm Pt tubular detector | 58 |
| Figure 3.11 | FIA peaks and calibration curve using 3.5-cm Pt tubular detector | 59 |
| Figure 3.12 | Reproducibility of the FIA peak heights for SA injection using 3-cm IER | 60 |
| Figure 3.13 | FIA peaks and calibration plot with 5-cm IER, loop size 200 μ L, flow rate 1.6 ml/min | 61 |
| Figure 3.14 | FIA peaks and calibration plot with 5-cm IER, loop size 200 μ L, | |

| | | |
|--------------------|---|----|
| | flow rate 3.1 ml/min | 63 |
| Figure 3.15 | FIA peaks and calibration plot obtained with Mixed CPG reactor | 64 |
| Figure 3.16 | FIA peaks and calibration plot for 4-cm IER | 65 |
| Figure 3.17 | Reproducibility of the FIA peak heights for SA injection using 4-cm IER | 66 |
| Figure 3.18 | Stability of the optimized enzyme reactor | 68 |
| Figure 3.19 | FIA peaks for bound SA (EPO)..... | 69 |
| Figure 3.20 | Effect of pH of PB on SA biosensor | 72 |
| Figure 3.21 | Effect of pH of PB on multipoint calibration of SA biosensor | 73 |
| Figure 3.22 | Effect of temperature on multipoint calibration of SA biosensor.. | 75 |
| Figure 3.23 | Effect of GA/T ratio on the response of SA biosensor | 76 |
| Figure 3.24 | Effect of total enzyme to BSA ratio on response of SA biosensor | 77 |
| Figure 3.25 | Effect of total amount of enzyme mixture on response of SA biosensor | 79 |
| Figure 3.26 | Stability of the SA biosensors of first and second batches | 80 |
| Figure 3.27 | Calibration plots for SA biosensors at 0, 4 and 8 day | 81 |
| Figure 3.28 | Amperometric <i>I-t</i> plot for SA biosensor response | 82 |
| Figure 3.29 | Calibration plots of three SA sensors prepared within one batch | 85 |
| Figure 3.30 | Within-day reproducibility of SA biosensors | 86 |
| Figure 3.31 | Multi-point calibration of SA biosensor in the range of 0-200 μM | 87 |
| Figure 3.32 | Cyclic voltammogram of the <i>m</i> -PDA on Pt electrode | 88 |
| Figure 3.33 | Amperometric response of bare and coated Pt electrode with Poly(<i>m</i> -PDA) to hydrogen peroxide | 89 |

| | | |
|--------------------|---|----|
| Figure 3.34 | Rejection properties of poly(<i>m</i> -PDA) of AA, AAP, and UA | 90 |
| Figure 3.35 | Amperometric responses of SA biosensor correspond to SA in blood simulation sample | 91 |
| Figure 3.36 | Assay of Epotin sample using SA biosensor and soluble neuraminidase enzyme | 93 |
| Figure 3.37 | Assay of free and total SA in a whole blood sample | 94 |
| Figure 3.38 | Multi-point calibration of Pyruvate biosensor | 97 |
| Figure 3.39 | Amperometric response of SA biosensor prepared with different enzymes immobilization methods | 99 |

List of Abbreviations

| | | |
|---------------------------|---|--|
| AA | : | Ascorbic acid |
| AAP | : | Acetamidophenol (acetaminophen) |
| Ag/AgCl | : | Silver silver chloride reference electrode |
| ANDSA | : | 7-aminonaphthelene-1,3-disulfonic acid |
| BSA | : | Bovine albumin serum |
| CE | : | Capillary electrophoresis |
| CHD | : | Coronary heart disease |
| CPG | : | Controlled pore glass |
| DMB | : | 1,2-diamino-4,5-methylenedioxybenzene |
| EPO | : | Erythropoietin |
| FIA | : | Flow injection analysis |
| GA | : | Glutaraldehyde |
| GC-MS | : | Gas chromatography with mass spectrometry detection |
| HPAEC- PAD | : | High performance anion-exchange chromatography with pulsed amperometric detector |
| HPLC | : | High performance liquid chromatography |
| IER | : | Immobilized enzyme reactor |
| ISE | : | Ion selective electrode |
| ISFET | : | Ion sensitive field-effect transistor |
| LC-ESI | : | Liquid chromatography with electrospray ionization |
| LC-ESI-MS | : | Liquid chromatography with electrospray ionization with mass spectrometry detection |
| MIP | : | Molecularly imprinted polymer |
| <i>m</i>-PDA | : | <i>m</i> -phenylenediamine |
| NANA- aldolase | : | <i>N</i> -acetylneuraminic acid aldolase |
| Neu5Ac | : | <i>N</i> -acetylneuraminic acid |
| Neu5Gc | : | <i>N</i> -glycolneuraminic acid |
| PE | : | Polyester |

| | | |
|---------------|---|-----------------------------------|
| PO | : | Pyruvate oxidase |
| Pt | : | Platinum |
| QCM | : | Quartz crystal microbalance |
| SA | : | Sialic acid |
| SPR | : | Surface plasmon resonance |
| Tos-Cl | : | <i>p</i> -toluensulfonyl chloride |
| TSA | : | Total sialic acid |
| UA | : | Uric acid |

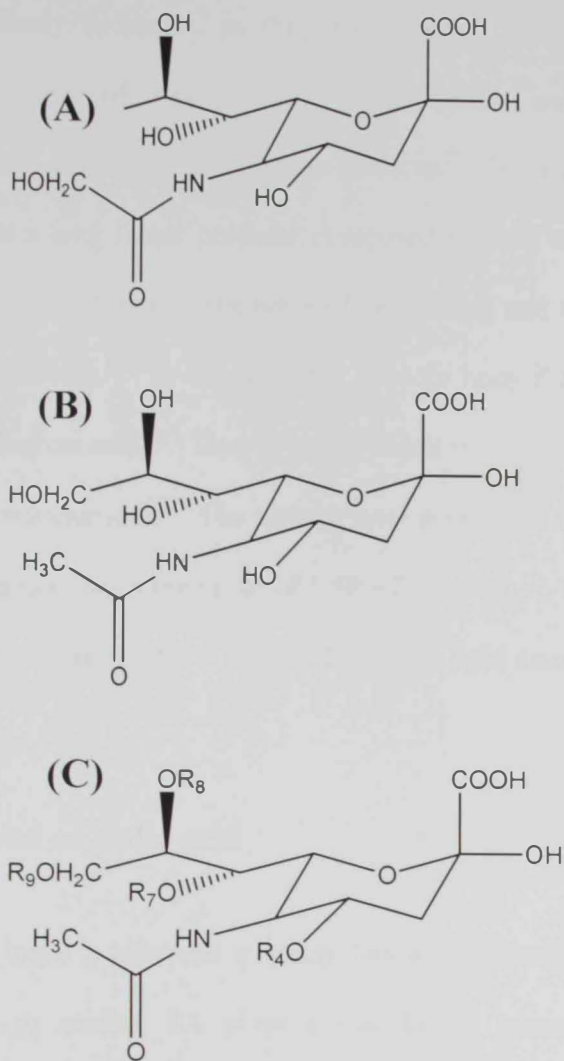
CHAPTER I

INTRODUCTION

1.1 Introduction

Sialic acid (SA) is a general term for a family of 43 derivatives of neuraminic acid, which is a 9-carbon carboxylated monosaccharide (**Figure 1.1**).^[1-3] Under physiological conditions, the carboxyl group has a negative charge which makes SA a strong organic acid (pK_a 2.2).^[2,4] SA derivatives can be divided into four major types neuraminic acid, *N*-acetyl-neuraminic acid, *N*-glycol-neuraminic acid and deamino-neuraminic acid.^[2] Neuraminic acid, which has an amino group in position 5 of the sugar ring, doesn't occur in nature. The other types of SA result from the substitution of the amino group of neuraminic acid with other functional groups, such as an acetomido, a glycol or a hydroxyl group. Deamino-neuraminic acid or 2-*keto*-3-deoxy-neuraminic acid is formed by the substitution of the amine group with a hydroxyl group. Deamino-neuraminic acid is found as a minor component in mammalian tissues and cells as well as in sperms and eggs of fish. Its elevated levels has been separated in fetal cord blood and ovarian cancer cells.^[1-2, 4] *N*-glycol-neuraminic acid (Neu5Gc) and *N*-acetyl-neuraminic (Neu5Ac) acid which form from the substitution of the amine group with a glycol or an acetomido group, respectively, are the most abundant forms of SA.^[2, 4-5] Neu5Gc acid is commonly found in many animal species. Yet, in humans, only trace amount of Neu5Gc acid is found, and only in particular types of cancer. Neu5Ac acid is the most commonly occurring SA derivative in humans.^[1-2, 5-7]

These main types of SA, can also be *O*-substituted at the hydroxyl groups at positions 4, 7, 8 and 9 with other groups, such as acetyl, methyl, lactyl or sulfate groups.^[2, 6-7] The *O*-substituted derivatives further increase the variety and number of SAs.^[6] *O*-acetylated derivatives of SA are normally found in the plasma of mammalian species.^[8]



R₄ acetyl

R₇ acetyl

R₈ acetyl, methyl, sulfate

R₉ acetyl, phosphate, lactoyl

Figure 1.1: The chemical structure of (A)- N-glycolylneuraminic acid, (B)- N-acetylneuraminic acid, (C)- representative structure of N-acetylneuraminic acid and their most common modifications.

SAs rarely occur freely in nature, as they are generally found as terminal sugar residues on oligosaccharides of glycoproteins, glycopeptides and glycolipids,^[1-2, 8-9] which exist on the inner and outer membrane surfaces.^[8] SA can also be found as polysialic acid, which is a long linear polymer composed entirely of negatively charged SA residues. Polysialic acid is found in the brain of vertebrates and is associated with the neural cell adhesion molecules.^[10] In humans, SA exist in body fluids including saliva, gastric juice, tears and human milk.^[11] They are also found in healthy human urine freely or complexes with oligosaccharides.^[2] The normal total sialic acid (TSA) level in serum and plasma has been found to be in the range of 1.58 – 2.22 mmol/L (0.52-0.73 g/L),^[5, 11] with the free form only constituting 0.5 – 3 $\mu\text{mol/L}$ and the lipid associated forms 10 – 50 $\mu\text{mol/L}$.^[2,5]

1.2 Physiological roles of sialic acid

SA is considered a major participant in many biological functions. Due to its large negative charge and high acidity, SA plays a role in the transport and binding of positively charged molecules and can increase the repulsion forces between different cells surfaces.^[4-5, 9, 12] The repulsive effects of negatively charged SA has been shown to prevent cell aggregation, as was observed when studying the adhesion of culture cell to their substratum.^[11] When needed, cell adhesion may be facilitated via positively charged substances or Ca^{2+} bridges which neutralize the repulsive effect of SA. SA also is hypothesized to have an important role in neural structure. Neural cell membranes contain 20 times more SA than the other types of membranes. Further more, Sialo-compounds have been shown to play an important role in the structural and functional establishment of synaptic pathways.^[11] SA also contributes in the cellular signaling processes. It is found as an essential component in many cell-surface receptors. For example it was found

that SA has a role in the cellular action of insulin and can also modulate amino acid transport in certain cells.^[12]

The potential of SA to be used as an antimicrobial agent is also enormous. Sialylated oligosaccharides in human milk can act as highly specific receptors for the variety of viruses, bacteria and parasites. Both free and bound sialylated oligosaccharides in human milk prevent the binding of rotavirus and cholera toxin associated with infant diarrhea, as well as *Escherichia coli* strains associated with neonatal meningitis and sepsis.^[1] Generally, the functions of SA in biological systems include conformational stabilization, protease resistance, charge, enhancement of water binding capacity, cellular recognition, protein targeting and developmental regulation.^[4-5, 8, 12]

1.3 Sialic acid as a biomarker

Biomarkers can be defined as living responses of a biological system to an environmental stressor. Hence, a biomarker can be an indicator of the exposure to this stressor. An example of biomarkers is a tumor marker, which is a substance, such as proteins, biochemicals, or enzymes, produced by the tumor cells or the body in response to tumor cells. As tumor cells multiply and tissue is damaged, the amount of these substances increase and leak into the bloodstream. Tumor marker levels in the blood can thus be used to screen people for certain types of cancer.^[13] SA is considered to be a biomarker for certain types of cancer and other diseases.^[1, 4-5, 8-9, 12]

Before starting discussing the role of sialic acid as a biomarker, a brief summary about cancer in UAE will be discussed. The first international scientific account of cancer in the UAE dates back to 1981 when it was documented that of the 209 liver patients in Al-Qassimi Hospital (Sharjah), five cases involved primary hepatoma. A retrospective

analysis of patients admitted to Tawam Hospital during years 1980 to 1984 indicated the presence of 1,357 cases of cancer. These included breast cancer (9%), head and neck cancer (9%), lung cancer (7%), non-Hodgkins lymphoma (6%), acute leukemia (5%), cancer of the cervix (5%), stomach cancer (5%), Hodgkin's lymphoma (4%), cancers of the colon and rectum (4%), thyroid cancer (4%), and others.^[14]

Based on a review of cases involving children with malignancies in UAE from 1983-1989, it appears that pediatric cancer may be on the rise in the UAE. On average, there were 20 new cases of cancer diagnosed in 1983 and annually from 1985-1987. However, this rate increased to 37 new cases in 1988 and 1989. UAE national children were the most affected (43% of all patients) followed by other Arabs (31%), South Asians (19%), and children of other nationalities (5.5%).^[14] During the twenty years between 1983 and 2002, there were 4,941 admissions to the Pediatric Oncology Unit in Tawam Hospital, including 1,014 new cases of pediatric cancer (ages 0-12). This translates to one new case per week.^[15] So the detection of cancer in early stages might increase the chances of controlling the disease and therefore saving patients' lives, especially those of children.

1.3.1 Sialic acid as a cancer biomarker

Disturbance in the metabolism of SA, either due to genetic error or at the post-translation level, may impair physiological function or lead to disease.^[1] Some genomic changes bringing about alterations in cell membrane and/or cell organelle components may cause degradation of cell growth and proliferation. Thus, it is not surprising that SA undergoes substantial variations during malignant transformation.^[16]

Increased serum concentrations of SA have been detected in a number of tumors, such as pancreatic cancer, skin squamous cell carcinoma, lung, prostate, breast, ovary,

colon and thyroid cancers.^[17-20] Elevated serum levels of TSA have been reported in the majority of patients with leukemia and solid tumors especially children.^[21] It was found that serum SA level in patients with endometrial cancer was substantially higher than in the healthy people.^[18, 20, 22] Furthermore, SA level has been correlated with the tumor size, positive lymph nodes metastasis, and advanced clinical stage in patients with head and neck squamous cell carcinoma.^[22] In the case of cholangiocarcinoma, – a type of cancer, the clinical features are increased liver mass, upper abdominal pain, jaundice and fever. The increase in SA levels has been positively correlated with tumor burden and the degree of metastasis, but a correlation between serum TSA levels and tumor types or staging of the cholangiocarcinoma could not be established.^[23]

In general, the elevated TSA concentrations are assumed to be due to the increased activity of sialyltransferase, leading to an increased amount of SA on the cell surface and the spontaneous release or shedding of aberrant SA containing cell surface glycoconjugates into the plasma.^[20, 23] In tumor metastasis, an increase in the level of cell surface sialylation in certain cell lines has been found to be linked to their metastatic potential,^[1] as the highly sialylated surfaces protect tumor cells from immune defense and thus facilitate metastatic spread.^[18] The increased sialylation may contribute to the survival of metastasizing cells in circulatory system and to adhesion of the cells to the endothelium at a secondary site.^[1]

Although the increased serum SA concentration showed a high sensitivity and positive predictive value, its clinical utility for screening cancers is limited because SA is non-specific for a given disease.^[20, 23] The non-specificity of SA came from considering it as a biomarker for other diseases such as: inflammation, metabolic disorders and other

health concerns such as pregnancy, aging and smoking,^[1, 2, 5, 11, 23-24] all which will be discussed later.

1.3.2 Sialic acid as a marker for other diseases

Decreased levels of SA have also been associated with some diseases, such as schizophrenia and Alzheimer's disease.^[1] In the case of schizophrenia, lower levels of SA content in the glycoproteins of the cerebrospinal fluid have been reported.^[1] Furthermore, when the schizophrenia was successfully treated, the SA content rose to normal levels.^[1] In the case of Alzheimer's patients, a decreased sialyltransferase activity, that affects the α -2,3-linked SA in serum glycoproteins has been reported in their serum. In these patients, ganglioside SA content in cerebral cortex was also decreased.^[1]

In other cases, elevated levels of SA have been reported in diseases such as type I and II diabetes, and cardiovascular diseases,^[1, 5] such as coronary heart disease (CHD).^[8] It was found that elevated plasma SA concentration is strongly related to the presence of microvascular complications in type I diabetes and cardiovascular morbidity in the general population.^[1] In type II diabetes, the circulating SA concentration is elevated in comparison with nondiabetic subjects.^[1] Links between SA and risk factors for vascular diseases, such as blood lipids, smoking, hyperfibrinogenemia and lipoprotein have also been reported.^[1, 5] Studies focused on the relationship between CHD and SA content have found that plasma SA levels are elevated in individuals with CHD, possibly due to elevations of plasma acute phase proteins released in response to inflammation.^[3] Other studies that have examined the relationship between lipoprotein-associated SA and the development of CHD have shown that individuals with low levels of lipoproteins-

associated SA are at increased risk of developing CHD. However, the factors that control the content of lipoprotein-associated SA are not known.^[3]

TSA was found to significantly increase in patients with chronic renal failure, chronic liver disease and pneumonia. Also, highly increased SA levels were observed in several inherited diseases in which SA accumulates in lysosomes.^[5] It was found that the concentration of SA increases with aging, smoking and pregnancy.^[2, 11] It was observed that SA is not related to gender as SA concentrations, are not different between females and males. In some studies,^[11] it was shown that the serum TSA increases with age in women but not men and this could be due to menopause. While in other studies,^[2, 12] no significant difference in serum TSA was found before and after menopause. Some studies have shown that smoking increases the serum SA concentration in men but not in women, however, no apparent explanation for this feature has been offered.^[11]

Furthermore, it was found that during pregnancy SA concentrations increases in maternal saliva and plasma.^[1, 2] SA in saliva increases to 3 folds of its concentration at the 21-40 weeks of gestation, corresponding to the period of rapid SA accumulation in the fetal brain. Some studies have shown significant correlations between maternal and retroplacental blood on the one side and between maternal and cord blood on the other side. This suggests that the mother synthesizes much of the SA, which crosses the placenta to contribute in the fetal growth in the third trimester.^[1]

1.3.3 Sialic acid and Erythropoietin

Adult humans produce approximately 2.3 million red blood cells every second.^[25] The main regulator of this process is erythropoietin (EPO), a glycoprotein hormone whose serum concentration is about one hundredth of most hormones in the body. EPO is produced in the kidneys, circulates in the plasma, and induces red blood cell production in the bone marrow, where it binds to erythroid progenitor cells.^[25] EPO has been used as a drug since 1988 primarily for the clinical treatment of anemia, especially anemia caused by renal failure.^[26] Also, EPO has been used as a standard drug in the treatment cancer, HIV infection and in the surgical setting to reduce allogenic blood transfusions.^[27]

Approximately 60% of the EPO molecule is protein and the remainder is carbohydrate. The carbohydrate content consists of small, branched-chain sugars, partially terminating in SA. The presence of SA ends on the carbohydrate slows the rate of clearance of EPO by the liver. Clearly, the longer EPO remains in the circulation, the greater the opportunity for it to stimulate erythroid progenitor cells located in the bone marrow.^[25] It was found that the removal of terminal SA from carbohydrates chains of urinary EPO increased their *in vitro* activity but abolished the *in vivo* activity completely. The latter is thought to be due to rapid metabolic clearance by binding of EPO to hepatic receptors recognizing exposed galactose residues.^[28] So, the number of the SA residues and the branching pattern of the N-linked oligosaccharides modify the pharmacodynamics, speed of catabolism and biologic activity of EPO.^[26]

Due to the great importance of SA and its physiological role as a biomarker, various colorimetric and chromatographic methods for its quantification have been developed. A survey of these methods will be discussed in the following section.

1.4 Analytical methods for the determination of sialic acid

The classical colorimetric methods suggested for SA determination suffer from sensitivity or selectivity limitations. These methods utilize different reagents such as perchloric acid/tryptophane,^[29] hydrochloric acid,^[30] diphenylamine,^[31] and ethanoic acid/sulphonic acid.^[32]

1.4.1 Colorimetric assays

1.4.1.1 Orcinol method

The orcinol reagent reacts with SA in the presence of ferric ions and hydrochloric acid at 100 °C. The chromophore produced is extracted by isoamyl alcohol after cooling and then measured spectrophotometrically at 572 nm.^[33] This method suffers from significant interferences in the presence of hexoses, pentoses, and uronic acid.

1.4.1.2 Resorcinol method

This method was first described by Svennerholm.^[34] SA is first released by heating with strong acid (hydrolysis) and then reacted with resorcinol and copper(II) ions to produce the chromophore which has an absorption maximum at 582 nm. Interferences from pentoses, 2-deoxyhexoses, and ketohexoses have been reported for this assay as well.

Jourdian *et al*^[35] enhanced the sensitivity of the resorcinol method (~ five-fold) by oxidizing SA residues with periodic acid prior to the addition of acidic resorcinol reagent. The periodate-resorcinol method was adapted for the microassay of total SA using the microtiter plate reader.^[36, 37] Various modifications of Jourdain's method have been described and used for the determination of free, bound and total SA in biological fluids.^[9]

The potential of such sialic speciation is attributed to the effect of the oxidation duration and temperature to measure either free, bound or total SA.

1.4.1.3 Periodic/thiobarbiturate method

This method is one of the most common methods used for the quantification of SA.^[12] In this method, the SA is first dissociated with acid hydrolysis. Periodic acid is then used to oxidize free SA to form formyl pyruvic acid, which in turn reacts with thiobarbiturate to produce red chromophore with an absorption maximum at 549 nm.^[38, 39] Interferences by substances that form formyl pyruvic acids have been reported. Several organic solvents have been suggested for the extraction of the produced chromophore such as cyclohexanone,^[39] butan-1-ol,^[38] and dimethylsulphoxide.^[40] Several recent studies utilized different variations of the periodic-thiobarbiturate method for the assay of SA in biological samples.^[41-43]

1.4.1.4 Other Colorimetric methods

A related colorimetric method to the periodic-thiobarbiturate method based on another sulfur containing organic reagent has been suggested as well.^[44] A colorimetric method for direct Sialoglycoproteins (e.g., Fetuin) has also been suggested.^[45] The method is based on the reaction with acidic ninhydrin reagent at 100°C which leads to the formation of a stable product with an absorption maximum at 470 nm. This method was applied for the determination of sialoglycoproteins in ascites fluids in tumor bearing mice.^[44]

1.4.2 Fluorometric assays

One of the earliest fluorometric assays was described by Hess and Rolde.^[46] In this method, SA is heated with 3,5-diaminobenzoic acid in the presence of dilute hydrochloric acid to form a green fluorescent compound. The assay has good sensitivity but suffers from interference from serum lipids. Other fluorescence assays include an adaptation of the periodic acid/thiobarbituric acid colorimetric assay in which the chromophore is excited at 550 nm and the emission measured at 570 nm.^[47] 2-deoxyribose has been reported to exert as a significant interference in this assay. A fluorometric assay suggested by Murayama and colleagues^[48] does not have the deoxyribose interference limitation. In this assay, the free SA is heated at 70 °C for 45 min with pyridoxine. The resultant fluorescent compound is then excited at a wavelength of 395 nm and with an emission wavelength of 470 nm. It has been observed, however, that certain ketoacids can give a similar fluorescence. A fluorometric method based on derivatization with 1,2-diamino-4,5-(methylenedioxy)benzene has also been suggested for the fluorometric detection of SA in HPLC methods.^[49]

1.4.3 Enzymatic assays

Several schemes have been suggested for the assay of SA based on a sequence of two or more enzymes, which could be either free or in immobilized form. Different enzyme combinations and their analytical products are illustrated in **Figure 1.2**. The enzymatic methods that utilize pyruvate could suffer from interference from endogenous pyruvate in the sample and so alternative enzymatic pathways have been investigated. One of these,^[50] uses neuraminidase to release SA in the free form, which is then acted upon by acylneuraminate pyruvate lyase to form pyruvic acid and N-acetyl-mannosamine. The

latter is then converted to N-acetyl-glucosamine by the enzyme acylglucosamine 2-epimerase and then to N-acetylglucosaminic acid and hydrogen peroxide by the enzyme N-acetylhexosamine oxidase. The hydrogen peroxide is then linked to peroxidase and a quinone dye, the chromophore having a wavelength maximum at 590 nm. The authors reported little interference but this scheme involves five enzymes to work in sequence.

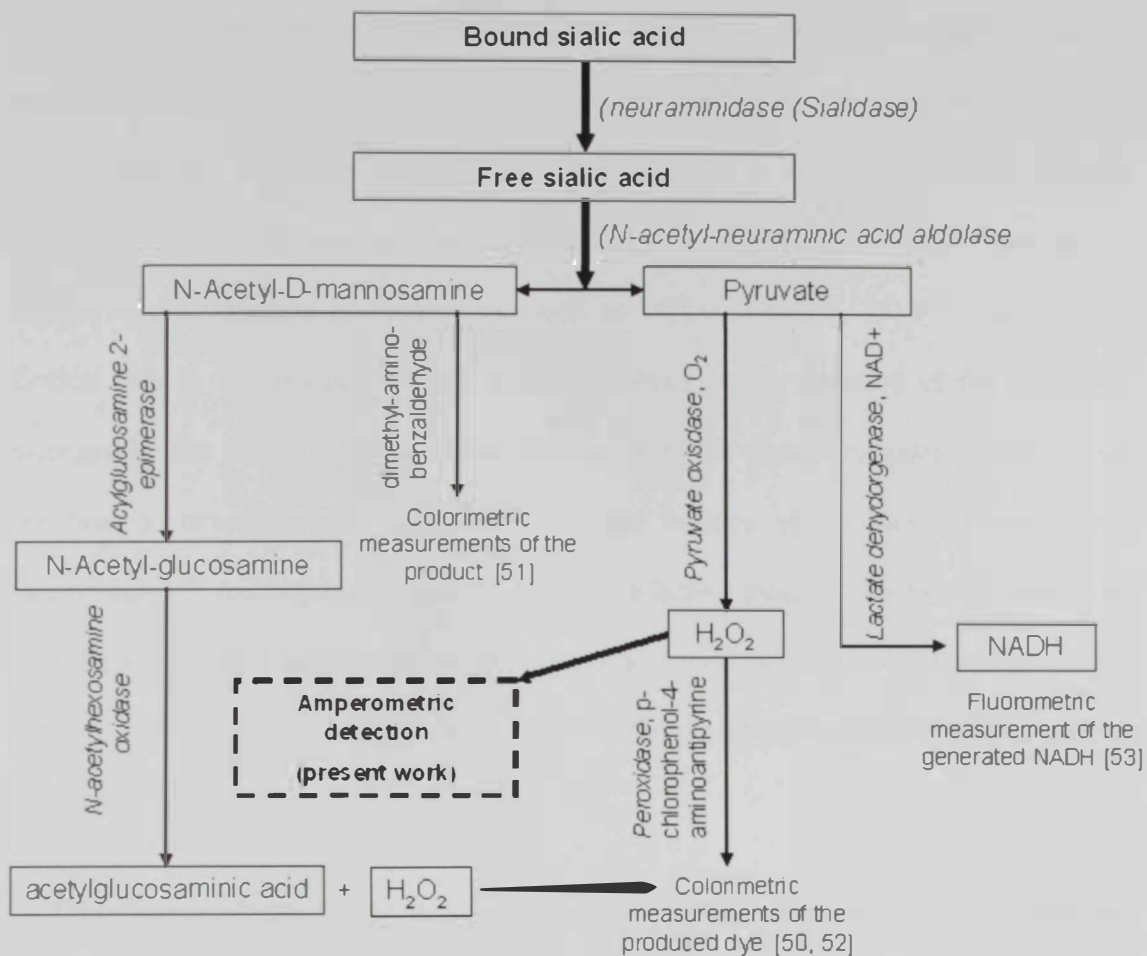


Figure 12: A scheme shows a summary of the enzymatic based methods.

1.4.4 Chromatographic methods

In general, two levels of SA analysis can be rationalized: (i) analysis of SA as monosaccharide constituents and (ii) structural analysis of the glycan chains of glycoconjugates. The latter is usually very complex due to the presence of the several monosaccharides with multiple and diverse substitution. Such analytical challenge is tackled by combination of techniques, such as HPLC, GC-MS, LC-ESI, and CE.^[54] Critical step in SA analysis is their liberation which entails isolation of the sialylated macromolecules and/or removal of SA residues from the glycoconjugates. A number of sialidase or neuraminidases (EC 3.2.1.18) from various microorganisms have been characterized.^[4] Acid hydrolysis treatments is an effective means to liberate SA residues as well. However, since acid treatments are always associated with some destruction of such carbohydrates residues, a balance between the release and destruction of SA should be optimized.^[2]

Direct chromatographic analysis of SA without prior derivatization has attracted the interest of many researchers. High performance anion-exchange chromatography with pulsed amperometric detection (HPAEC-PAD) is a powerful tool for the analysis of carbohydrates including SA. This subject has been recently reviewed by Rohrer.^[55] The highly alkaline eluents used in HPAEC-PAD limited the range of the analyzed SA to non-substituted ones such as Neu5Ac. A direct reversed-phase ion-pair HPLC method for the analysis of five underivatized SA has been reported as well.^[7] Most carbohydrates do not possess ionizable groups and their hydroxyl groups are ionized only in extreme alkaline conditions (pH>11). SAs are unique in that aspect due to the presence of carboxyl groups. Dong et al utilized this feature and reported the separation of underivatized Neu5Ac and Neu5Gc in borate-phosphate buffer (pH 8.95) by capillary electrophoresis (CE).^[56]

Numerous chromatographic methods for determination of SA following derivatization have been suggested to assay different types of SA. Analysis of De-*O*-acetylated SA can be derivatized with *p*-toluenesulfonylchloride (Tos-Cl) to yield tosyl derivatives, which are completely resolved by liquid chromatography.^[57] The reversed phase HPLC analysis of SA after labeling with 1,2-diamino-4,5-methylenedioxybenzene (DMB) is one of the most widely used and highly sensitive methods for the determination of SA.^[58] The acidic conditions (acetic acid) used in the DMB derivatization reaction is believed to prevent the migration of acetyl groups from one hydroxyl group to another, and this allows the analysis of *O*-acetylated derivatives as well.^[58]

Both chromogenic and fluorogenic derivatization have been suggested for the analysis of SA by capillary chromatography. The most widely used derivatization scheme is the reductive amination. The carbonyl group of a reducing sugar reacts with the amino group of the label and forms a Schiff base, which is reduced to a stable secondary amine. Guttman^[59] used 9-aminoacridone as a fluorescent label for the determination of SA by CE. Mechref et al^[60] introduced a different derivatization scheme for SA which involved condensation of the carboxylic acid group of Neu5AC with the amino group of 7-aminonaphthelene-1,3-disulfonic acid (ANDSA). Another derivatization schemes based on the conversion of reducing sugars to *N*-methylglycamines^[61] as well as per-*O*-benzoylation procedures^[62] have been reported for the determination of SA by CE.

Hyphenated chromatographic techniques such as gas chromatography with mass spectrometry (GC-MS) have been successfully used for the determination for SA. Many of these methods use a methanolysis step to release SA followed by derivatization to form a heptafluorobutyrate derivatives.^[63] Liquid chromatography with electrospray ionization-mass spectrometry detection (LC-ESI-MS) technique for the determination of SAs has

been suggested as well.^[64] The powerful potential of LC-ESI-MS could be due to the combination of both retention and mass spectra data, which could allow for simultaneous determination of about 13 members of the SA family with differences in the substitution with *N*- or *O*-acetyl, or glycolyl ester groups.^[65]

1.5 Determination of sialic acid by chemical sensors and biosensors

Despite of the physiological significance of SA and the numerous optical and chromatographic methods reported for the determination of SA, a comprehensive literature search revealed a very limited number of publications describing the development of either chemical sensors or biosensors for the determination of SA. Two sensors were developed by Takeuchi and coworkers based on SA-molecularly imprinted polymers (MIP) that allow the recognition for SA recognition in both a quartz crystal microbalance (QCM)^[66] and a surface plasmon resonance (SPR).^[67]

Up to the author's knowledge, only one publication has been cited for the determination of bound sialic using a potentiometric biosensor.^[68] This biosensor was based on an immobilized sialidase on top of a H^+ -sensitive plastic indicator electrode. The cleavage of the linkage to the macromolecular substrate catalyzed by sialidase leads to the liberation of SA (pK_a 2.6). The resultant local pH drop constituted the basis of bound SA quantitation.

Therefore, the aim of the present work was to combine, for the first time, the NANA-aldolase-PO enzyme sequence with the amperometric transduction for the generated hydrogen peroxide to allow new, simple, and reliable electroanalytical methods for the determination of free and bound Neu5Ac, which are the most common forms of SA in humans. In the following sections, a brief overview of the definition, classification,

techniques, and applications of biosensors with special emphasize on electrochemical biosensors will be given.

1.6. Biosensors

According to the IUPAC recommendations,^[69] an electrochemical biosensor is a self-contained integrated device, which is capable of providing specific quantitative or semi-quantitative analytical information using a biological recognition element (biochemical receptor) which is retained in direct spatial contact with an electrochemical transduction element. The biological recognition element transforms information from the biochemical domain, usually an analyte concentration, into a chemical or physical output signal. The purpose of the recognition element is to provide the sensor with a high degree of selectivity for the analyte to be measured.^[70] The role of the transduction element (transducer) is to translate the information received from the biological recognition element into a measurable electrical signal.

Biosensors can be classified according to either the nature of the biorecognition element or the transducer. The biorecognition element can be systems containing enzyme (mono or multi-enzyme), whole cells (microorganisms such as bacteria, fungi, eukariotic cells, yeast), cells organelles and plant or animal tissue slice.^[71] According to the nature of the transduction element, electrochemical biosensors can be further classified into conductometric, potentiometric and amperometric biosensors.^[72-74]

Conductometric biosensors are based on the principle of change of the sample conductivity when the biological element metabolizes uncharged substrate such as carbohydrates or urea into ionic species.^[75] The limitation of the conductometric transduction is the interference of the ionic background of the real samples which

necessitated the use of the dual measurements.^[76] In biosensors based on potentiometric transducers a membrane or sensitive surface to a desired species generates a proportional potential to the logarithms of the concentration of the active species measured in relation to a reference electrode. The types of potentiometric transducers can be either ion selective electrodes (ISEs) or ion sensitive field effect transistors (ISFETs). Both types transducers have been utilized to construct potentiometric biosensors for several species.^[77-81]

Biosensors based on enzymes, as a biological recognition element, and amperometric transduction modes have received the greatest attention to date by far. As they offer several advantages in terms of sensitivity (10^{-5} - 10^{-8} M, range of concentrations can be measured), ease and versatility of construction, simplicity and cost. In addition to the general advantages provided by the biosensors, such as minimum sample treatment (ideally no reagents are required for the assays using biosensors), virtually nondestructive, fast response, they can be used for small sample volumes and offer a wide scope of applications.^[71-72, 82-83]

Because of biosensors exceptional performance capabilities, they have been found successfully used in diverse fields such as clinical diagnosis,^[70, 72] food analysis,^[71, 73, 84] process control, biotechnology and environmental monitoring.^[85-87]

As mentioned before, biosensors based on enzymes, as a biological recognition element have received by far the greatest attention to date, thus, improvements in enzymes stability via immobilization can enable further practical applications. It can reduce the required amount of enzymes, prolong the lifetime of enzyme reactors, increase the potential for enzyme reuse, or maintain the good signal of biosensor.^[83, 88] Some of

the commonly used enzymes immobilization techniques will be briefly explained in the following section.

1.6.1 Enzyme Immobilization

Generally, the biological recognition components, *e.g.*, enzymes can be immobilized either physically, chemically or combination of them. The common physical methods are adsorption to water-insoluble carrier and entrapment in water-insoluble polymeric gels. Chemical immobilization is realized by covalent coupling to derivatized carrier or by intermolecular crosslinking of the biomolecule.^[76, 89] Examples of these methods will be explained briefly.

1.6.1.1. Adsorption

The adsorption of an enzyme onto the electrode surface is the simplest immobilization method. However, biosensors based on adsorbed enzymes are usually of short operational life-time because of continuous leaching out of the enzyme from the vicinity of the electrode surface.^[76, 90] Anionic and cationic ion exchange resins, active charcoal, silica gel, clay, aluminum oxide, porous glass, and ceramics are being currently used as active material. Ideally, the carrier should exhibit high affinity and capacity for the biomolecule and the latter must remain active in the adsorbed state. The carrier should also neither adsorb reaction products nor inhibitors of the biocatalyst.^[76, 85]

1.6.1.2. Gel entrapment

Entrapment in polymeric gels prevents the biomolecules from diffusing away from the reaction mixture. Gel entrapment is as mild a procedure as adsorption, as the biomolecules are not covalently bound to the matrix, membrane, or to each other. The

method is therefore widely employed. The most important matrices used are alginate, carageenan, collagen, cellulose triacetate, polyacrylamide, gelatin, agar, silicon rubber,^[76] sol-gel,^[91] poly(carbamoyl) sulfonate hydrogel.^[92]

1.6.1.3. Covalent attachment

To covalently couple biomolecules, such as enzymes or antibodies, to carriers the dissolved protein is either reacted with an activated water-insoluble carrier or copolymerized with a reactive monomer. The reaction should involve only groups that are not essential for the biological activity of the biomolecule. The immobilization is conducted in three steps: activation of the carrier, coupling of the biomolecule, and removal of adsorbed biomolecules. A disadvantage of covalent coupling is the frequently occurring loss of enzyme activity.^[76, 93]

1.6.1.4. Crosslinking

The protein molecules may be crosslinked with each other or with another, functionally inert protein (e.g. albumin or gelatin). The biomacromolecules can also be adsorbed to a water insoluble carrier or entrapped in a gel and then crosslinked. Among others, bisdiazobenzidine, bisisocyanate derivatives,^[76] glutaraldehyde,^[91,94-95] and epichlorohydrin^[94] have been used as bifunctional reagents.

The advantages of crosslinking are the simple procedure and the strong chemical binding of the biomolecules. Furthermore, the choice of the degree of crosslinking permits the physical properties and the particle size to be influenced. The main drawback is the possibility of activity losses due to chemical alterations of the catalytically essential sites of the protein.^[76]

It has been found that, the properties of immobilized enzymes are governed by the properties of both, the enzyme and the support material. A number of desirable characteristics should be common to any material considered for immobilizing enzymes. These include: high affinity to proteins, availability of reactive functional groups for direct reactions of enzymes and for chemical modifications, hydrophilicity, mechanical stability and rigidity, regenerability, and ease of preparation in different geometrical configurations that provide the system with permeability and surface area suitable for a chosen biotransformation.^[89]

1.6.2. Interference to a biosensor response

Electrochemical biosensors, in spite of the use of analyte specific molecular recognition elements, are susceptible to interference from indigenous electroactive compounds such as, uric acid, dopamine, and ascorbate. Ascorbate is the most troublesome due to its comparatively high concentration and broad oxidation potential range. Several methods have been employed to produce a combination anionic size exclusion barrier to interfering species, including electropolymerization of pyrrole and o-phenylenediamine, cellulose acetate, and polyestersulfonic acid for applications measuring nitric oxide, glucose, pyruvate, and glutamate. Electropolymerized films show excellent permselectivity for short periods of time, but tend to fail rapidly when operated at 37°C.^[70]

1.7 Objectives

The Objectives of the present work are:

1. Optimization of the experimental conditions for sialic acid conversion, by the action of two successive enzymes, into hydrogen peroxide which constitutes the principle of the analytical signal.
2. Development of a flow injection analysis system for the determination of SA based on immobilized enzyme reactor (IER).
3. Design, fabrication and characterization of SA enzymatic biosensor(s).
4. Assessment of the reliability of such developed amperometric method and biosensor(s) for the determination of SA in urine and/or blood samples from healthy individuals and patients diagnosed with cancer.

CHAPTER II

**MATERIALS AND
METHODS**

2. Materials and Method

2.1 Materials and Reagents

N-acetylneuraminic acid (Neu5Ac) was purchased from Toronto Research Chemicals (Canada). N-acetylneuraminic acid aldolase (NANA aldolase) (EC 4.1.3.3) from microorganism (24.8U/mg), pyruvate oxidase (PO) (EC 1.2.3.3) from microorganism (10.9 U/mg) and neuraminidase (EC 3.2.1.18) from microorganism (71.8 U/mg) were received as lyophilized powders from (Toyobo enzymes, Sorachim, France). Aminopropyl controlled pore glass (CPG) (200-400 mesh, with average pore size of 500 Å and 170 Å with amine content of 45 and 70 µmol/g glass, respectively) and thiamine pyrophosphate (TPP), acetaminophen (4-acetamidophenol) (AAP) and uric acid (UA) were received from Sigma (USA). Glutaraldehyde (GA) (25% aqueous solution, grade II) and bovine serum albumin (BSA), fraction V were received from Sigma-Aldrich Chemie GmbH (Germany). 1,3-diaminobenzene (*m*-phenylenediamine (*m*-PDA)), *L*-ascorbic acid (AA) and 4-morpholinepropanesulfonic acid (MOPS) were received from Aldrich (USA). 1-mL Erythropoietin (Epotin) samples (4000U/vial) were received from Julphar Pharmaceutical Co. (UAE). Chitosan (low molecular weight) was received from Fluka (USA). Ultra-bind membranes were received from Gelman Sciences (USA). Polyester membranes (6 µm thick) with pore size of 1.0 microns were received from Osmonics Inc. All other chemicals were of analytical reagent grade. Enzyme solutions were prepared immediately before the use in 0.1 M phosphate buffer. Thiamine pyrophosphate and SA stock solutions in 0.1M phosphate buffer (PB) were prepared freshly every 3 days and stored in refrigerator at 4 °C when not in use. All chemicals were used without further

purification and other chemicals were of the highest available purity. All solutions were prepared using deionized water.

2.2 Apparatus

All amperometric measurements, cyclic voltammetry (CV) experiments, and electrodeposition were carried out using a Princeton Applied Research Scanning Potentiostat/Galvanostat (EG&G Model 362). The potential and current analog outputs of the potentiostat were recorded using an ADC 16 data acquisition interface card (Pico Technology, UK) connected to a PC installed with PicoLog software (Pico Technology, UK) for data display and storage. pH measurements were made using a combination glass electrode and a Thermo-Orion pH/mV meter. A peristaltic pump (Masterflex, Model 7554-95 country) and a manual sample injection valve (Rheodyne, USA Model 7125) fitted with either 50 or 200 μL sample injection loop were used in the flow injection system. A digital circulating water bath (Julabo, Model EC-5, Germany) was used throughout for temperature control. All batch experiments were carried out in a 10-mL double-jacket thermostated cell, using three-electrode electrochemical cell configuration. An Ag/AgCl and platinum (Pt) wire were used as reference and counter electrodes, respectively, whereas the working electrode type varied with the experiment type.

2.3 Investigation of the dual enzyme system by homogenous catalysis

This study was carried out using homogeneous enzymatic catalysis using a Pt disk electrode (1.6 mm in diameter, BAS) as working electrode. The Pt electrode was polished using alumina slurries, rinsed with deionized water and sonicated in distilled for 5 minutes. After this treatment, the Pt electrode was subjected to several potential cycles cycling between -0.25 and +1.25V vs Ag/AgCl in 0.5M H_2SO_4 at a scan rate of 50mV/sec.

In all amperometric measurements, the Pt electrode was polarized at 0.6 V (unless otherwise stated) in the background buffer and the background current was allowed to decay before the sample was introduced into the measurement cell.

2.3.1 Effect of buffer type

A 5-mL aliquot of either 0.1M phosphate or MOPS buffer (pH 7.2) was transferred to a 10-mL double-jacketed cell thermostated at 28°C. TPP and SA were added to give 0.5 and 1.5 mM, respectively. The cell was turned on and the background current was allowed to decay. Then a 20- μ L aliquot of the tested buffer containing NANA-aldolase (4.04 U) and PO (4.09 U) was added to initiate the generation of hydrogen peroxide. The anodic current, which corresponds to the oxidation of hydrogen peroxide, was recorded for 250 seconds at 2 Hz sampling rate.

2.3.2 Effect of the TPP cofactor concentration

A 5-mL aliquot of 0.1M PB pH 7.2 was transferred to a 10-mL double-jacketed cell thermostated at 37°C. TPP which is the cofactor of PO, was added to give a concentration ranges from 0 to 1.6mM. SA was added to give a final concentration of 1.5 mM. Then a 20- μ L aliquot of the PB containing NANA-aldolase (4.04 U) and PO (4.09 U) was added to initiate the generation of hydrogen peroxide. The corresponding anodic current was recorded as described above. The effect of TPP using MOPS buffer was tested similarly.

2.3.3 Effect of Temperature

A 5-mL aliquot of 0.1M PB pH 7.2 was transferred to a 10-mL double-jacketed cell thermostated at the required temperature in the range of 20-58°C. TPP and SA were added to give 0.5 and 1.5 mM, respectively. Then a 20- μ L aliquot of the PB containing

NANA-aldolase (4.04 U) and PO (4.09 U) was added to initiate the generation of hydrogen peroxide. The corresponding anodic current was recorded as described above.

2.3.4 Optimization of pH

A 5-mL aliquot of 0.1M PB -adjusted to the required pH value in the range of 4.5-8.52 - was transferred to a 10-mL double-jacketed cell thermostated at 37 °C. TPP and SA were added to give 0.5 and 1.5 mM, respectively. Then a 20- μ L aliquot of the PB containing NANA-aldolase (4.04 U) and PO (4.09 U) was added to initiate the generation of hydrogen peroxide. The anodic current which corresponds to the generated hydrogen peroxide for each pH value was recorded as described above. The experiments with pH 5.6, 6.3, 6.6, 6.9 and 7.2 were carried out at 37 °C.

2.3.5 Effect of NANA-aldolase/PO activity ratio

A 5-mL aliquot of 0.1M PB pH 7.2 was transferred to a 10-mL double-jacketed cell thermostated at 37°C. TPP and SA were added to a final concentration of 0.5 and 1.5 mM, respectively. An aliquot of NANA-aldolase was then added, and after background current stabilization, an aliquot of PO was added. The PO concentration was fixed to be 4.09 U in all the experiments, while the NAN-aldolase was added in different concentration to the ratio of NANA-aldolase/PO as 0.246, 0.493, 0.739, 0.986, 1.232, 1.479, 1.725 and 1.972, respectively. The anodic current, which corresponds to the generated hydrogen peroxide for each NANA-aldolase/PO ratio, was recorded as described above.

2.3.6 Effect of the freshness of TPP cofactor

A 5-mL aliquot of 0.1M PB pH 7.2 was transferred to a 10-mL double-jacketed cell thermostated at 37°C. TPP fresh and old stock solutions were used for this study and

diluted with PB to 0.5 mM, respectively. SA concentration was fixed at 1.5 mM. Then a 20- μ L aliquot of the PB containing NANA-aldolase (4.04 U) and PO (4.09 U) was added to initiate the generation of hydrogen peroxide. The anodic current, which corresponds to the generated hydrogen peroxide, was recorded for 250 seconds.

2.3.7 Effect of SA freshness

A 5-mL aliquot of 0.1M PB pH 7.2 was transferred to a 10-mL double-jacketed cell thermostated at 37°C. TPP was added to give 0.5 mM. SA fresh and old stock solutions were used for this study and diluted with PB to 1.5 mM, respectively. Then a 20- μ L aliquot of the PB containing NANA-aldolase (4.04 U) and PO (4.09 U) was added to initiate the generation of hydrogen peroxide. The anodic current, which corresponds to the generated hydrogen peroxide, was recorded for 250 seconds.

2.3.8 Effect of enzymes freshness

A 5-mL aliquot of 0.1M PB pH 7.2 was transferred to a double-jacketed cell thermostated at 37°C. Fresh TPP and SA were added to give 0.5 and 1.5 mM, respectively. Then a 20- μ L aliquot of the PB containing NANA-aldolase (4.04 U) and PO (4.09 U) was added to initiate the generation of hydrogen peroxide. The anodic current, which corresponds to the generated hydrogen peroxide, was recorded for 250 seconds. The experiment was repeated using one-week old solution of the two enzymes, one week old NANA and fresh PO, and one week old PO and fresh NANA, respectively.

2.4 Flow injection analysis

The flow-injection-analysis (FIA) setup used for the determination of SA was constructed as shown in **Figure 2.1**. A carrier solution (0.1 M PB pH 7.2 containing

1.0mM TPP) was propelled through the system at the desired flow rate by means of the peristaltic pump. The components of the system were connected with Norprene tubes (0.8 mm i.d.). A manual injection valve (Rheodyne, Model 7125) fitted with either 50- or 200- μ L injection loop was used for sample injection. The injected SA sample was transferred to the immobilized enzyme reactor (IER) in which both of NANA-aldolase and PO were co-immobilized and a corresponding amount of hydrogen peroxide was formed and transferred to the detector. The details of both of the IER and the detector were given in the following sections.

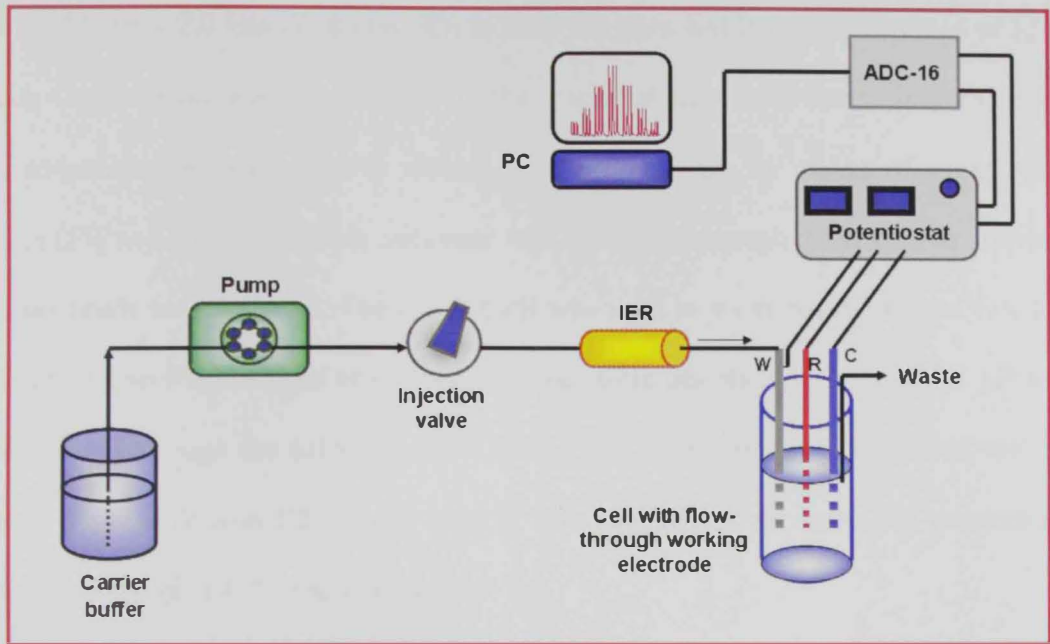


Figure 2.1: Schematic diagram of the FIA experimental setup for SA determination.

2.4.1 Preparation of the immobilized enzyme reactors (IER)

NANA aldolase and PO were co-immobilized on controlled pore glass (CPG) according to the literature method.^[96] Controlled pore glass particles (average pore size 500Å or 170 Å), obtained from Sigma chemical company, were packed into a glass column (70 mm x 2.0 mm i.d, 8 mm OD) to have the glass bed length in the range of 3.0–5.0 cm. Cotton plugs were used to secure the glass bed from both sides. Stainless steel tubes served as inlet and outlet to reactor fixed at both ends by means of epoxy. GA solution (5% v/v) in 0.1M sodium carbonate was circulated through the reactor to activate the glass beads for two hours. Then, 0.1M PB was used to wash out the excess GA for one hour. A specified amount of the two enzymes were dissolved in 2mL of PB pH 6.3 and circulated through the column for two hours. The excess enzymes were removed by washing the reactor with PB for one hour at flow rate of ~ 1 mL/min. The reactors as prepared were kept at 4 °C when not in use.

2.4.2 Preparation of the flow-through amperometric detector for FIA setup

Platinum tubes (1.32 mm ID, 1.47 mm OD, 99.9% metal basis, Alfa Aesar) of either 1.5 or 3.5 cm length polarized at 0.6V were used as a flow-through working electrode in the present work. The Pt tube was electrochemically cleaned by potential cycling between -0.25V and +1.25V vs Ag/AgCl in 0.5M H₂SO₄ at a scan rate of 50mV/sec. The details of the connection of the tubular Pt anode were shown in **Figure 2.2**. The Pt tube working electrode was placed along with the counter and reference electrodes in a plastic container where the effluent buffer accumulated till a certain height above which it was removed using the second channel of the peristaltic pump. The outer surface of the Pt tube and its electrical connection

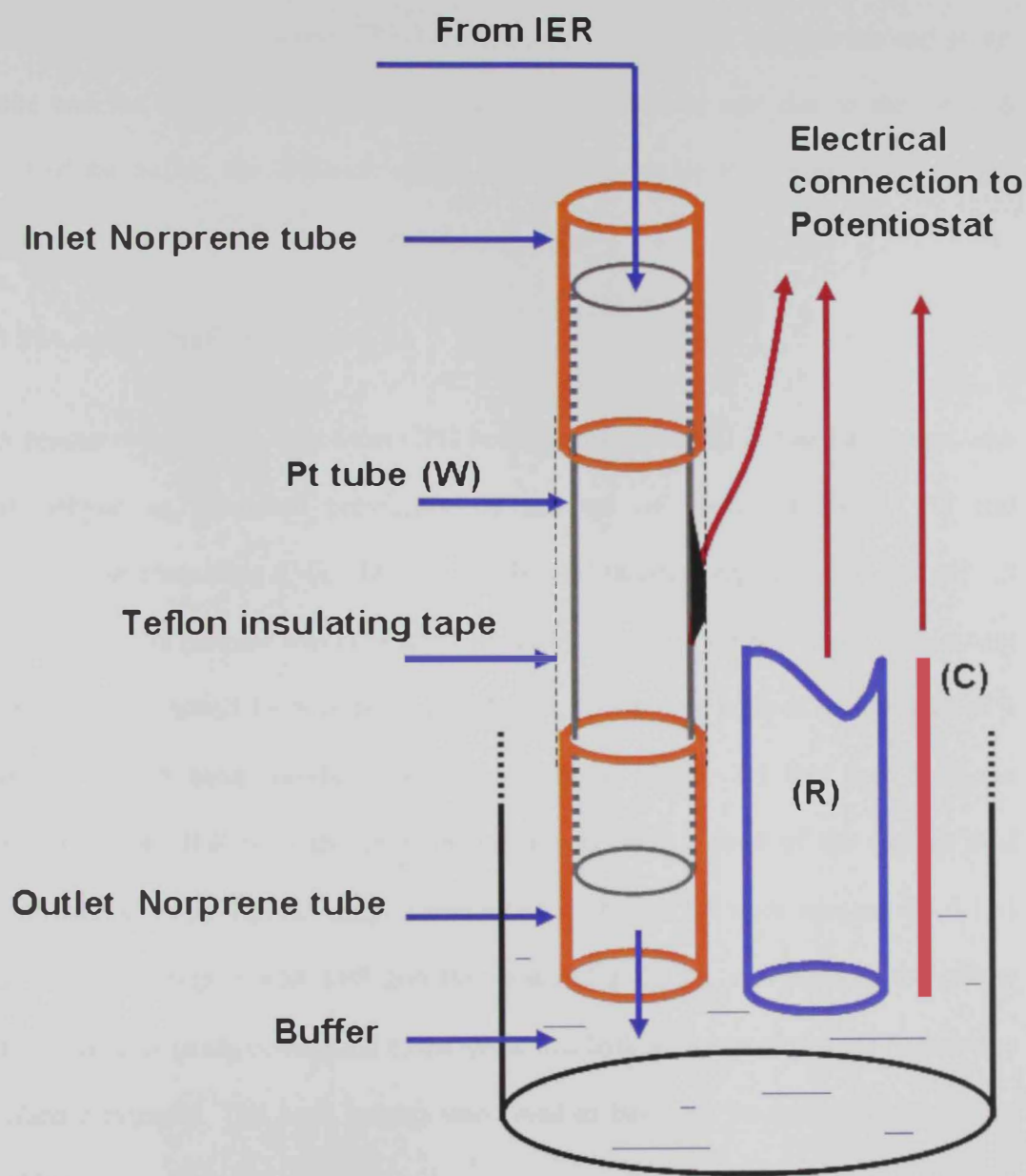


Figure 2.2: Detailed construction of the tubular Pt detector and the electrochemical cell.

wire were isolated from the solution using Teflon tape. A piece of a Noprene tube was connected to the end of the tubular detector (shown in **Figure 2.2**) was found to be essential to stabilize the baseline. This tube increased the distance between the end of the Pt tube and the effluent buffer accumulated in the container and due to the forward motion of the buffer, the diffusion of the hydrogen peroxide from previous injections back into the tubular anode was prevented.

2.4.3 FIA determination of bound SA

A reactor was packed with 4-cm CPG bed (average size 500 Å) and activated with glutaraldehyde as described previously. A mixture of NANA aldolase, PO and Neuraminidase containing 434U, 285.6U and 366.2U respectively in 2mL of PB pH 7.3 was prepared. The mixture was circulated through the column for two hours. The excess enzymes were removed by washing with PB pH 7.3 for one hour at a flow rate of 1 mL/min.. An FIA setup similar to that described in **Figure 2.1** was used with the exception that an IER with the three enzymes was used instead of the regular dual enzyme reactor. 50- μ L Epotin samples which contain bound SA were injected. PB 0.1 M of pH 7.3 containing 2 mM TPP and theromstated at 37 °C was used as the carrier solution. The FIA peaks correspond to the generated hydrogen peroxide were recorded as described previously. The peak heights were used as basis for the quantification of the bound SA.

2.5 Construction of SA biosensor

2.5.1 Electrochemical polymerization of *m*-PDA

Pt disc electrodes (2 mm in diameter and 6 mm body diameter, CH instruments, USA) were cleaned by polishing and electrochemical treatment as described previously. Then, poly(*m*-PDA) film, which acts as inner rejection layer for interfering species, was prepared by electropolymerization using cyclic voltammetry. The film was grown from a gently stirred aqueous solution containing 10 mM *m*-phenylenediamine in 0.1M PB pH 7.2. The potential of the Pt working electrode was cycled between +0.1 and +0.7V vs Ag/AgCl at scan rate 2 mV/sec for 12 cycles (2 hours).

2.5.2 Enzyme immobilization

Both of NANA-aldolase and PO were co-immobilized by crosslinking with glutaraldehyde and BSA. A 15- μ L aliquot of the given enzyme-BSA-GA mixture solution in PB was quickly pipetted onto the center of microporous polyester membrane (PE) (25 mm in diameter). The enzyme layer was allowed to reticulate and to dry in air at room temperature. Then, the PE membrane was fixed on top of the platinum electrode in such away that the enzyme layer faced the Pt electrode. This novel arrangement of the sensor design eliminated the problem of the enzyme layer adhesion to the surface of the Pt electrode transducer. SA biosensors prepared as such were kept at 4°C when not in use. The biosensor configuration is shown in **Figure 2.3**.

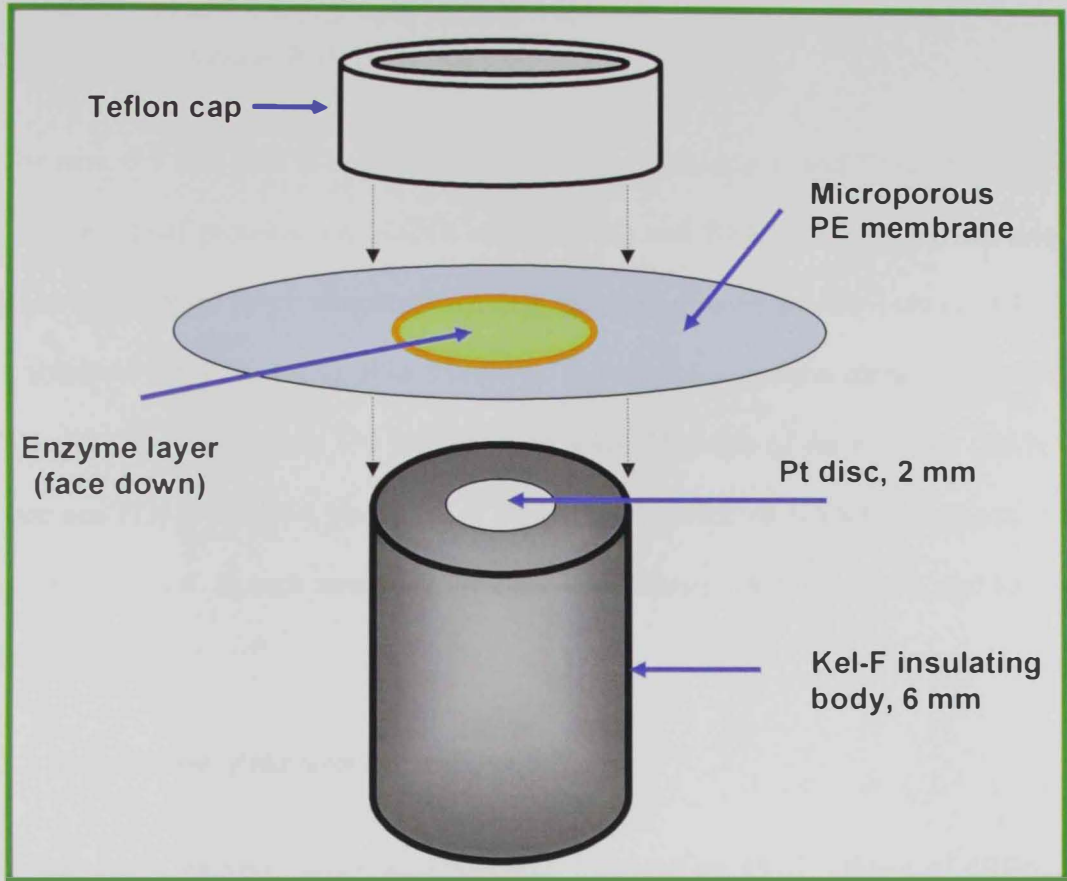


Figure 2.3: Construction of SA biosensor based on an immobilized layer enzyme layer onto microporous PE membrane.

2.5.3 Optimization of Enzyme layer

2.5.3.1 Effect of Glutraldehyde (GA)

The term G/T was used to compare the extent of crosslinking. G and T refer to the w/v % of GA and total proteins, i.e., NANA aldolase, PO and BSA. Three biosensors were prepared by pipetting 15- μ L aliquot of different enzymes mixture solutions obtained from stock solutions GA 0.9% (w/v), BSA 9% (w/v), and enzymes solution contains 4% (w/v) NANA-aldolase (99.2 U) and 6% (w/v) PO (65.4 U). The ratio of the enzymes (NANA aldolase and PO) to the BSA was fixed to be 1:1 and the ratio of NANA aldolase to PO was fixed at 1.5:1.0. In each sensor, G/T values were adjusted to 0.027, 0.048, and 0.075, respectively.

2.5.3.2 Optimization of the total enzymes ratio

In this study, enzyme layers were prepared by pipetting 15- μ L aliquot of different enzymes mixture solutions containing 2.8, 3.3 and 4.4 % (w/v) of total enzymes were the ratio of NANA aldolase to PO was fixed at 1.5:1.0 which was obtained from enzymes solution contains 4% (w/v) NANA-aldolase (99.2 U) and 6% (w/v) PO (65.4 U). The G/T was fixed to be 0.048 (0.3% w/v). The total protein content (NANA, PO and BSA) was fixed to be 6.3% (w/v) which was adjusted by adding suitable volumes of BSA solution 9% (w/v).

2.5.3.3 Optimization of Enzyme layer thickness

A mixture of the two enzymes and BSA was prepared with the total enzymes content of 3.3% (w/v) (NANA aldolase and PO in 1.5:1.0 ratio) and BSA 3% (w/v). The G/T ratio was kept at 0.048. Different aliquots of the enzyme-BSA-GA mixture (10, 15 and

20- μ L) were pipetted on top three different PE membranes. The enzyme layers were allowed to dry and used in the biosensor construction as described above.

2.5.4 Effect of temperature and pH on the response of SA biosensor

Three similar biosensors were prepared by pipetting 15- μ L aliquot of enzyme mixture of composition 2.2, 1.1, 3.0 and 0.3% (w/v) NANA aldolase, PO, BSA and GA, respectively and G/T factor of 0.048. The sensitivity of these biosensors constructed with such enzyme layer was evaluated at different temperatures, i.e., 25, 30, 34 and 37 °C. The experiments were carried out using 5-mL aliquot of PB pH 7.2 containing 2 mM of TPP. The sensitivity of the same electrodes was tested under different pH values in the range of 5.6-8.5 at 37 °C.

2.5.5 Stability and selectivity of SA biosensor

Two batches of three biosensors each were prepared using the enzyme layer described in the previous section and PE membranes (pore size 1 μ m). The stability and the sensitivity of the two batches were tested for two weeks at both optimum pH and temperature. The sensors were kept in at 4°C when not in use. The interference caused by the AA, AAP and UA was checked with and without the inner electropolymeric layer. The efficiency of the poly(*m*-PDA) inner layer to reject the interfering species was checked for two weeks.

2.5.6 Amperometric Measurements

A conventional three-electrode system was used for all amperometric batch measurements. A Pt wire served as the counter electrode and an Ag/AgCl electrode as the reference electrode. The sensor was polarized at +0.6V. All the experiments were performed in a 10-mL double-jacket-thermostated cell containing a magnetically stirred 5mL PB containing 2 mM TPP at 37°C. The background current was allowed to stabilize before SA addition. The generated current was recorded as described previously.

2.5.7 SA measurements in protein solution and biological samples

To mimic serum samples, a 5% w/v BSA solution containing 2 mM SA, 0.2 mM AA, 0.2 mM AAP and 0.2 mM UA in 0.1M sodium bicarbonate pH 7.4 was prepared. The response of SA biosensor to this complex solution was compared with the response to 2 mM SA in simple PB.

Erythropoietin samples (Epotin) were tested for the bound SA. The hydrolysis of SA was carried out by the addition of enough amounts of neuraminidase and then the liberated SA was measured. Blood sample for a healthy volunteer and a serum sample for a cancer patient were also tested for free and bound SA. These samples were kept in anticoagulant tubes. The bound SA in the blood and serum samples was hydrolyzed by adding enough amount of neuraminidase.

2.5.8 Immobilization of the two enzymes using chitosan and ultra-bind membrane

Chitosan membrane prepared by solvent evaporation method^[89] was used to co-immobilize NANA and PO. A 0.3% Chitosan solution was prepared in 3% w/v acetic acid. A 20- μ L aliquot was taken from the solution and placed on a PE membrane (pore

size 1 μ m) and left to dry at 65°C. Upon drying the membrane is neutralized with a 50- μ L aliquot of 5 mM sodium hydroxide and the excess sodium NaOH was washed off using 0.1M PB. A 50- μ L aliquot of enzymes solution contains 30 U of NANA-aldolase and 19.5 U of PO, were added and left for drying at room temperature. Then, a 50- μ L aliquot of 0.01% GA added to the membrane for crosslinking and left for one hour. The excess GA was washed off using 0.1M PB pH 7.3. Another 50- μ L aliquot of enzymes solution was added and left for drying and excess enzymes was washed off.

A third approach for enzyme immobilization was tested as well. This approach based on the Ultrabind membranes which have aldehyde groups. Circular sections of Ultrabind membrane were simply soaked in a mixture of the two enzymes in PB pH 7.0 overnight at 4 °C for enzyme immobilization.

CHAPTER III

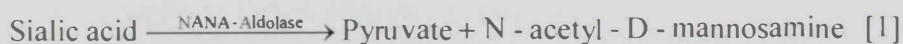
RESULTS AND DISCUSSIONS

3. Results and Discussion

3.1. The dual enzyme system

The concept of using a tandem of two or more enzymes, which act on a given target, analyte to produce (or uptake) a more detectable compound (or ion) has been utilized in the construction of several biosensors and enzymatic analytical systems.^[76] Among several possible intermediates, pyruvate has been a frequent intermediate species produced by the action of the first enzyme. This normally suggested the second enzyme as either Lactate dehydrogenase^[53] or more commonly pyruvate oxidase (PO).^[50, 52] Several reports utilized different enzymes such as phytase,^[97] citrate lyase -oxaloacetate decarboxylase couple,^[98] ornithine carbamyl transferase,^[99] L-alanine dehydrogenase,^[100] amino acid oxidase,^[101] octopine dehydrogenase^[102] coupled with PO to construct biosensors for phytic acid, citrate – isocitrate, alanine, and octopine. Moreover, PO has been co-immobilized with NANA-aldolase to construct analytical system for SA.^[50-53] The generated hydrogen peroxide in this system was measured colorimetrically.

Despite of the analytical usefulness of the NANA-aldolase-PO dual enzyme system^[50-53] for the quantitation of SA, up to the author knowledge that this system has not been utilized in the construction of any biosensor for direct SA determination so far. Hence, the primary objective of this project was to develop the first enzyme biosensor based on NANA-aldolase-PO dual enzyme system. The sequence action of these two enzymes is as follow



Anodic oxidation of the generated hydrogen peroxide offered the basis for quantification for SA biosensor. Although, the ultimate goal was to construct SA biosensor, this project was carried out in three subsequent phases with an individual objective for each phase. These phases are: (i) investigation of the NANA-aldolase-PO system and to check its suitability for the amperometric transduction mode using simple homogenous enzyme catalysis; (ii) Design, construction and optimization of a flow injection system based on a co-immobilized NANA-aldolase and PO in an enzyme reactor for FIA determination of SA; and (iii) final construction and optimization of prototype SA sensor and the verification of its analytical utility. The realization of each of the as described individual objectives is discussed in details in the following sections.

3.2 Investigation of the optimization of the condition

In this initial study, the effect of different variables were investigated using simple homogenous enzyme catalysis, i.e., enzymes were soluble in the aqueous sample. In addition to the advantage of being simple, addition of enzymes in soluble form eliminated any possible variations in any series of experiments due to the immobilization step itself. This initial study was of particular importance for the following reasons: (i) to check the activity and stability of the purchased enzymes, (ii) to explore the feasibility of hydrogen peroxide detection under the experimental conditions optimum for the enzymes; and (iii) to investigate all the experimental variables, which affect the overall activity of the dual enzyme system and/or the anodic detection of hydrogen peroxide. The outcome of such initial study utilized in the subsequent phases of this project will be discussed later.

3.2.1 Effect of buffer type on the generated current signal

The effect of buffer type was investigated using phosphate and MOPS buffers. All other variables, i.e., temperature, pH, enzyme activity, cofactor concentration were fixed at arbitrarily reasonable values comparable to some literature relevant results.^[103-104] The obtained rate curves were plotted in **Figure 3.1** and showed that the generated anodic current was about 6 times higher than that obtained in MOPS buffer. Hence, PB was used throughout the remaining work.

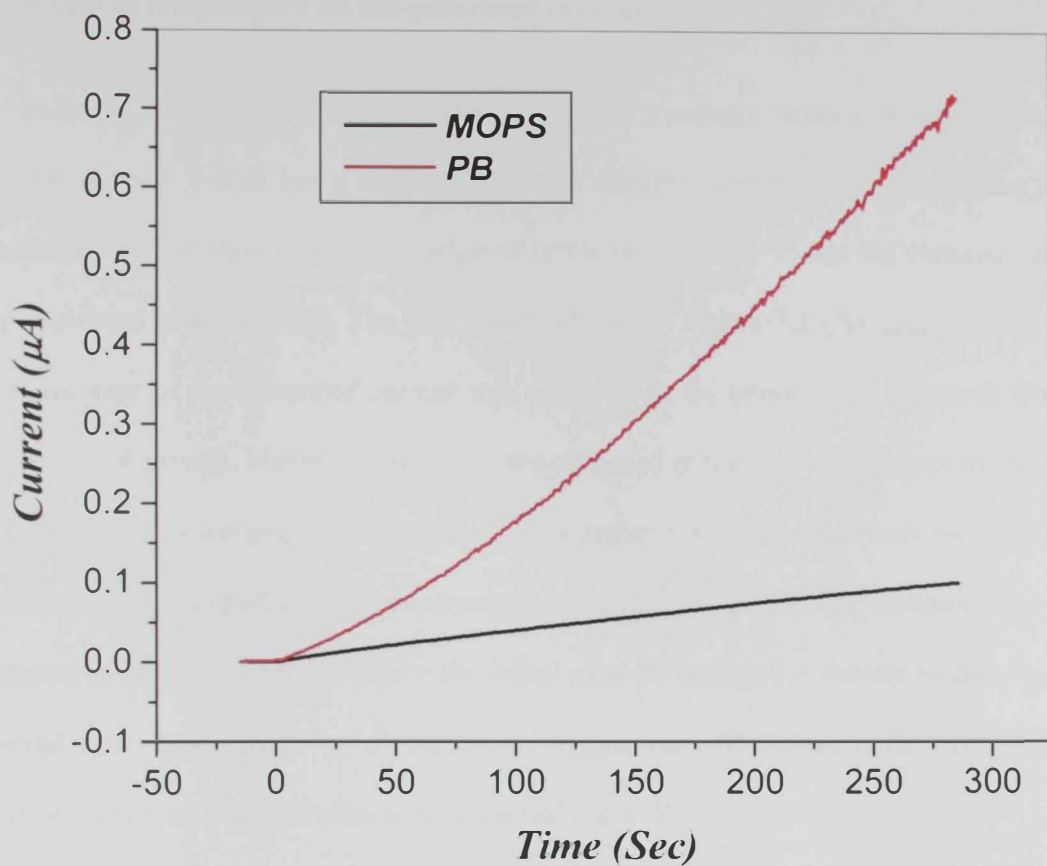


Figure 3.1: Effect of buffer type on the generated anodic current. pH 7.2, temperature: 28 °C, SA: 1.5 mM, TPP: 0.5 mM, NANA-aldolase: 0.81 U/ml, PO: 0.82 U/ml.

3.2.2 Effect of temperature on the generated current signal

Similar to chemical reaction, the rates of enzyme reactions increase with increasing temperature; with a limit being set by the thermal stability. The effect of temperature on both sensitivity and stability was investigated in the range 10-58 °C and the obtained data were presented in **Figure 3.2**. The rate curves shown in Figure 3.2 (A) indicated that a steady increase of the generated current was observed as the temperature increased from 10 to 37 °C. Although, higher initial rates were observed at higher temperatures (up to 50 °C) the stability of the enzymes was less at such higher temperatures as indicated by the decrease of the generated current at temperatures higher than 37 °C. This observation was illustrated in Figure 3.2 (B), in which the initial rates as well as the current signals were observed after 200 seconds as a function of temperature. Therefore, unless otherwise stated, all subsequent measurements were carried out at 37 °C.

3.2.3 Effect of TPP cofactor concentration

The effect of TPP concentration was investigated in PB of pH 7.2 at 37 °C. The data obtained was presented in **Figure 3.3**. The anodic current signal was increased with TPP concentration up to ~ 0.5 mM with a little further enhancement at higher TPP concentration. A similar effect of TPP was observed with MOPS (data not presented). Hence, TPP was added to the buffer solution at 0.5 mM throughout the subsequent work. A small reduction in the current signal was observed when TPP cofactor of more than 3 days old was used. Hence, TPP was prepared freshly every 2-3 days.

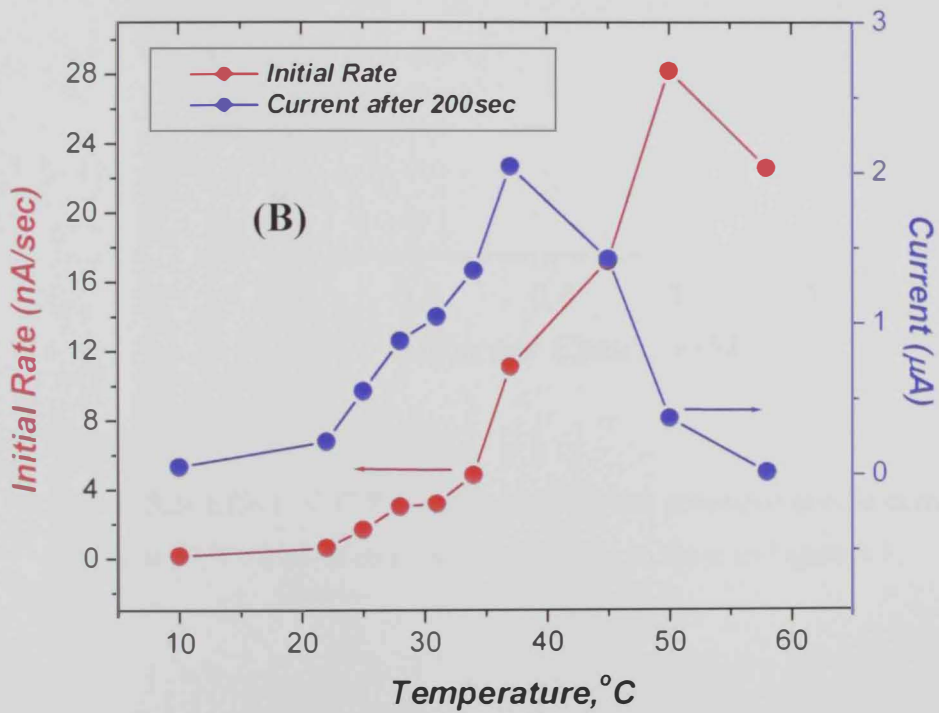
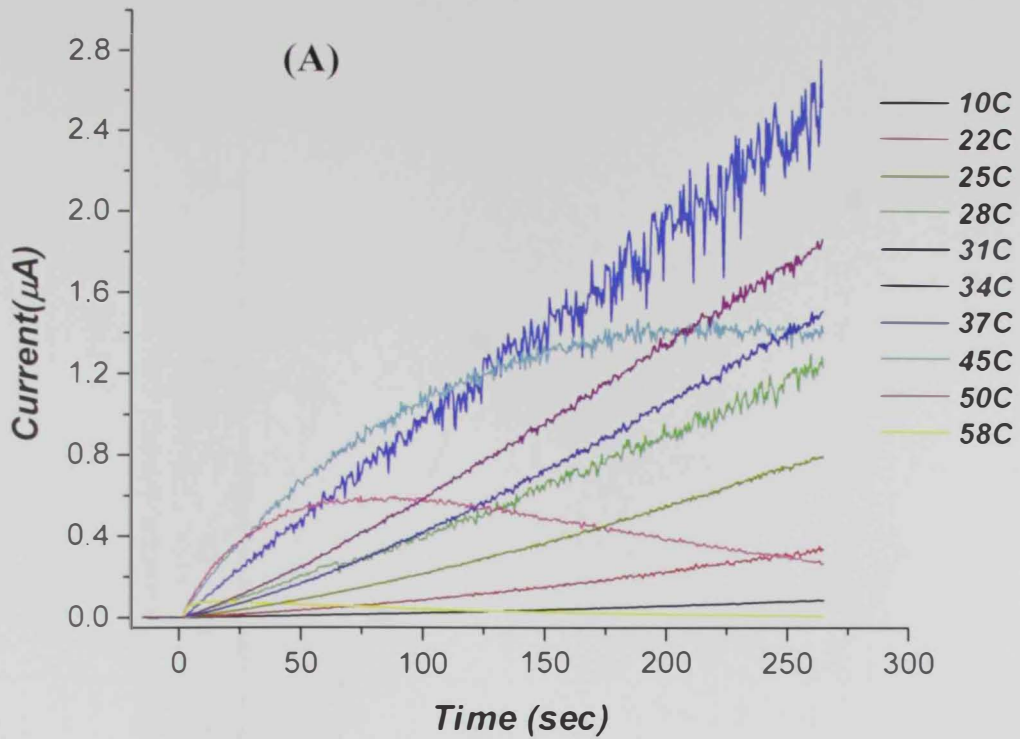


Figure 3.2: Effect of temperature on the generated anodic current. PB pH 7.2, SA: 1.5 mM, TPP: 0.5 mM, NANA-aldolase: 0.81 U/ml, PO: 0.82 U/ml. A: Rate curves; B: initial rates and the generated current values after 200 sec.

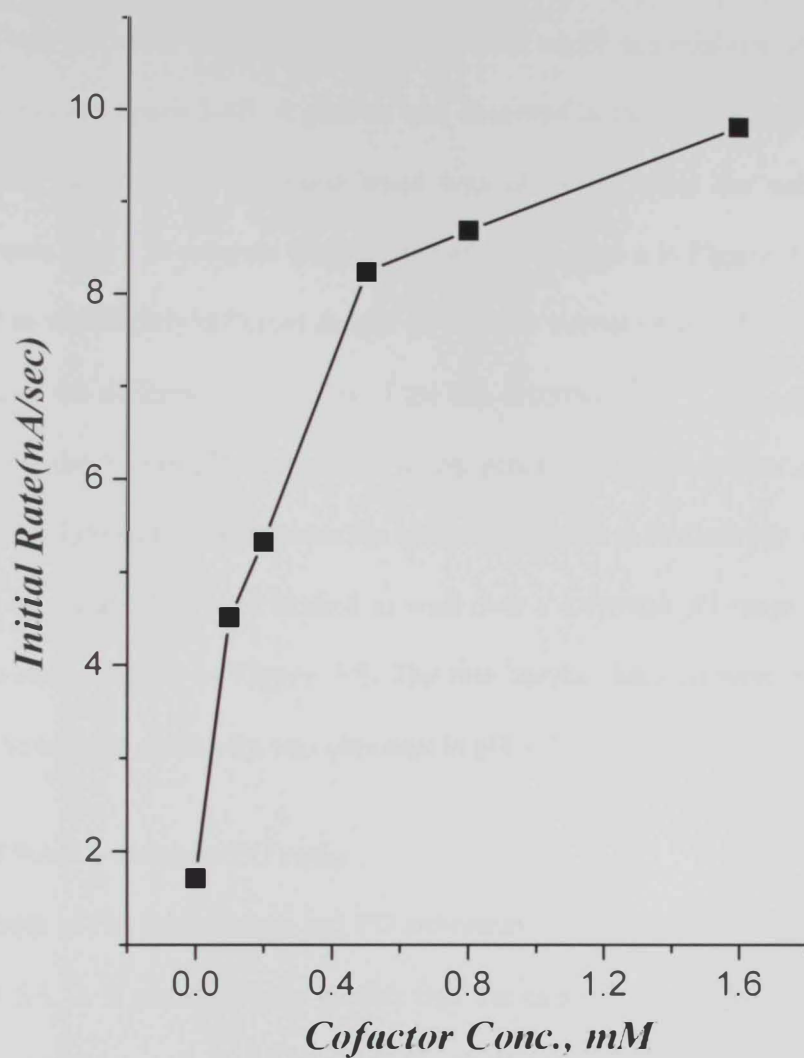


Figure 3.3: Effect of TTP concentration on the generated anodic current. PB pH 7.2 at 37 °C. Rest of conditions are similar to those in Figure 3.1.

3.2.4 Effect of pH on the generated current signal

The rate curves obtained in sixteen different PBs of pH values in the range of 4.5-8.5 were obtained and plotted in **Figure 3.4**. The initial rate, which is a measure of sensitivity, was plotted vs. pH in **Figure 3.4B**. A plateau was observed in the pH range of 5.6-6.3. A slightly different pattern with the same trend was observed when the values of the generated currents after 150 seconds were plotted vs. pH as shown in **Figure 3.4 (B)**. This was attributed to the slightly different shapes of the rate curves obtained at different pH values because of the different pH profiles of the two enzymes.^[103-104] It is appropriate to mention here that the overall pH dependence of the generated anodic current is attributed in part to the variations of hydrogen peroxide oxidation current at Pt electrode with pH.

The effect of pH at 37 °C was studied as well over a narrower pH range around the optimum pH value obtained in **Figure 3.5**. The rate curves obtained were presented in **Figure 3.5**. The highest sensitivity was obtained in pH 6.3.

3.2.5 Effect of NANA-aldolase/PO ratio

Although both of NANA-aldolase and PO are essential for the generation of hydrogen peroxide from SA, it is reasonable to predict that the ratio of the enzymes will have a dramatic effect on the current signal. It was also predicted that either very small or very large activity ratios would lead to small currents due to the limiting effect of one of the enzymes, respectively. Therefore, this study was carried out using NANA-aldolase/PO activity ratio in the range of ~ 0.25-2.0. The data obtained (**Figure 3.6**) indicated that the current signal increased with increasing NANA-aldolase/PO ratio and a plateau was observed at ratios greater than 1.5. Therefore, this ratio was used throughout the subsequent work unless otherwise stated.

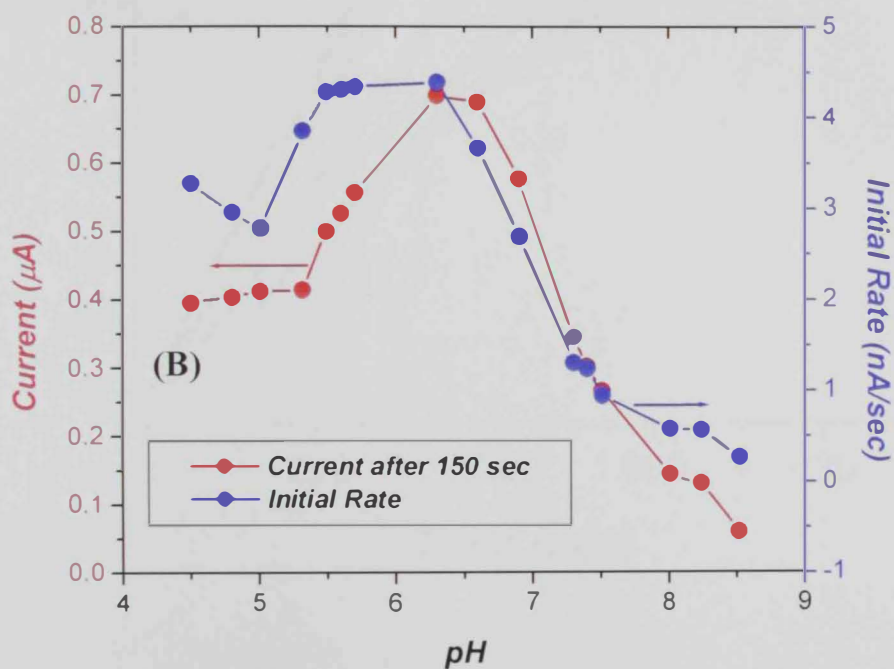
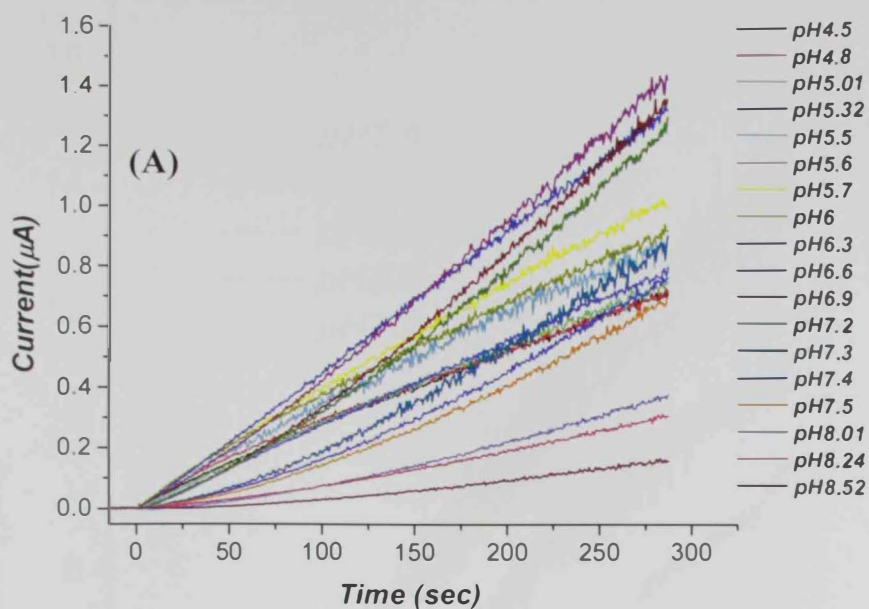


Figure 3.4: Effect of pH of the PB on the generated anodic current (A). at 28 °C, SA: 1.5 mM, TPP: 0.5 mM, NANA-aldolase: 0.646 U/ml, PO: 0.654 U/ml. (B) Initial rates and current values after 150 sec calculated from the data presented in (A).

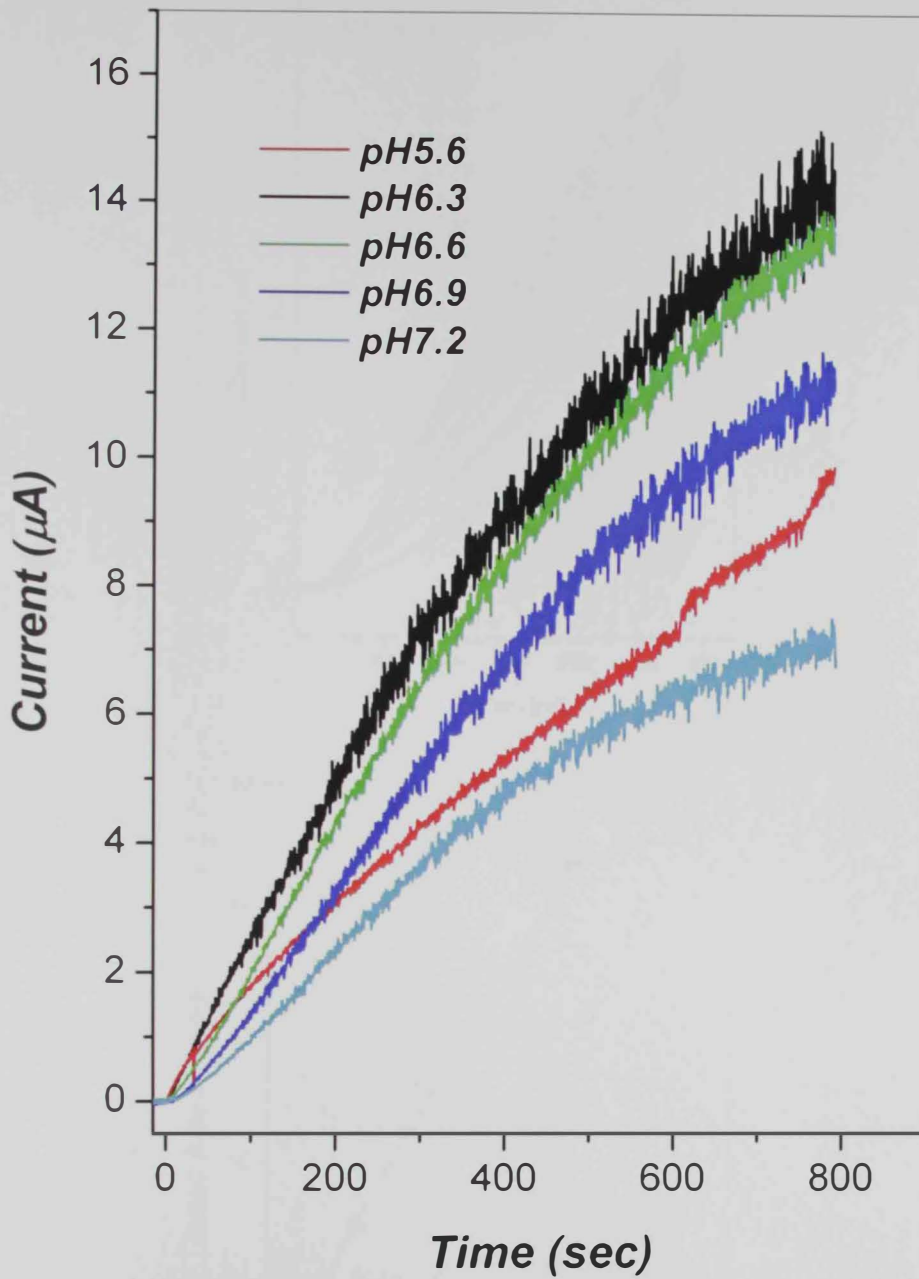


Figure 3.5: Effect of pH of PB on the generated anodic current curves at 37 °C. Rest of conditions are similar to those used in Figure 3.4.

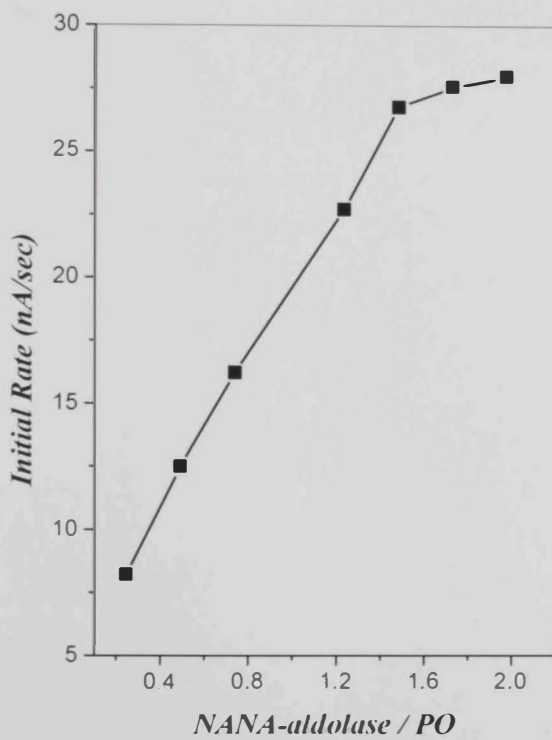
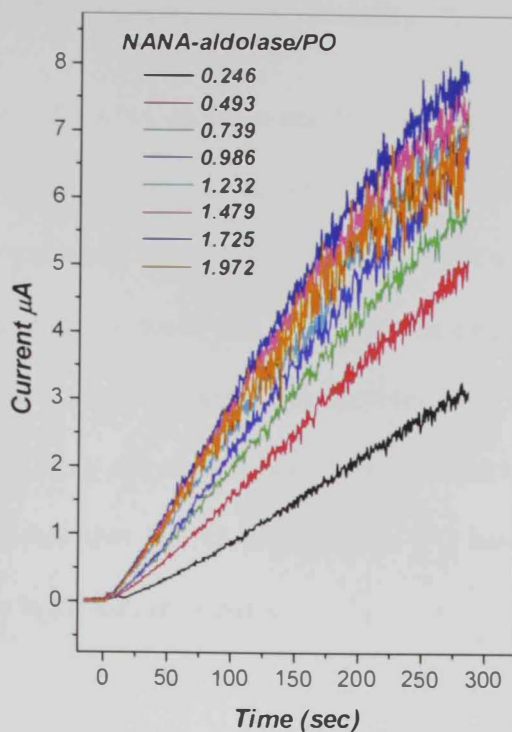


Figure 3.6: Effect of NANA-aldolase/PO activity ratio on the generated anodic current in PB pH 7.2 at 37 °C. TPP: 0.5 mM and SA 1.5 mM.

3.2.6 Evaluation of the NANA-aldolase and PO stability

To evaluate the stability of NANA-aldolase and PO dissolved in 0.1 M PB pH 7.2 and stored at -20 °C, four experiments were carried out as follows: (i) both enzymes are fresh; (ii) both enzymes are one week old; (iii) fresh PO and one week old NANA-aldolase; and (iv) fresh NANA-aldolase and one week old PO. The data obtained were presented in **Figure 3.7**. The current signal obtained with both enzymes were one week old was 50% of the signal obtained with fresh enzymes under identical experimental conditions. The last two experiments indicated that NANA-aldolase and PO have different stability as indicated by the difference in the current signals.

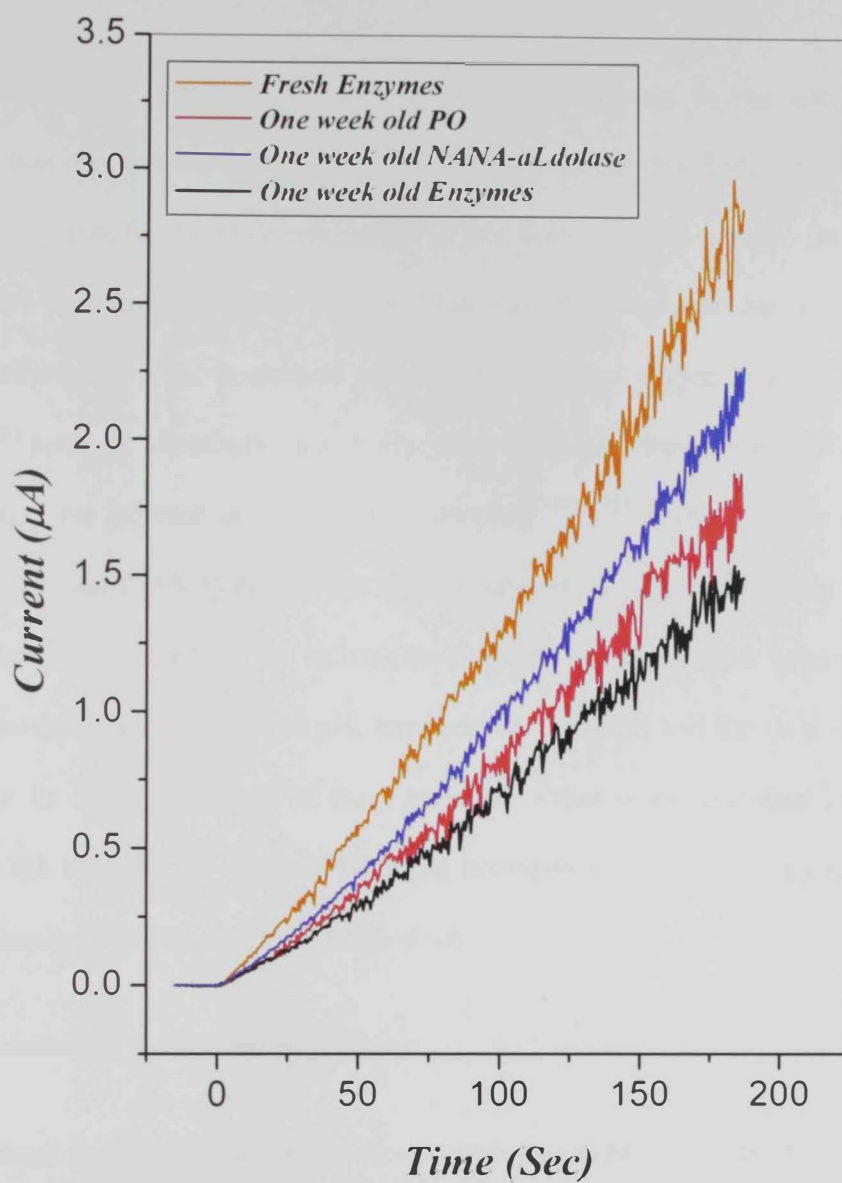


Figure 3.7: Stability of NANA-aldolase and PO enzymes. Rate curves generated in PB pH 7.2 at 37 °C. SA 1.5 mM, TPP 0.5 mM, NANA-aldolase 0.81 U/mL, PO 0.82 U/mL.

3.3 Flow injection analysis of SA

The feasibility of coupling the NANA-aldolase-PO system to the amperometric transduction was demonstrated in the previous section to utilize this finding to construct a flow injection system for direct determination of SA; both enzymes were co-immobilized in a controlled-pore glass in a tube reactor. This was attempted because of the several advantages offered by FIA, in general and the immobilized enzyme reactors (IER) in particular^[105] such as simplicity, feasibility, high sampling frequency and degree of automation and low expense of reagents and samples,^{[106],[107]} Several factors can affect the sensitivity of such FIA system. Such factors include (i) sensitivity of the hydrogen peroxide detector; (ii) activity of the enzyme reactor; (iii) injected sample volume, and (iv) other experimental variables such as pH, temperature, cofactor, and the flow rate of the carrier buffer. In this study, each of these variables either were optimized or selected according to the conclusions obtained from the homogenous catalysis study to enhance the overall sensitivity of FIA determination of SA.

3.3.1 Optimization of the platinum detector

Flow-through hydrogen peroxide electrode can be assembled in different geometries. However, the most obvious choice was to use a platinum disc electrode positioned in a suitable flow cell. This arrangement provided reasonable hydrogen peroxide sensitivity. To further enhance the sensitivity, a Pt tubular detector was suggested as a detector for hydrogen peroxide. Tubular detectors have been used as electrochemical detectors in HPLC and capillary liquid chromatography systems,^[108-109] as they can be either amperometric or potentiometric detectors.^[110] Although, it is generally accepted that increasing the electrode area does not enhance the signal/noise ratio,^[111] a different

conclusion can be made in case of FIA because non-steady state signals are measured and electrodes with larger surface areas will exhaustively oxidize hydrogen peroxide and produce larger signals. In batch measurements, such large electrodes which are capable of exhaustive electrolysis of the sample are not expected to give steady-state signal – (especially at low analyte concentrations) because of the fast analyte depletion. This should not be of concern in FIA because transient (non steady state signals) are measured anyway.^[105]

This prediction was validated by injecting different hydrogen peroxide concentrations in the flow system equipped with Pt disc electrode and tubular Pt electrode, respectively. The obtained FIA peaks (**Figure 3.8**) with the Pt tubular detector were much more sensitive than those obtained with Pt disc electrode. This conclusion was further confirmed by the fact that Pt tubular detector of shorter length exhibited lower sensitivity, as will be discussed below. Based on this finding, Pt tubular detectors were used throughout the subsequent work to enhance the sensitivity of hydrogen peroxide detection.

3.3.2 Optimization of the experimental conditions and the IER

The next important step was to optimize the construction of the IER and the experimental conditions to achieve the highest possible sensitivity. To do so, different variables were explored such as (i) length of the IER; (ii), the pore size and the amine loading of the commercial CPG and the amount of the added enzymes; and (iii) the other FIA system variables. The data presented in **Figure 3.9** show the effect of the carrier flow rate on the peak current. As the flow rate was decreased both of the sensitivity and the peak time increased. The increased sensitivity can be attributed to the longer time available for the enzymatic reaction as the sample passes through the IER as well as the

enhanced detector signal observed at slower flow rate and thus because of the longer time available for the detector to oxidize H_2O_2 . Therefore, flow rate can be selected depending on the required selectivity and the sampling frequency.

Data presented in **Figures 3.10** and **3.11** shows the comparison of the detection sensitivity of the same IER with two Pt tubular detectors of different lengths. The longer detector exhibited about 20% higher sensitivity. However, in each case a linear calibration plot for SA was obtained over the tested range of 1-30 mM.

The reproducibility of the peak height obtained with the FIA system employing the 1.5- and 3.5-cm Pt tubular detectors was assessed by successive injection of 30 and 5.25 mM SA for 20 times, respectively. The data presented in **Figure 3.12** showed coefficient of variation (Standard deviation/mean) for the peak height equal to 1.4 and 0.75%, respectively. The higher precision obtained with the longer Pt tubular detector could be attributed for the longer sample residence time which was responsible for the higher sensitivity as well.

To further enhance the sensitivity of FIA determination of SA to sub-millimolar level, a longer IER (i.e., 5-cm long) was prepared. In this case, larger amount of each enzyme, i.e., 500 U NANA-aldolase and 400 U PO were used as. In addition, a larger sample injection loop (200 μ L) was employed. The combined effects of these three variables resulted in 285% enhancement of the sensitivity as shown in **Figure 3.13**. It is worth mentioning that the reported relative sensitivities achieved with different experimental condition were based on the ratios of the slopes of the relevant calibration graphs.

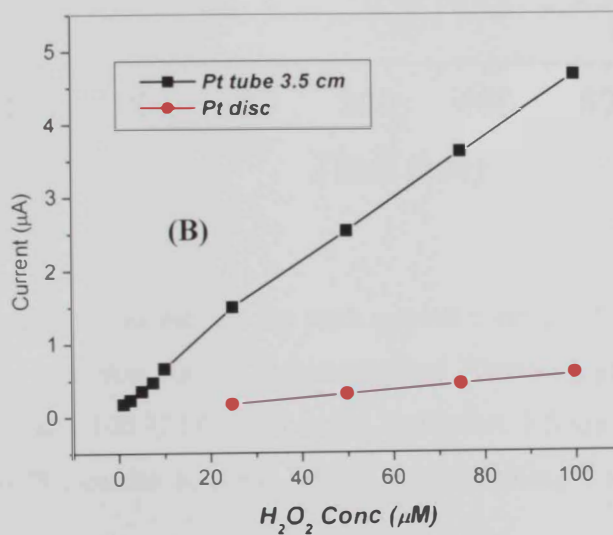
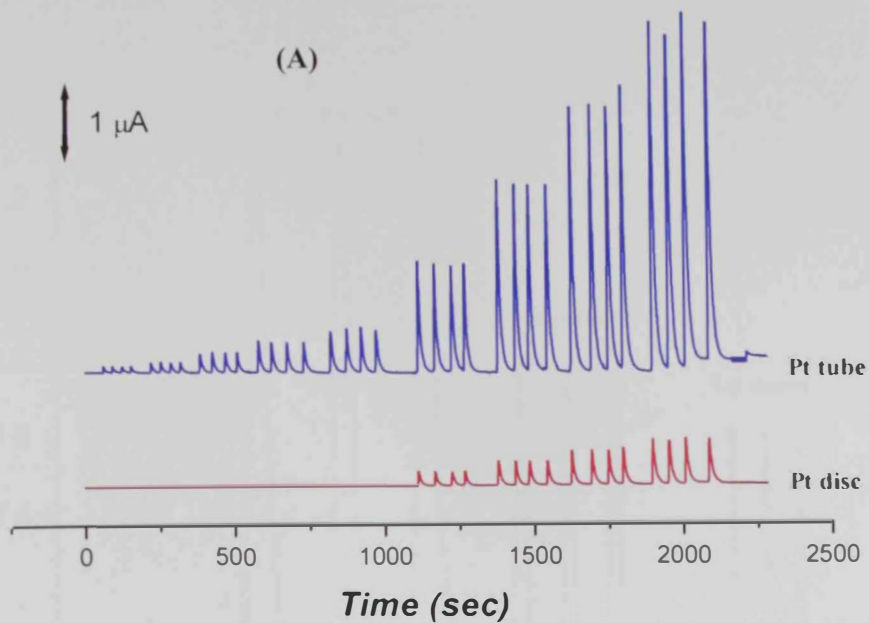


Figure 3.8: Comparison between the Pt disc and Pt tube (3.5 cm in length) electrodes as detectors in FIA detection of hydrogen peroxide. A: FIA peaks; B: peak heights plotted against H_2O_2 concentration. PB pH 7.0 used as carrier solution: Applied potential 0.6 V.

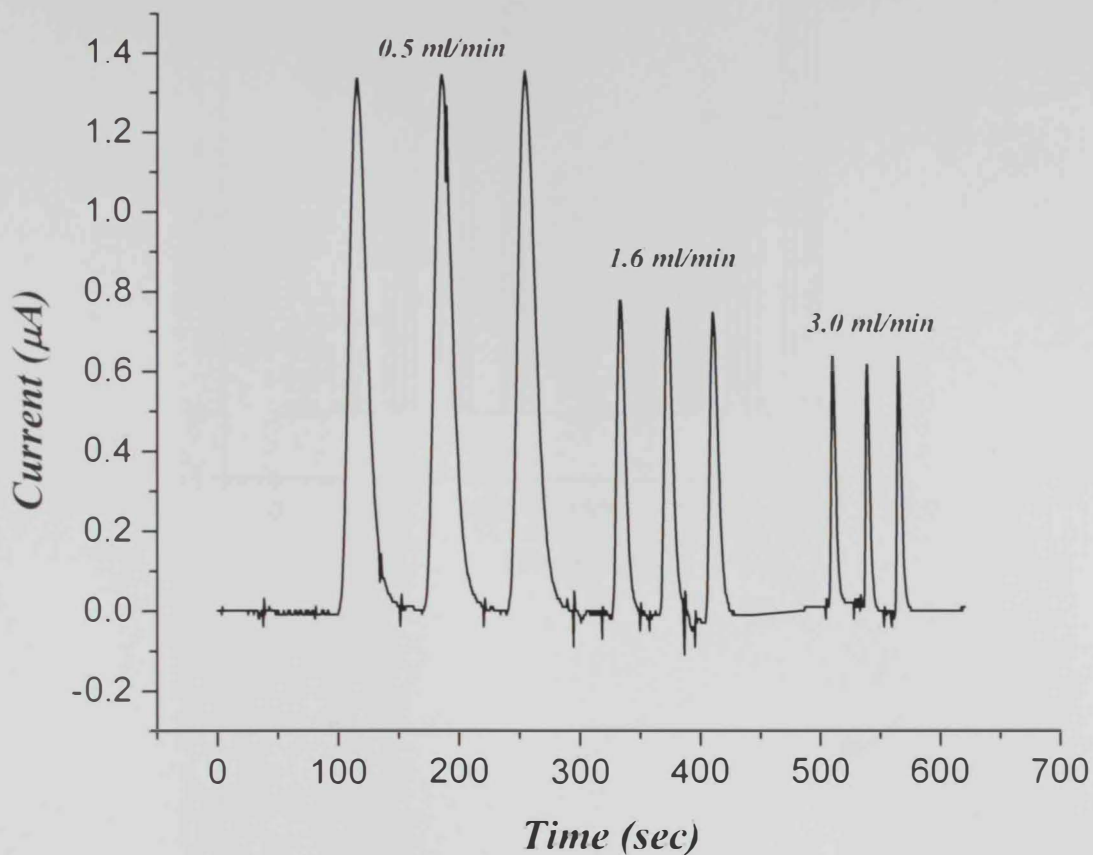


Figure 3.9: Effect of carrier flow rate on the peak current correspond to 5.25 mM SA. 3-cm IER (CPG, average pore size 500 Å, Amine content 70mmol/g glass) activated with 150 U NANA-aldolase and 100 U PO used in the activation. 1.5-cm Pt tubular detector polarized at 0.6 V, 34 °C, carrier solution PB pH 6.3 containing 1 mM TPP, Injection loop volume 50µL.

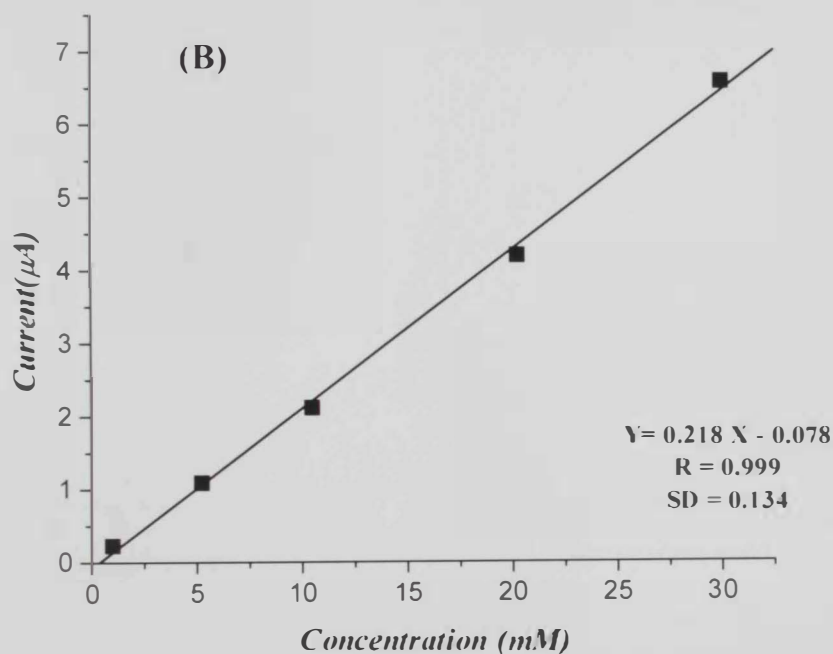
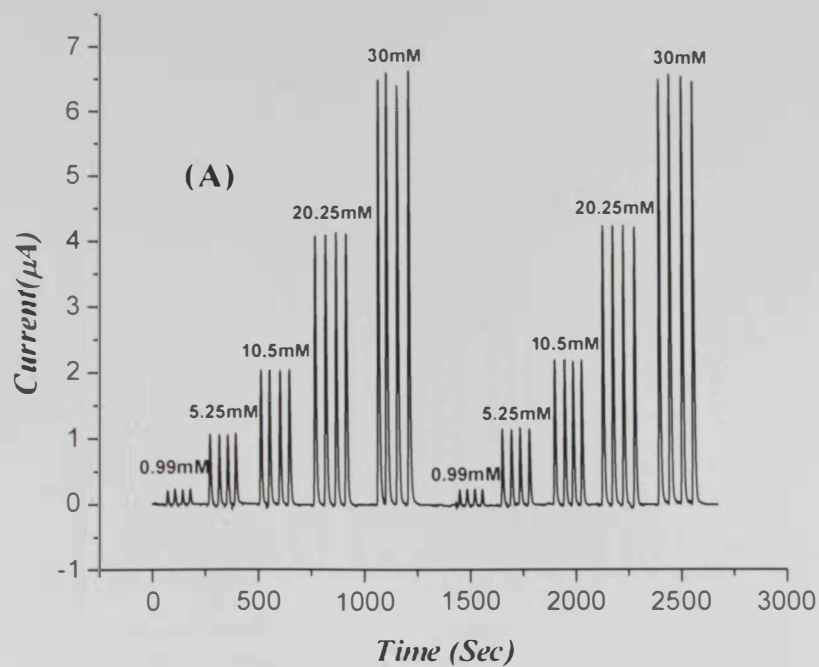


Figure 3.10: FIA peaks (A) and calibration curve (B) obtained 1.5-cm Pt tubular detector polarized at 0.6 V and Flow rate 1.6ml/min. The rest of conditions are similar to those mentioned in Figure 3.9.

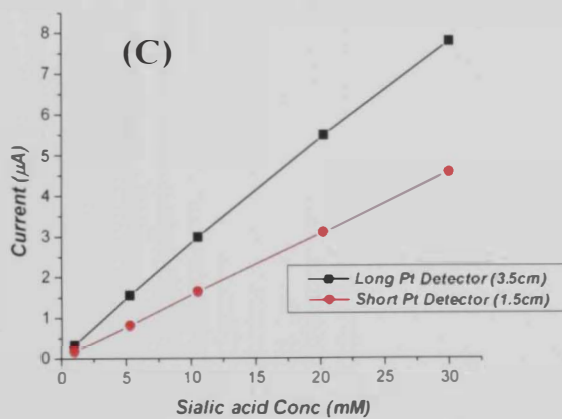
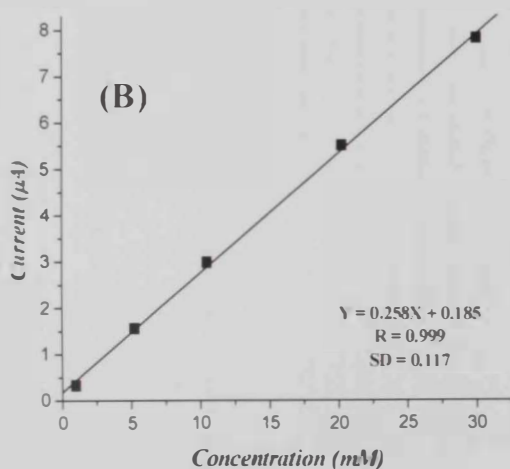
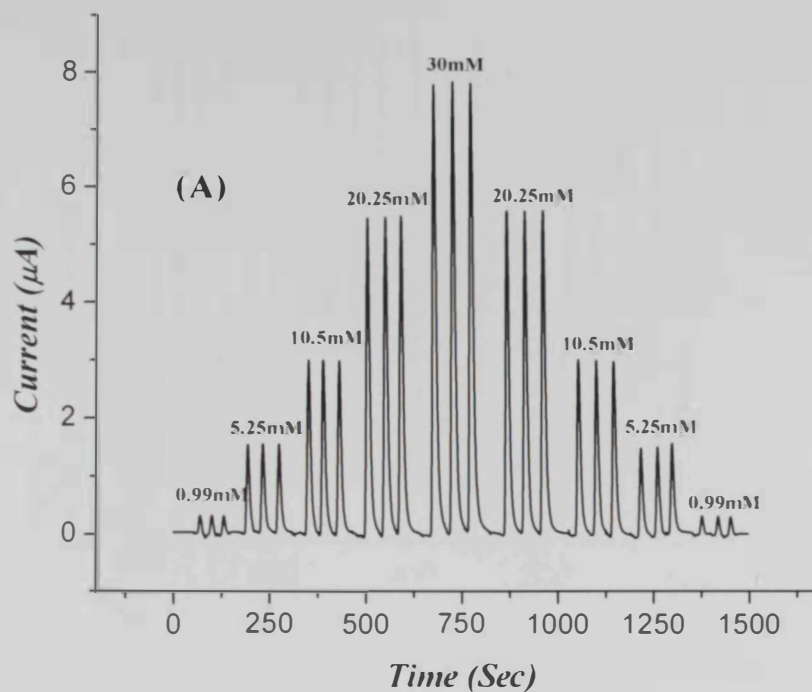


Figure 3.11: FIA peaks for SA (A) and calibration curve (B) using 3.5-cm Pt tubular detector flow rate 1.6 ml/min. The rest of the conditions are similar to those mentioned in Figure 3.9. (C) comparison between the sensitivities obtained with both detectors.

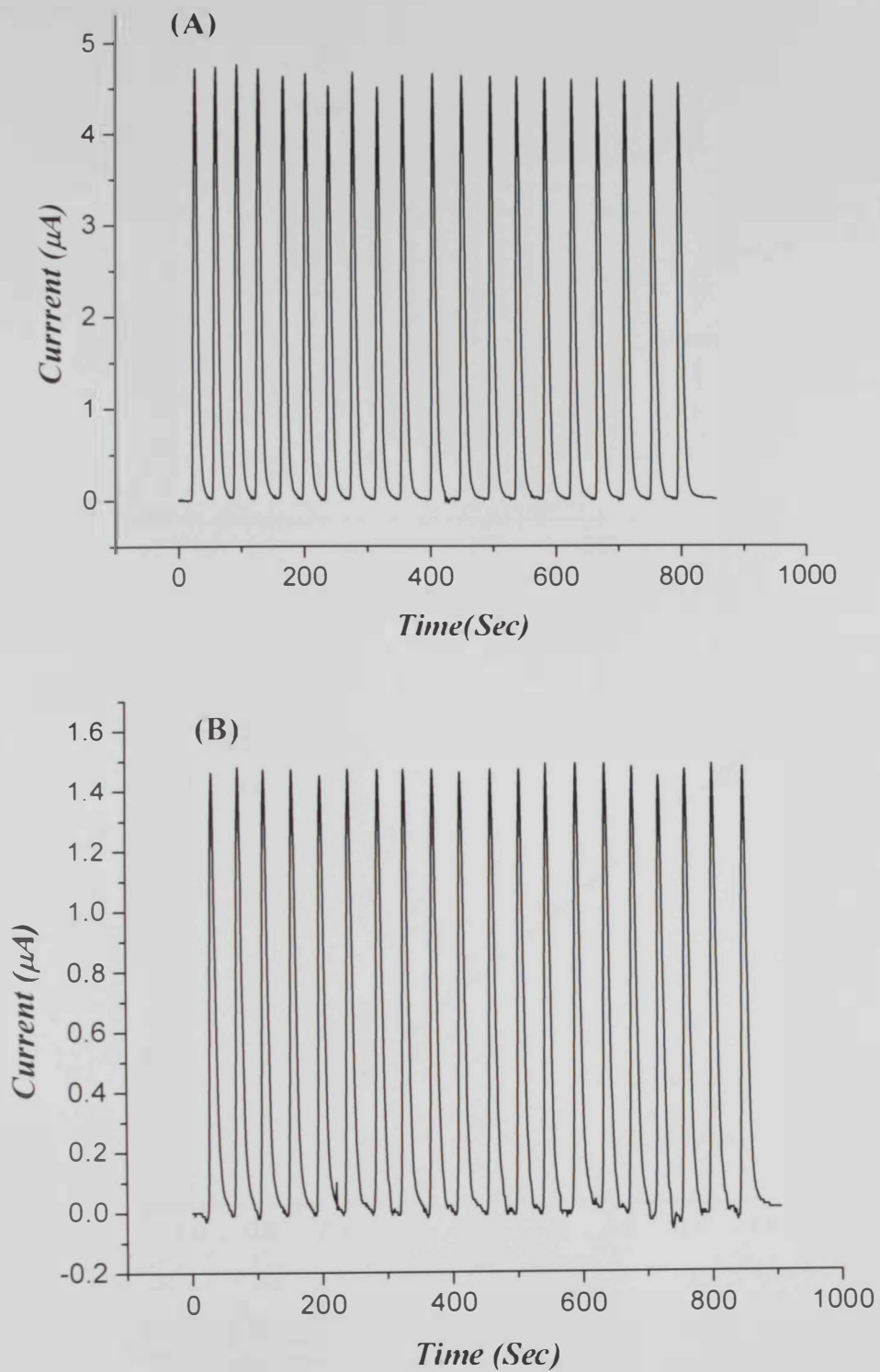


Figure 3.12: Reproducibility of the FIA peak heights for SA injection. The same setup described in Figure 3.10 (A) and 3.11 (B) using 30 and 5.25 mM SA, respectively.

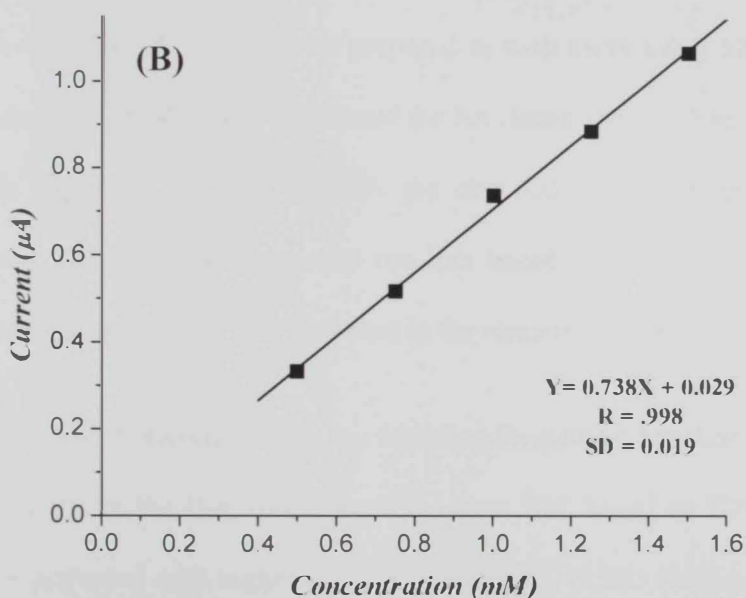
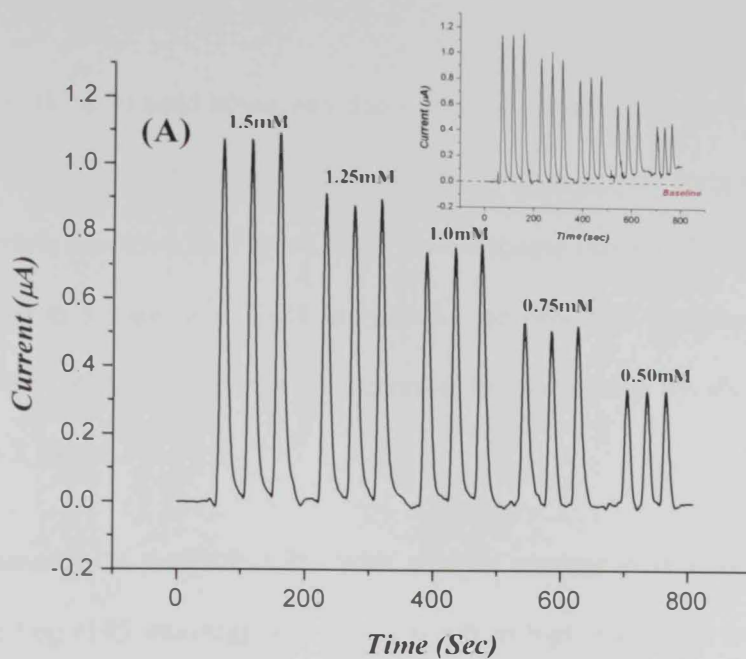


Figure 3.13: FIA peaks (A) and calibration plot (B) obtained with 5-cm IER loaded with higher amount of enzyme and 3.5-cm detector, loop size 200 μL , flow rate 1.6 ml/min. The rest of conditions are similar to those mentioned in Figure 3.9. Insert in (A) represents the original data prior to baseline correction.

Unfortunately, the enhanced sensitivity due to the increased length of the reactor and the increased size of the injection loop was associated with relatively long recovery time and drifting baseline as shown in **Figure 3.13**. To overcome this problem, the flow was increased from 1.6 to 3.0 mL/min. Such increase in the flow rate partially resolved the resolved the tailing problem, however it decreased the sensitivity by about ~ 11% as shown in **Figure 3.14**.

Another commercially available CPG with smaller average pore (170 Å) but with higher amine loading (145 mmol/g) that would result in higher enzyme immobilization was also tested. However, reactors prepared with such type of CPG imposed very high pressure in the flow system. Therefore, a 1:1 mixture of the two types of the CPG was used to prepare a new IER. A 3-cm reactor prepared in such away using 500 and 400 of NANA-aldolase and PO, respectively was tested for SA determination. The data obtained were presented in **Figure 3.15**. Unfortunately the obtained calibration graph was less sensitive and linear that those obtained with reactors based on 500 Å CPG. Therefore, CPG with average pore size 170 Å was excluded in the remaining work.

The best compromise between sensitivity, sampling frequency, baseline stability, and moderate back pressure of the IER was offered by 4-cm IER based on CPG of average pore size of 500 Å activated with higher amount of enzymes. (750U NANA-aldolase and 500 U PO),. PB of higher pH 7.3 at flow rate of 0.33 mL and sample injection volume of 50 µL. FIA peaks, calibration plot, and reproducibility of the peak heights at two different concentrations were presented in **Figures 3.16** and **3.17**, respectively.

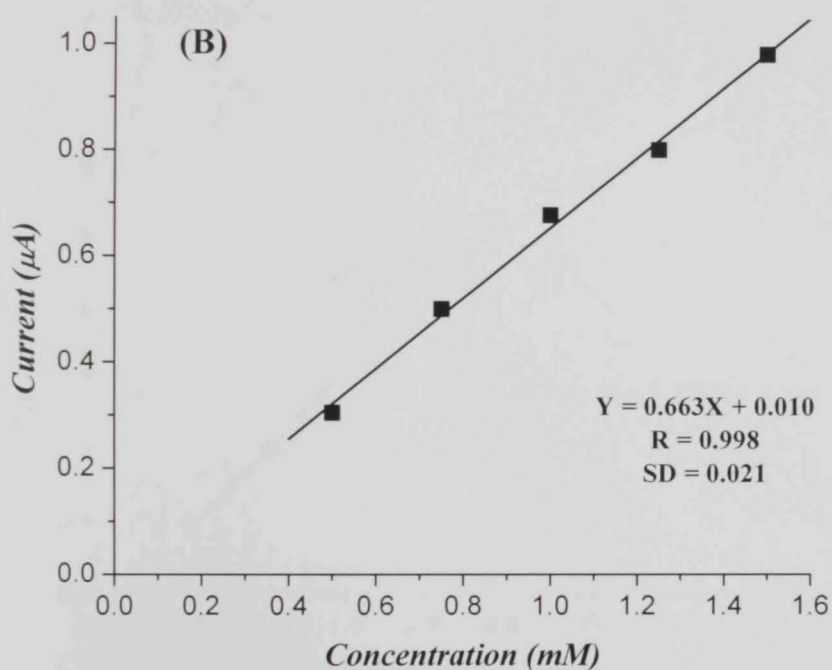
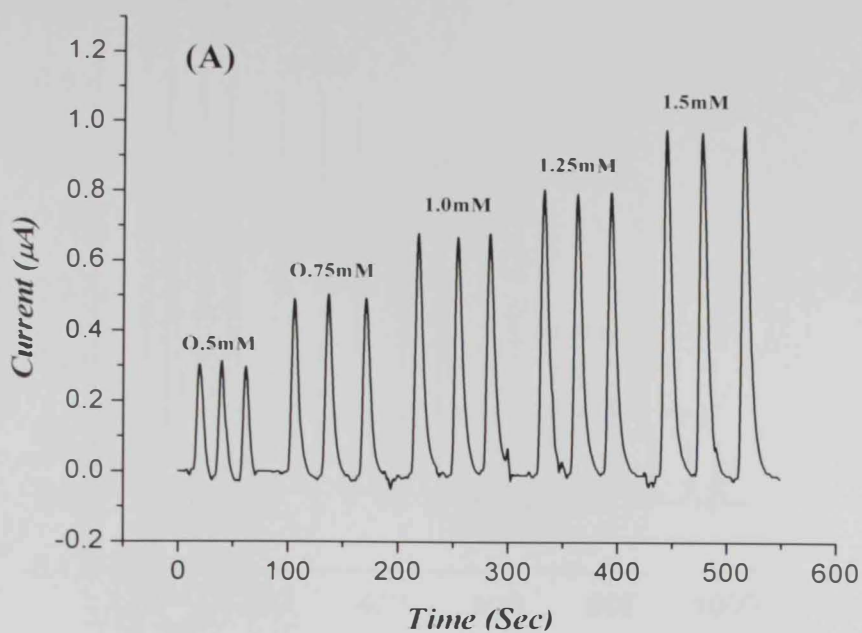


Figure 3.14: FIA peaks (A) and calibration plot (B) obtained with carrier buffer flow rate 3.1 mL/min and 200 μL sample injection volume. 3.5-cm Pt tubular detector. The rest of conditions are similar to those mentioned in Figure 3.9.

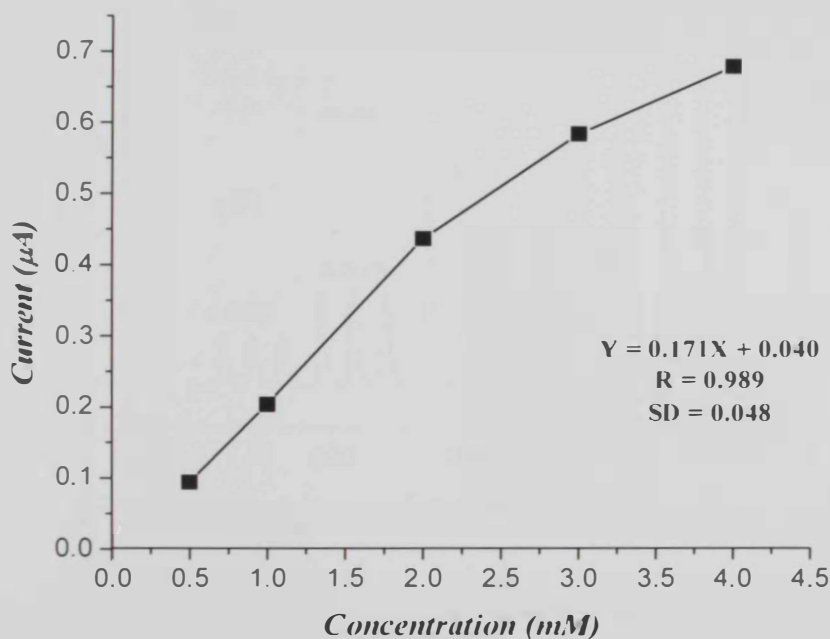
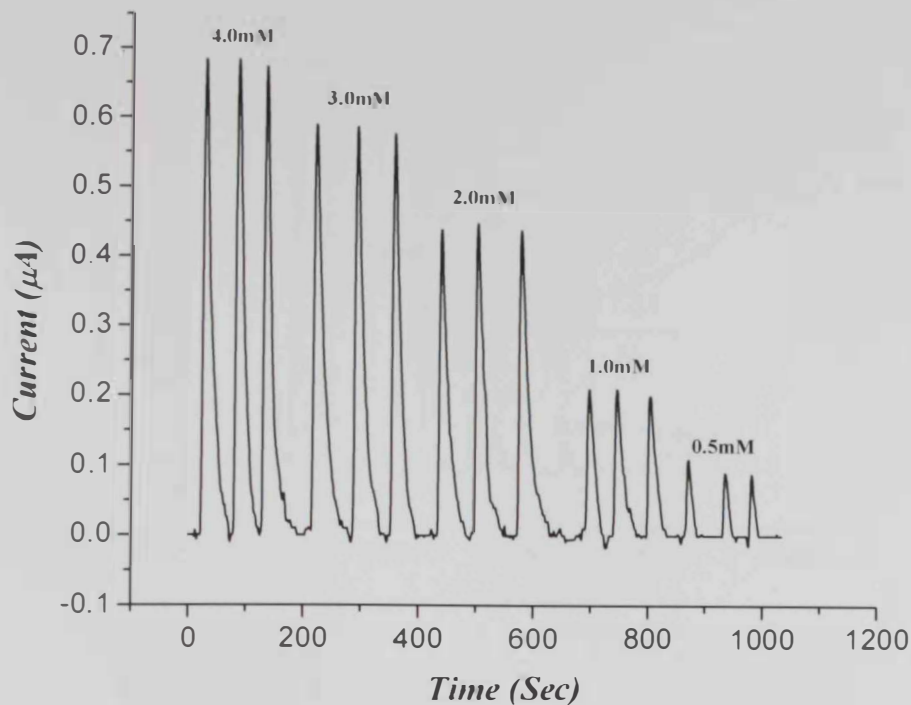


Figure 3.15: FIA peaks (A) and calibration plot (B) obtained with Mixed CPG reactor. Flow rate 1.6ml/min and sample injection loop 50 µL. The rest of conditions are similar to those mentioned in Figure 3.9.

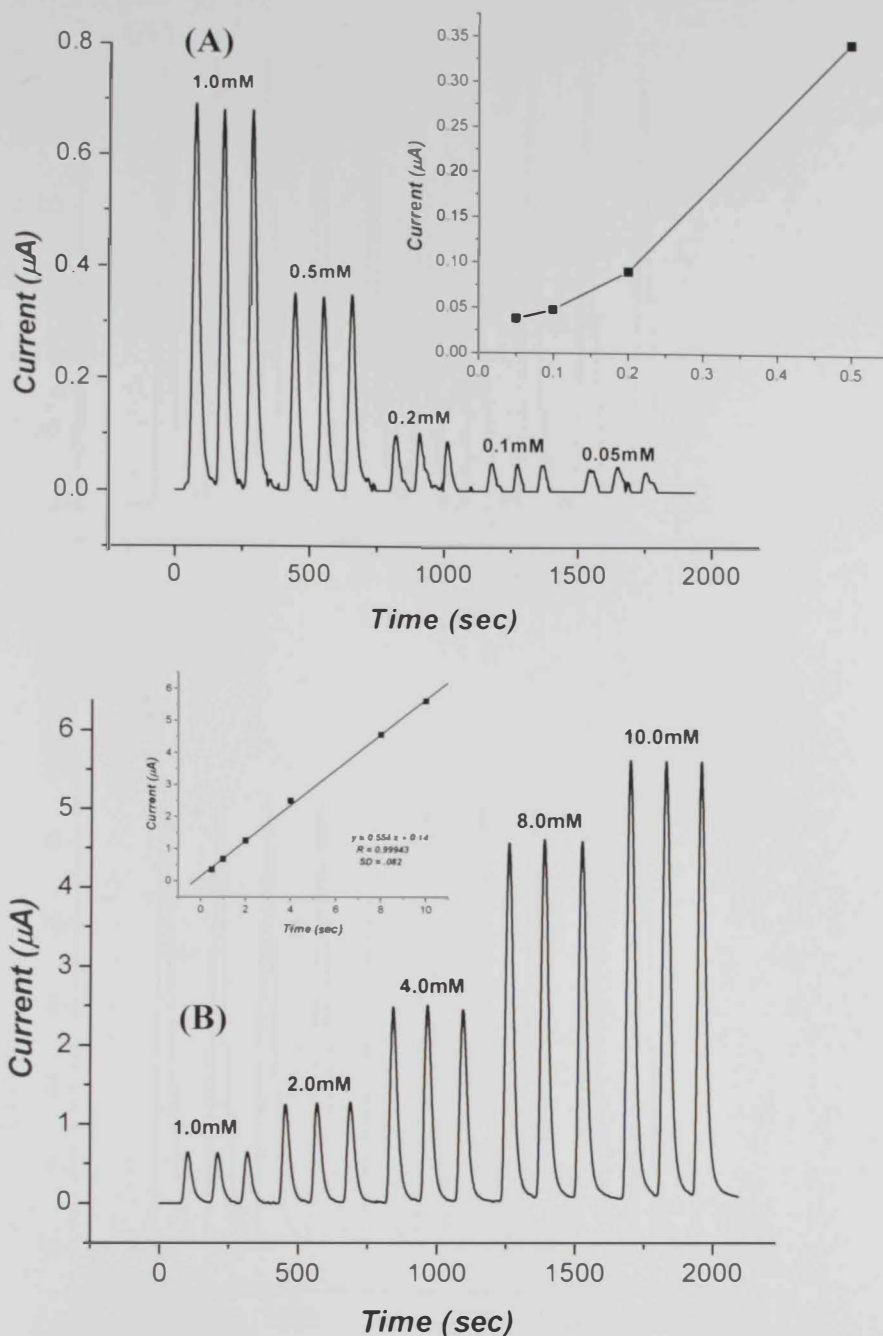


Figure 3.16: FIA peaks for 50 μL SA samples. 4-cm IER based on CPG with pore size 500 Å and activated with 750 U NANA-aldolase and 500 U of PO. PB carrier pH 7.3 and flow rate 0.33 mL/min. The rest of conditions are similar to those mentioned in Figure 3.9. Graphs A and B correspond to peaks obtained in 0.05-1.0 mM and 1-10 mM SA ranges, respectively. Inserts: calibration plots of with each tested concentration range.

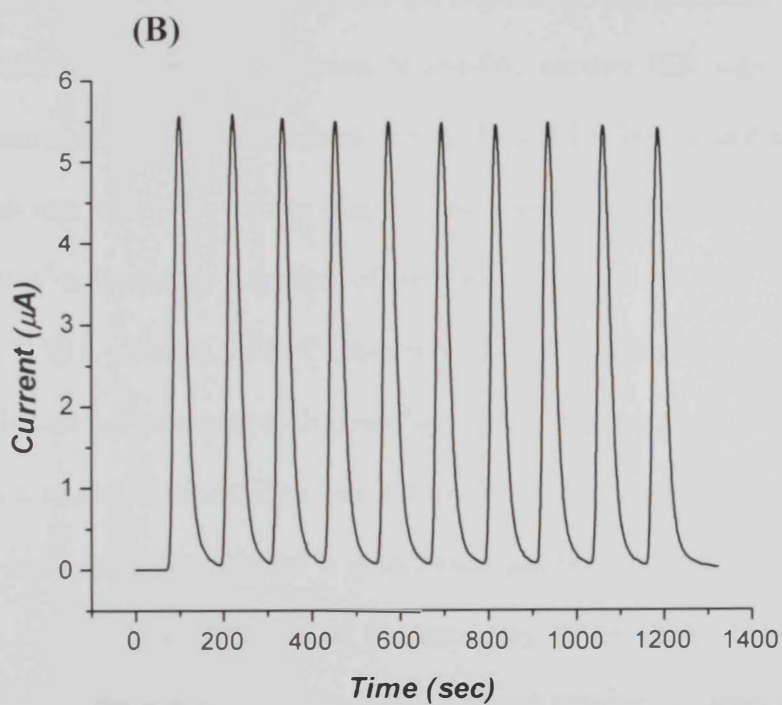
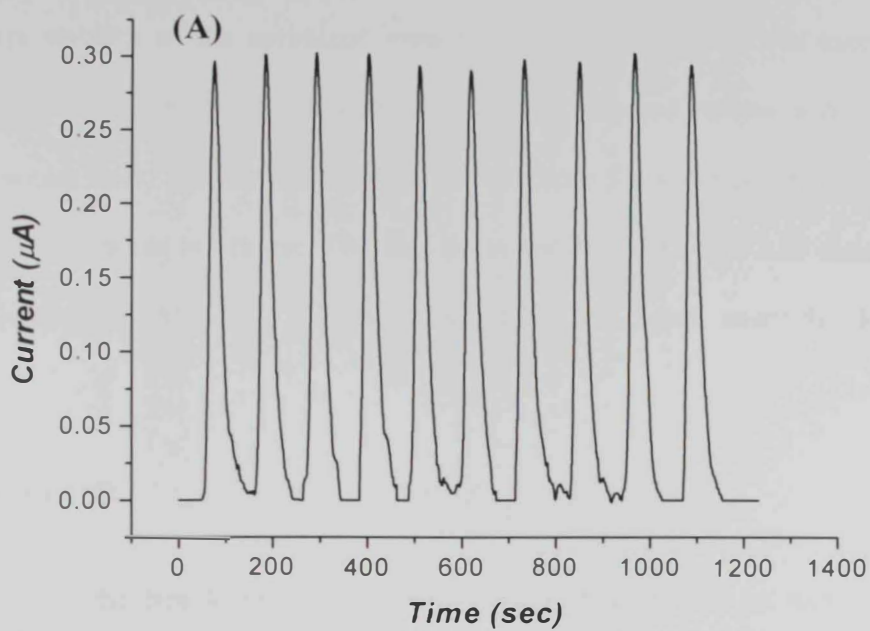


Figure 3.17: Reproducibility of FIA peak heights obtained for 50 μL SA samples using the optimized conditions at 0.5 mM (A) and 10 mM (B) SA, respectively.

Long-term stability of the optimized immobilized enzyme reactor was assessed by comparing the calibration plots obtained with freshly prepared reactor and the same reactor one month later. The reactor was used for hundreds for SA injections and kept in refrigerator at 4 °C when not in use. The data presented in the **Figure 3.18** showed that the reactor retained ~ 16% of its original activity after one month under the described conditions.

3.3.3 Bound SA IER

In addition to the free form, SA occurs as well in bound form as terminal sugar residues on oligosaccharides.^[1-2, 8-9] To extend the potential of the described FIA method to determine such physiologically relevant bound-SA, another IER was prepared by immobilizing neuraminidase enzyme, which releases bound SA from its conjugates, along with NANA-aldolase and PO. A 3-cm reactor was prepared based on CPG of average pore size of 500 Å^o activated by a mixture of enzymes containing 366, 434, and 286 U of neuraminidase, NANA-aldolase, and PO, respectively. Epotin injection sample was used as a source of bound SA to assess such described FIA system because Fetuin (a typical protein used as a source of bound-SA) was not available. At higher flow rate, no peaks were detected, while the system started to detect hydrogen peroxide peaks at slower flow rate. This was explained on the basis of the necessary longer sample residence time within the reactor for the action of the three immobilized enzymes to generate hydrogen peroxide. The data presented in **Figure 3.19** shows the FIA peaks correspond to diluted (1:1 with PB) and undiluted Epotin sample. The proportional peak heights obtained for diluted and undiluted samples nicely indicated the potential of such FIA simple system for the quantitation of bound-SA using a suitable calibrant such as Fetuin.

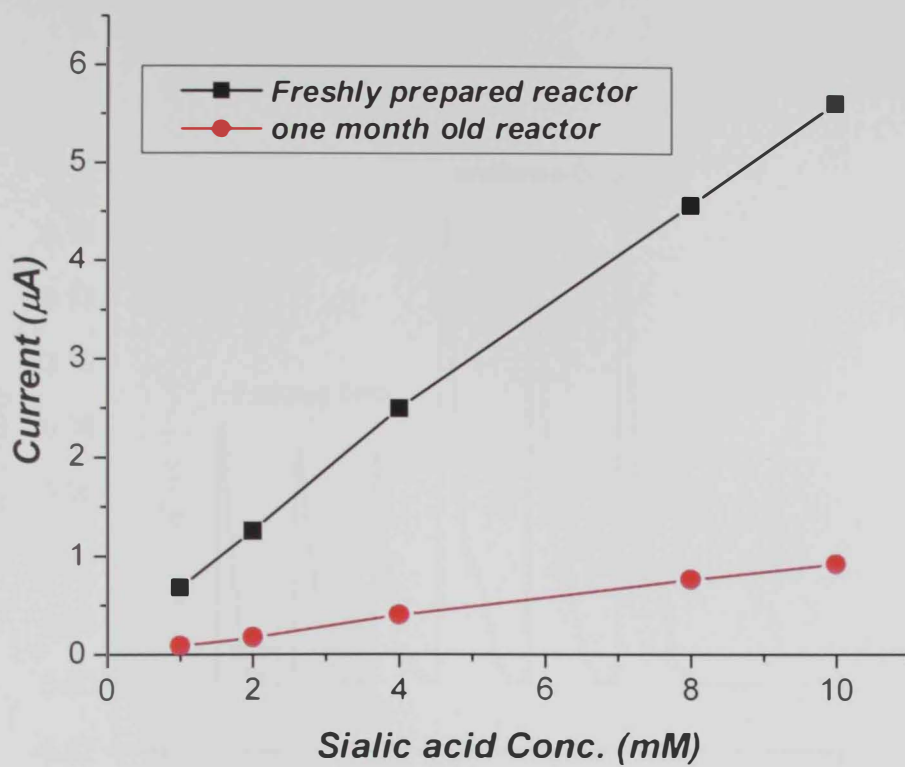


Figure 3.18: Stability of the optimized enzyme reactor. The reactor was kept in refrigerator at 4 °C when not in use.

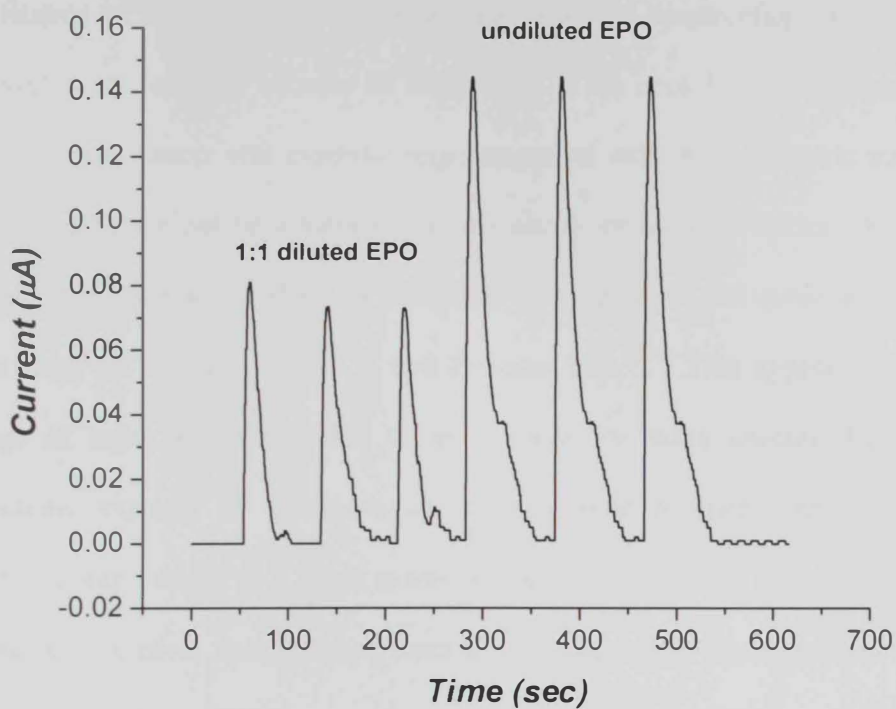


Figure 3.19: FIA peaks obtained for both 1:1 diluted and undiluted Epotin (EPO) sample. Carrier solution PB pH 7.3 containing 2 mM TPP, Injection loop size 50 µL.

3.4 Preparation, characterization and application of SA amperometric biosensor

Although development of an FIA system for the determination of SA necessitated the immobilization of both enzymes to prepare the IER, the construction of the biosensor represented more challenge because an integration of the immobilized enzymes with the amperometric transducer was essential requirement as well. Amperometric transduction of hydrogen peroxide can be achieved by either anodic or cathodic modes. The reduction of hydrogen peroxide occurred at low potentials by a variety of electronic mediators such as peroxidase,^[112-114] hemoglobin,^[115] and Prussian blue.^[116] This approach offered the advantage of being less vulnerable to interference by redox species. However, the complications imposed by incorporating the electronic mediators and their limited stability^[117] compromised to a great extent the advantage of their enhanced selectivity. Therefore, the classical anodic amperometric transduction of hydrogen peroxide at Pt electrode polarized at +0.6 V was adapted in this project to develop a prototype SA amperometric biosensor.

Preliminary investigations to co-immobilize NANA-aldolase and PO using GA crosslinking indicated that PO activity was strongly affected by the amount of GA used. This explains the observation, that previous biosensors which incorporated PO were constructed by physical entrapment of PO on polymeric matrices rather than covalent immobilization. A similar sensitivity to GA crosslinking was reported by Marzouk et al for pyruvate oxidase.^[118] The authors reported an optimized GA:lactate oxidase:BSA ratio which proved efficient in the immobilization of such delicate enzyme using the harsh GA crosslinking method. Therefore, a similar ratio similar to that published for

lactate oxidase immobilization^[118] was selected as a reasonable start to co-immobilize NANA-aldolase-PO to construct SA biosensor, which will be subsequently optimized.

An additional novelty introduced in the current SA biosensor construction was the utilization of microporous PE membranes for casting the enzyme layer, which adhered strongly to the PE membrane. This eliminated the need for the strong adhesion between the enzyme layer and the electrode substrate. The enzyme layer was then positioned in close proximity to the Pt electrode surface by means of a Teflon cap.

3.4.1 Effect of pH of the SA biosensor response

The initially tested enzyme layer which was based on enzyme-BSA-GA ratio similar to those previously optimized values^[118] provided a reasonable response to SA. Consequently, biosensors prepared using such enzyme layer were used study the effect of pH and temperature on the sensor response. The enzyme layer was prepared by pipetting 15- μ l aliquot of an enzyme mixture solution prepared by mixing equal volumes of 0.9% GA, 9% BSA and 10% enzyme solution (4% NANA-aldolase (99.2U) and 6% PO (65.4U)) on a polyester membrane (1 μ m pore size).

The effect of pH was studied by measuring the SA biosensor current response to 1 mM SA in PB in the pH range of 5.6-8.5. The obtained responses were presented in **Figure 3.20**. It was observed that the sensor response was significantly deteriorated after being exposed to buffers of pH values greater than 8 as shown in **Figure 3.20 B**. The shift of the optimum pH by about 1 pH unit to a higher value from the value obtained by homogenous catalysis could be reasonably attributed the change of the enzyme characteristics upon immobilization by crosslinking.^[104]

To avoid the damage of the enzyme layer at high pH values, Multipoint calibration responses of SA biosensor were obtained in PBs in the pH range 5.60 -7.65 only as shown in **Figure 3.21**. It was evident that although of the effect of pH on the sensor sensitivity, its linear response was retained over the tested concentration range.

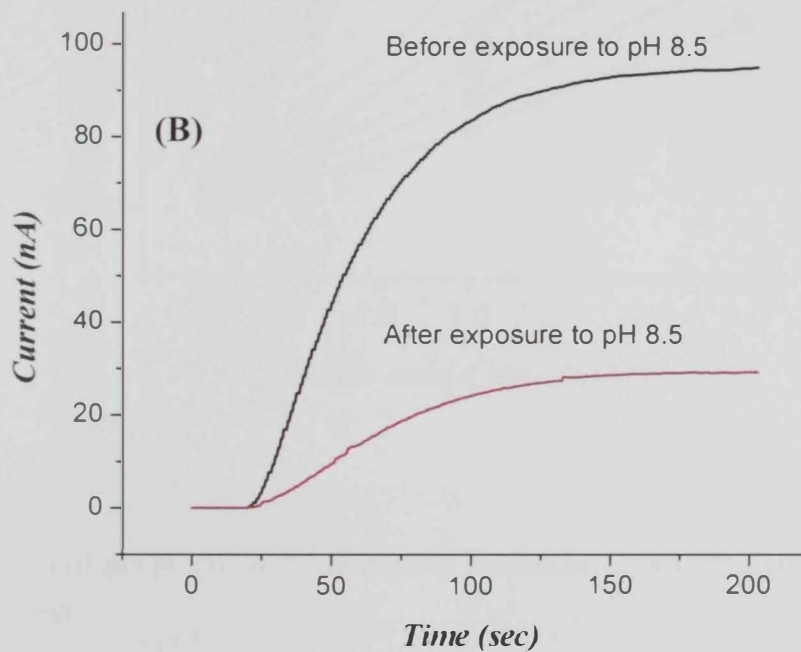
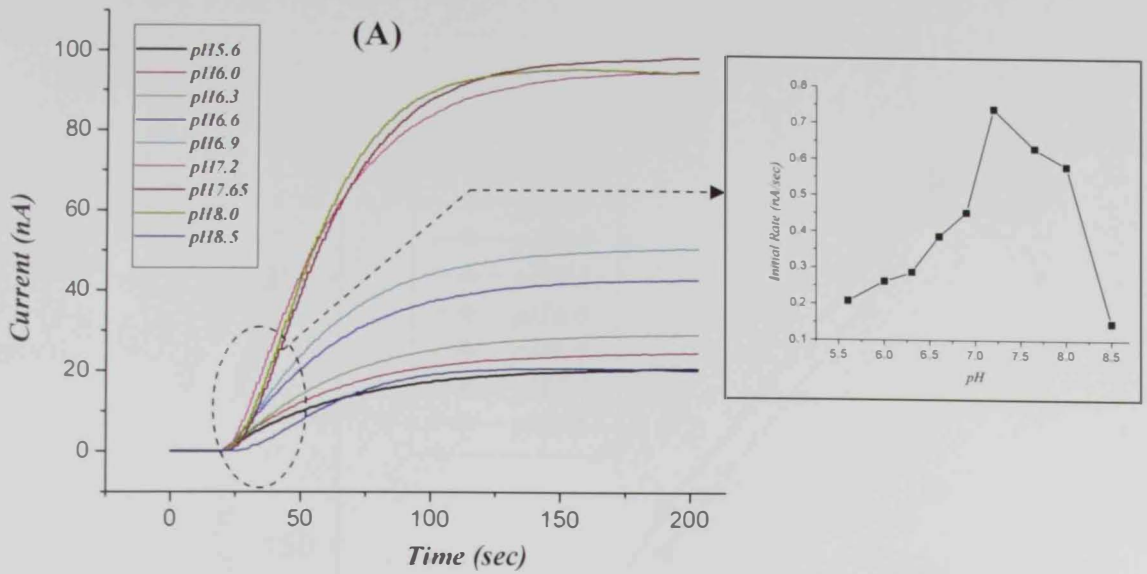


Figure 3.20: (A) Effect of pH of the PB on the SA biosensor response to 1 mM SA; the insert shows the effect of pH on the initial rate. (B) SA biosensor response to 1 mM SA at pH 7.2 before and after exposure to PB pH 8.5

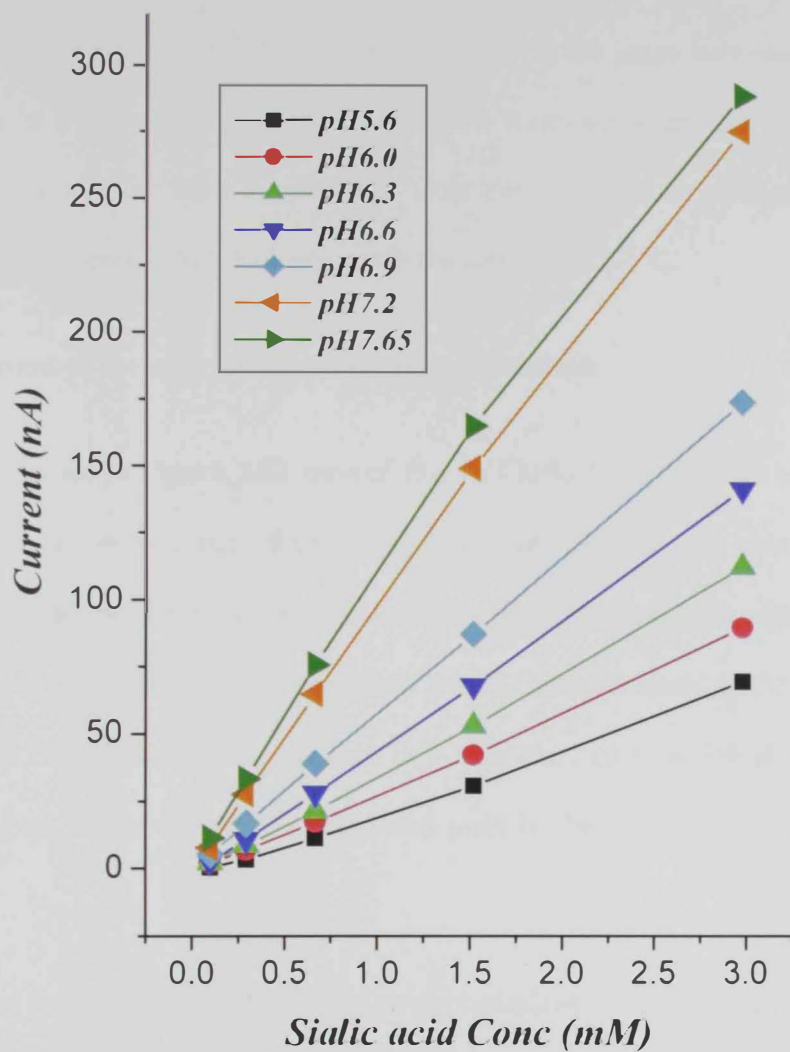


Figure 3.21: Effect of pH of PB on the multipoint calibration of SA biosensor at 37 °C and using 2 mM TPP.

3.4.2 Effect of temperature of the SA biosensor response

The effect of temperature on SA biosensor response in the range between 25 and 37 °C was shown in **Figure 3.22**. Higher temperature were not attempted to avoid the deactivation of the enzyme layer as predicted from the homogenous catalysis data. All subsequent measurements with SA biosensors were carried out 37 °C.

3.4.3 Optimization of the enzyme immobilization conditions

The data presented in **Figure 3.23** showed that G/T ratio has a dramatic effect on the sensor response. At low G/T (i.e., 0.03) unstable sensor response was obtained which could be attributed to inefficient enzyme immobilization. Whereas at high value (i.e., G/T = 0.08) the sensor showed diminished sensitivity which could attributed to the deleterious effect of GA on PO. Therefore, the average G/T ratio (i.e., 0.05) which showed stable response and good sensitivity was selected and used in the subsequent enzyme layer preparations.

The effect of total enzymes to BSA ratio at the optimized G/T value was investigated and the obtained data were presented in **Figure 3.24**. The highest sensitivity was obtained with enzyme layer with the total enzyme % (w/v) ~ equal to BSA %. Either lower or higher enzyme to BSA ratios resulted in lower sensitivity. In the first case, the decreased sensitivity could be attributed to the low enzyme content in the enzyme layer whereas in the second case the decreased sensitivity could be attributed to inefficient enzyme immobilization because of the decreased BSA content.

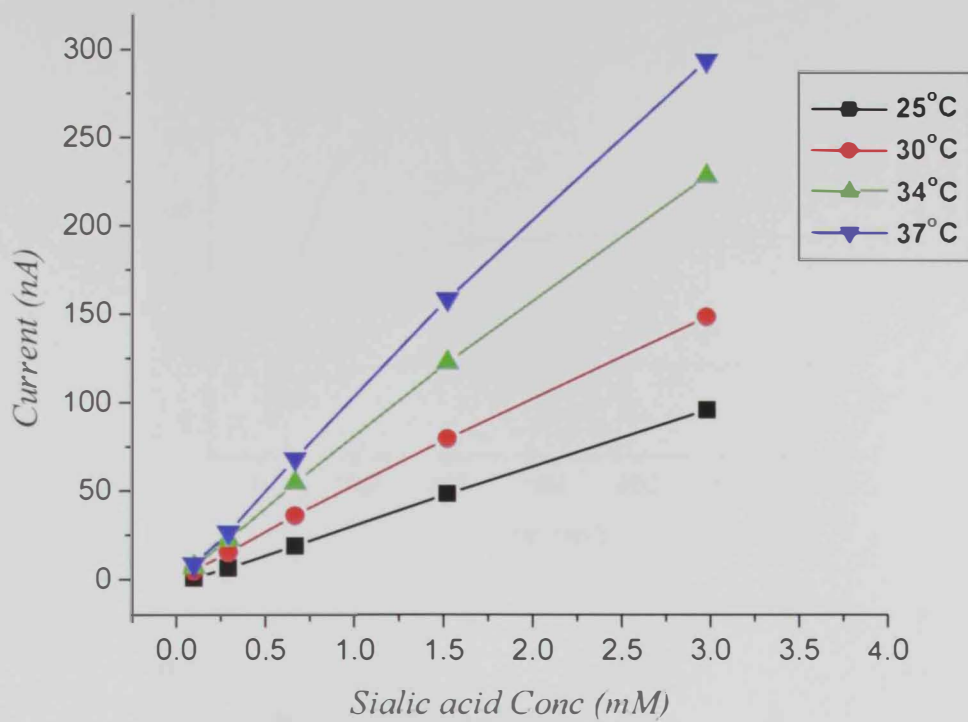


Figure 3.22: Effect of temperature on the multipoint calibration of SA biosensor in 0.1 M PB pH 7.3 containing 2 mM TPP.

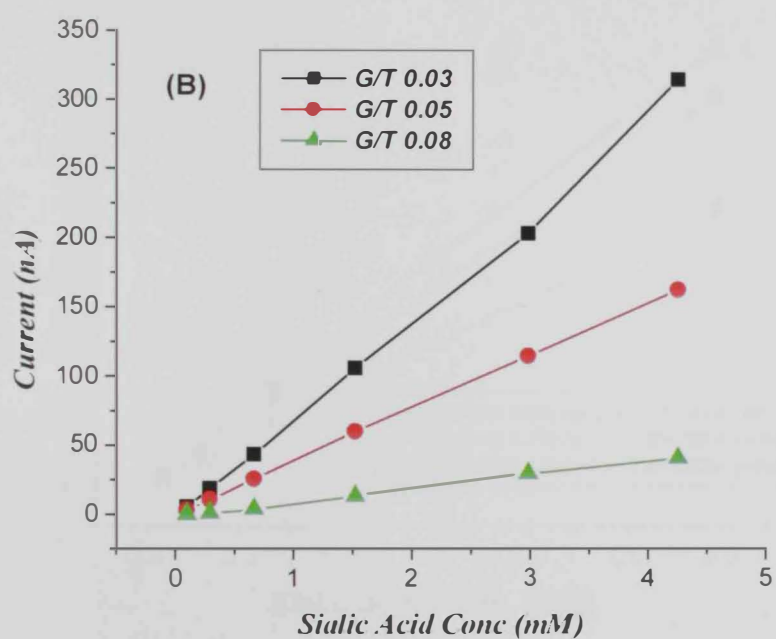
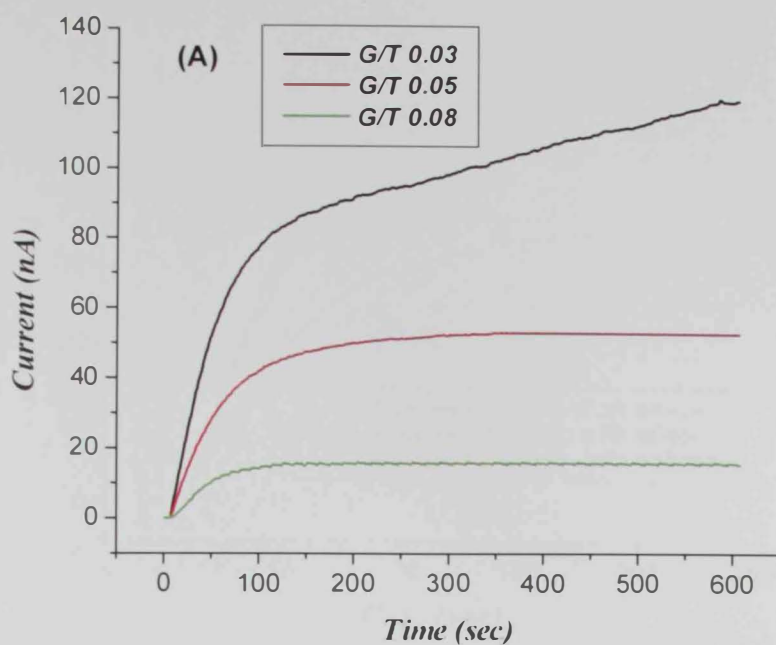


Figure 3.23: Effect of GA/T ratio on the response of SA biosensor. (A) The time response obtained for 2 mM SA; (B) multipoint calibration of SA biosensors based on enzyme layers of different G/T ratio.

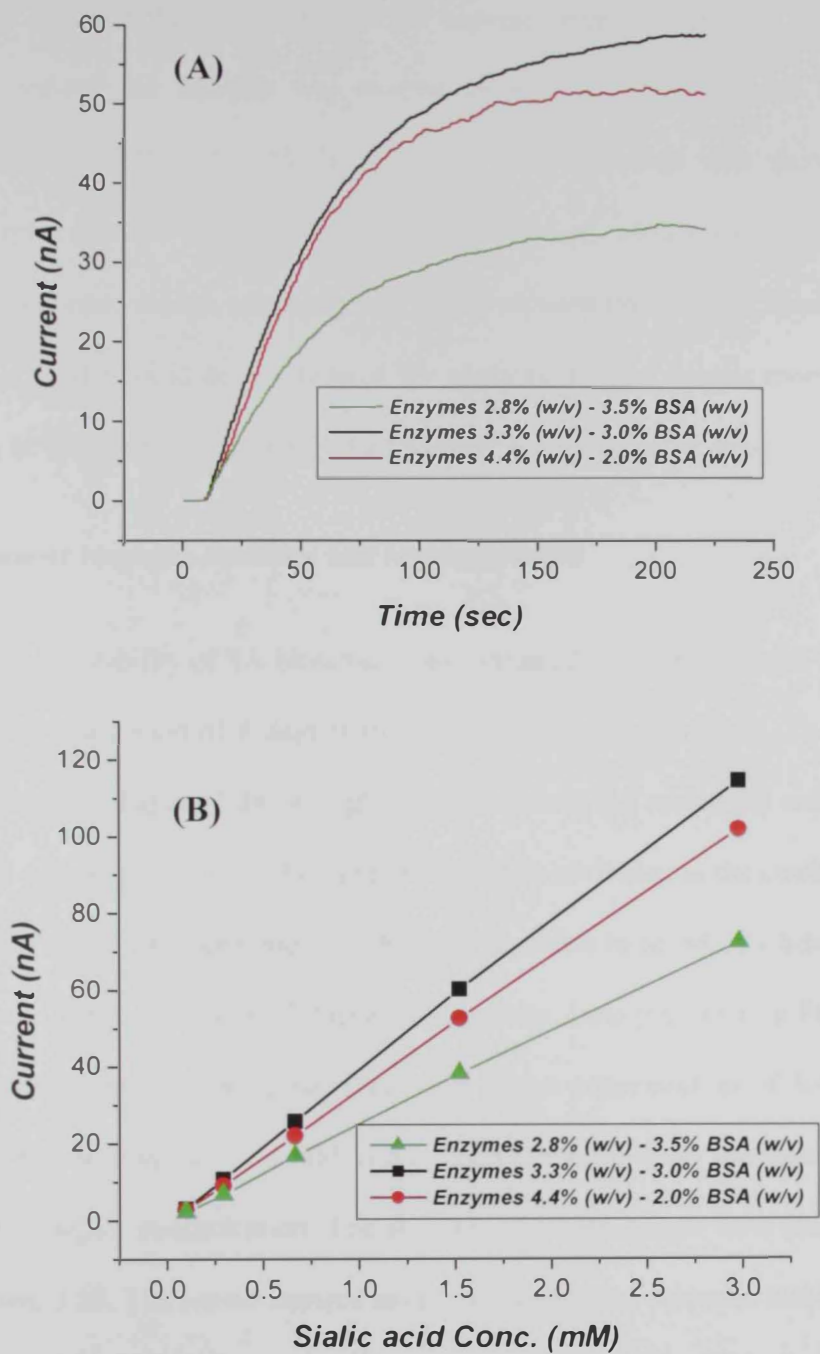


Figure 3.24: Effect of total enzyme to BSA ratio (at a fixed G/T ratio of 0.05) on the response of SA biosensor. (A) The time response obtained for 2 mM SA; (B) multipoint calibration of SA biosensors based on enzyme layers of enzymes to BSA ratio.

The further optimize the construction of the enzyme layer, the effect of total amount of the optimized-enzyme mixture was studied as well and the obtained data were presented in **Figure 3.25**. Although the sensitivity was enhanced with increasing the amount of enzyme mixture within the tested range, the 15- μL aliquot was selected as the best compromise between high sensitivity and short response time ($t_{95\%} = 90 \text{ sec}$). Larger amounts (e.g., 20 μL) could be nicely used for applications that require more sensitive determination of SA but on the expense of a relatively longer response time ($\sim 3 \text{ min}$).

3.4.4 SA biosensor response, stability and reproducibility

The operational stability of SA biosensor was evaluated by comparing the calibration plots obtained over a period of 8 days with two batches (3 sensors each). The obtained data were presented in **Figure 3.26**. A slight enhancement of the sensitivity was observed within the first 4-5 days in both batches and this could be attributed to the conformational relaxation of the crosslinked enzymes.^[118] A slight decrease in sensitivity was observed afterwards due to the gradual loss of the enzyme activity. Data presented in **Figure 3.27** showed the three calibration plots obtained with wider concentration of SA. Sensors showed linear response up to $\sim 3.5 \text{ mM}$ and a slight deviation from the linear response was observed at higher concentration. The stability of SA biosensor time response was shown in **Figure 3.28**. The sensor showed excellent steady state response stability which was attributed to the careful optimization of the enzyme layer construction.

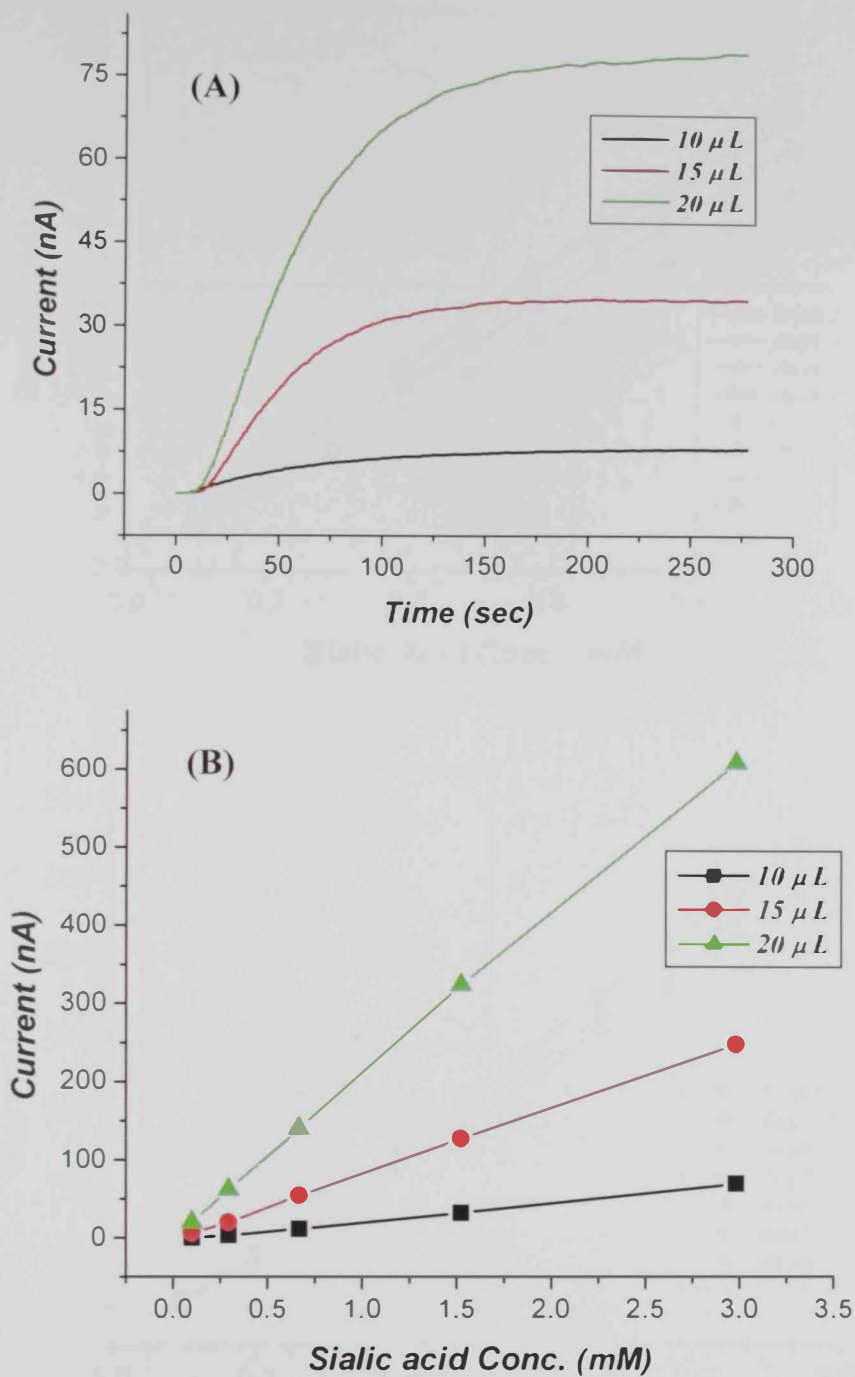


Figure 3.25: Effect of the total amount of the enzyme mixture on the response of SA biosensor. (A) The time response obtained for 0.4 mM SA; (B) multipoint calibration of SA biosensors based on enzyme layers of enzymes to BSA ratio

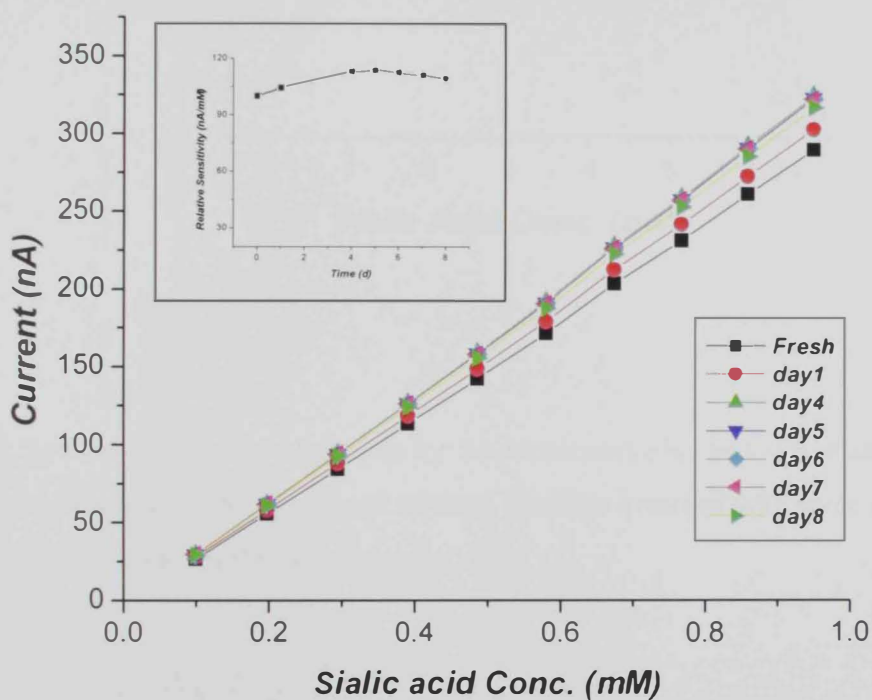
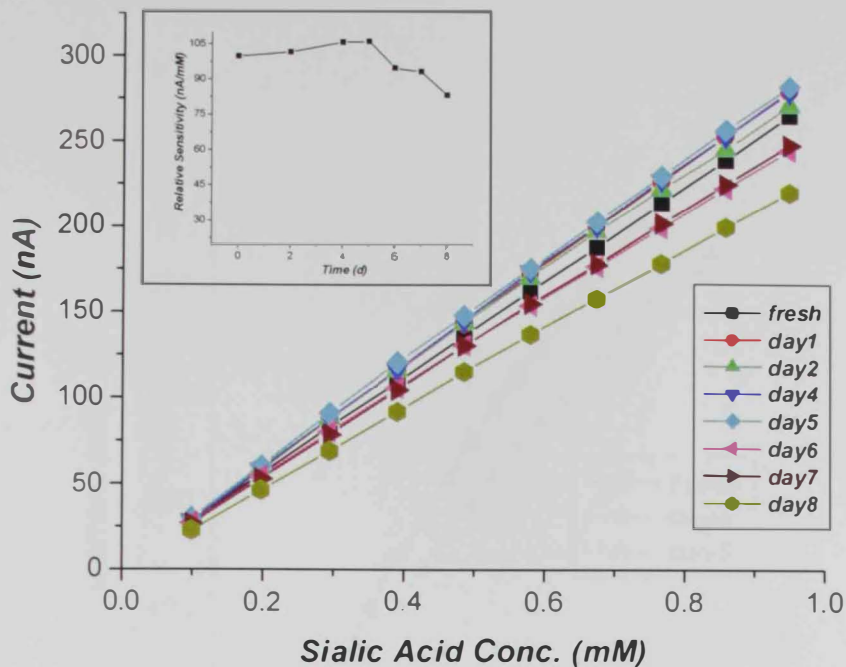


Figure 3.26: Stability of the SA biosensors of the first (A) and the second (B) batch. Each calibration plot corresponds to the average of the three sensors readings calibrated in separate experiments. Insert in each figure shows the relative sensitivity.

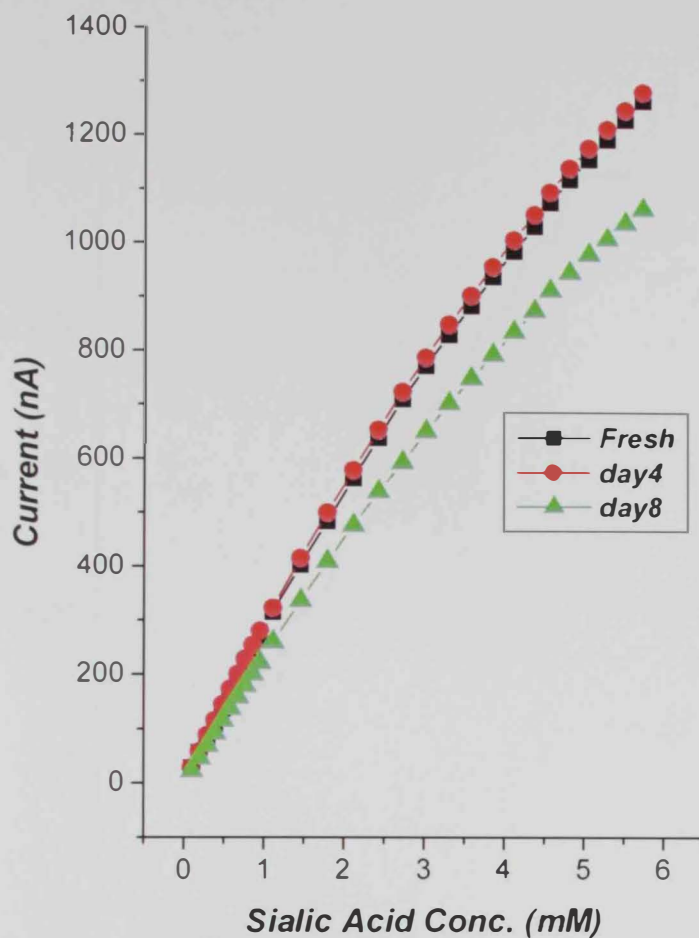


Figure 3.27: Several-point calibration plots for SA biosensors obtained at 0, 4 and 8 day. Each data point corresponds to an average of three readings obtained with three different SA biosensors prepared using the optimized enzyme.

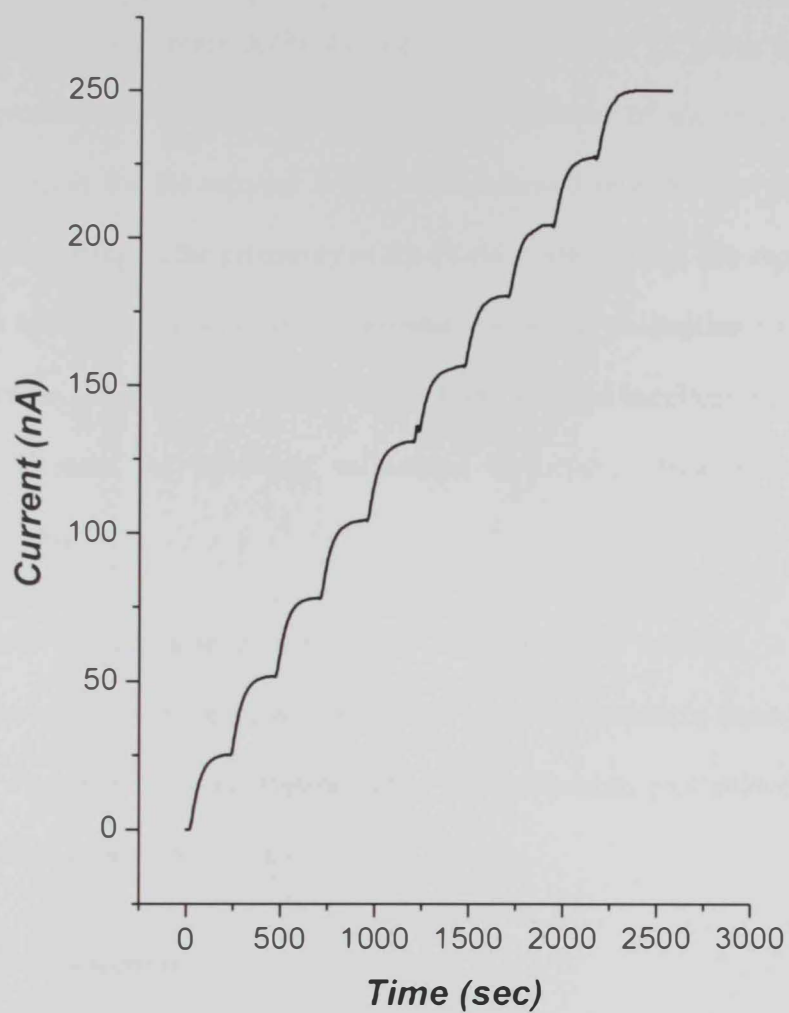


Figure 3.28: Amperometric $I-t$ plot for SA biosensor response. Each step corresponds to a 100 μM increment of SA concentration in the range of 0-1 mM. SA

Within batch reproducibility of SA biosensor fabrication was assessed by comparing the response sensitivity obtained with different sensors from prepared similarly in one batch. The data obtained (**Figure 3.29**) showed CV of 11 % ($n = 3$). It was believed that such good reproducibility attributed to the novel utilization of the microporous PE membrane as support for the enzyme layer, which allowed reproducible enzyme layer thickness and positioning in the proximity of the Pt electrode surface. The reproducibility of the same SA biosensor was assessed by repeating the sensor calibration for three times within the same day. The data obtained (**Figure 3.30**) revealed excellent reproducibility, which would decrease the necessary calibration frequency, while maintaining the measurement accuracy.

To complete, the characterization of the SA biosensor response, a multipoint calibration at low micromolar range was performed under the optimized condition and the data obtained were presented in **Figure 3.31**. The calibration plot showed excellent linearity ($r = 0.9998$) with SD of 0.067.

3.4.5 SA biosensor selectivity

The inherent problem of the hydrogen peroxide anodic detection system is the non-selective oxidation of other species, likely to be present in the sample solution, at the relatively high-applied working potential necessary for oxidation. Several approaches have been developed to overcome this limitation as discussed before.^[70, 119] However, electropolymeric films provide many attractive features, such as self-limiting coverage to the electrode surface, generation of very thin layers (~ 10 nm), strong adhesion to the electrode surface, ease of thickness control by changing the polymerization time, and convenience of automation.

Ideally, the polymeric films should have 100% permeability for the hydrogen peroxide signal molecules and reject completely the penetration of the interfering molecules. The poly(*m*-PDA) inner layer previously described^[118] was adapted in the present work. Typical cyclic voltammogram for oxidative electropolymerization of *m*-PDA from stirred 10 mM PB solution is shown in **Figure 3.32**. The process was totally irreversible, no reduction current was observed on reversing the potential scan. The decrease in the current was attributed to the polymer growth on the electrode surface and hence the monomer molecules could not penetrate through the film. The modified platinum electrodes with poly(*m*-PDA) showed favorable retention of the hydrogen peroxide signal (~ 90 %) obtained with the same bare platinum prior to the modification (**Figure 3.33**). The rejection properties of the pol(*m*-PDA) inner layer towards AA, AAP and UA, which are potential interfering species for hydrogen detection in biological media, were shown in **Figure 3.34**.

The reliability of SA biosensor was further assessed by comparing its response to SA dissolved in PB and in bicarbonate carbonate buffer containing 5 % BSA and the highest physiological levels (~0.2 mM) of each of AA, AAP and UA, respectively. The later solution was used to mimic the complexity of the human serum matrix. The data obtained and presented in **Figure 3.35** showed the selective sensor response towards SA regardless of the complexity of the sample matrix. In this experiment, the SA recovery was only 96% and could be attributed to the experimental error in pipetting such viscous sample.

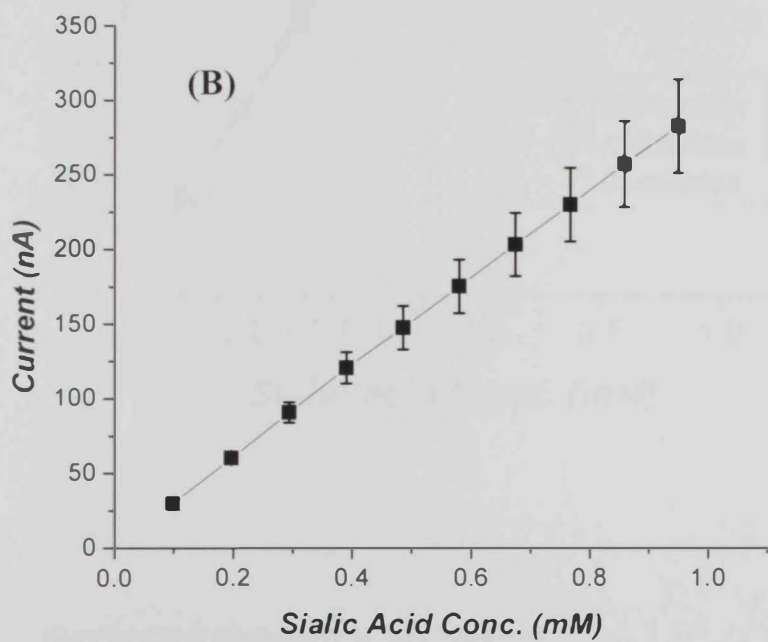
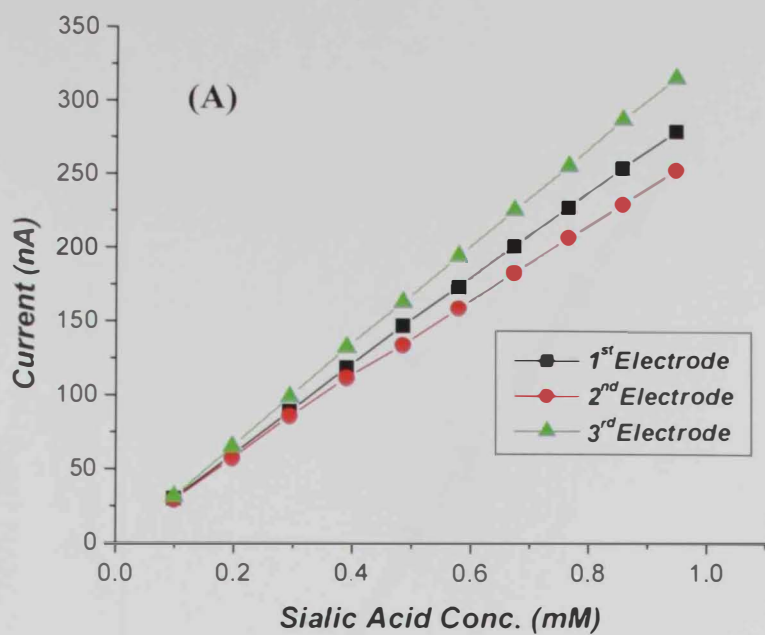


Figure 3.29: Calibration plots of three SA sensors prepared within one batch (A). The mean values and error bars which correspond to the standard deviation ($n=3$) are presented in (B).

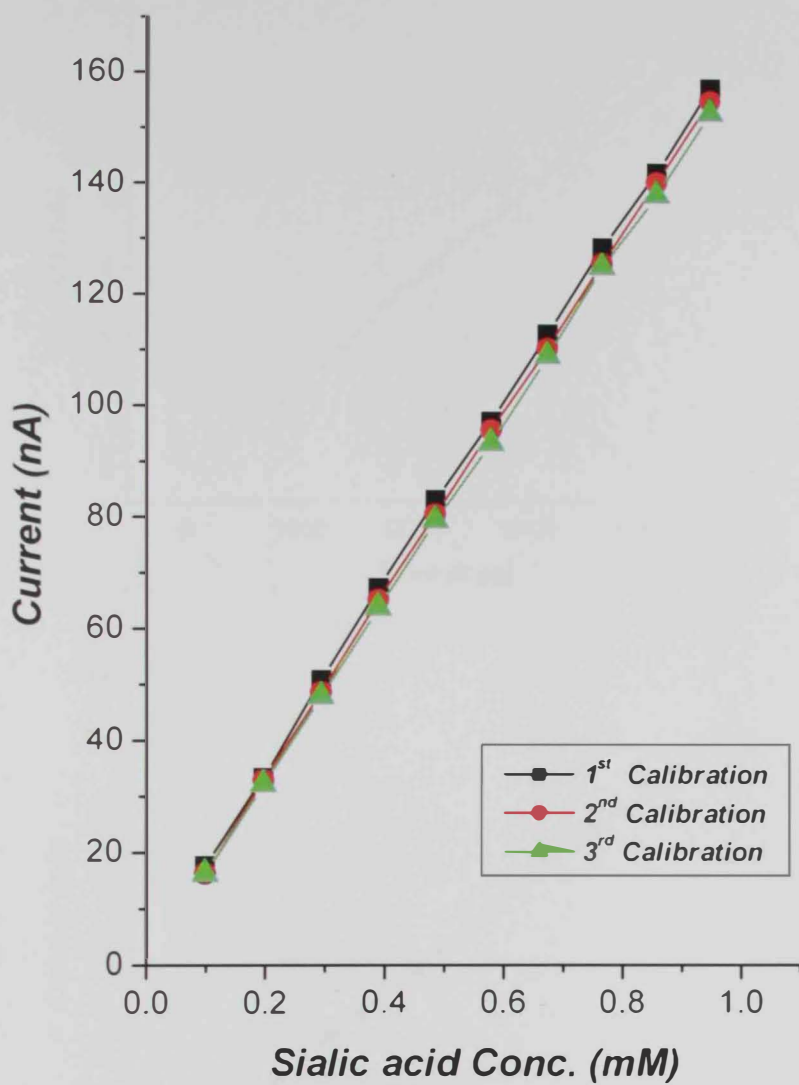


Figure 3.30: Within-day reproducibility of SA biosensors.

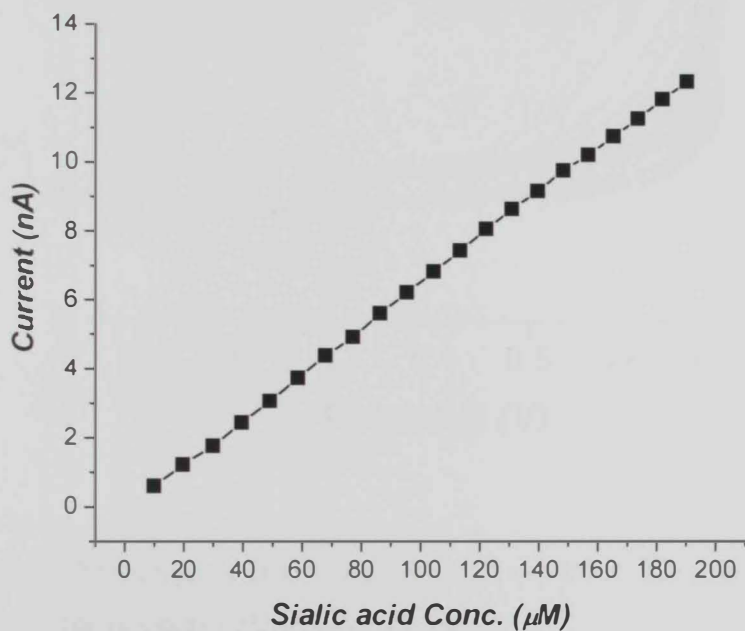
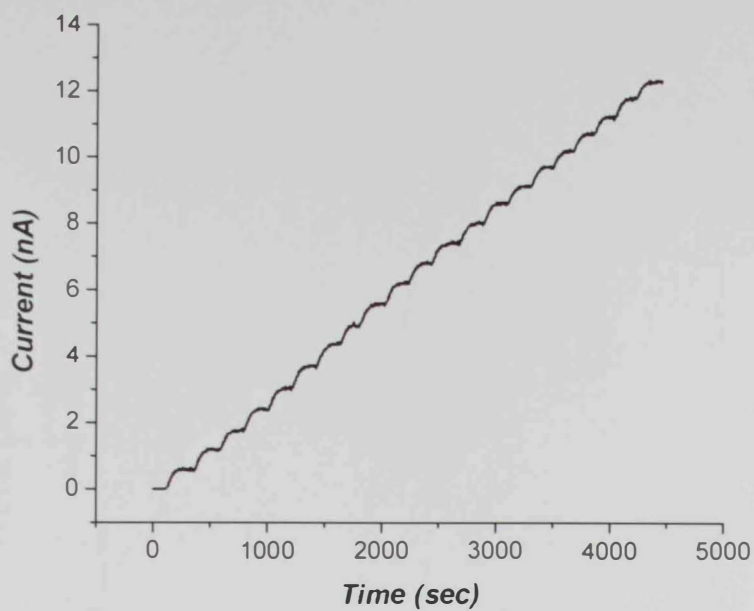


Figure 3.31: Multi-point calibration of SA biosensor in the range of 0-200 μM . (A) amperometric $I-t$ plot; (B) calibration plot based on the steady state current values obtained from (A). Each addition corresponds to 10 μM increment in SA concentration.

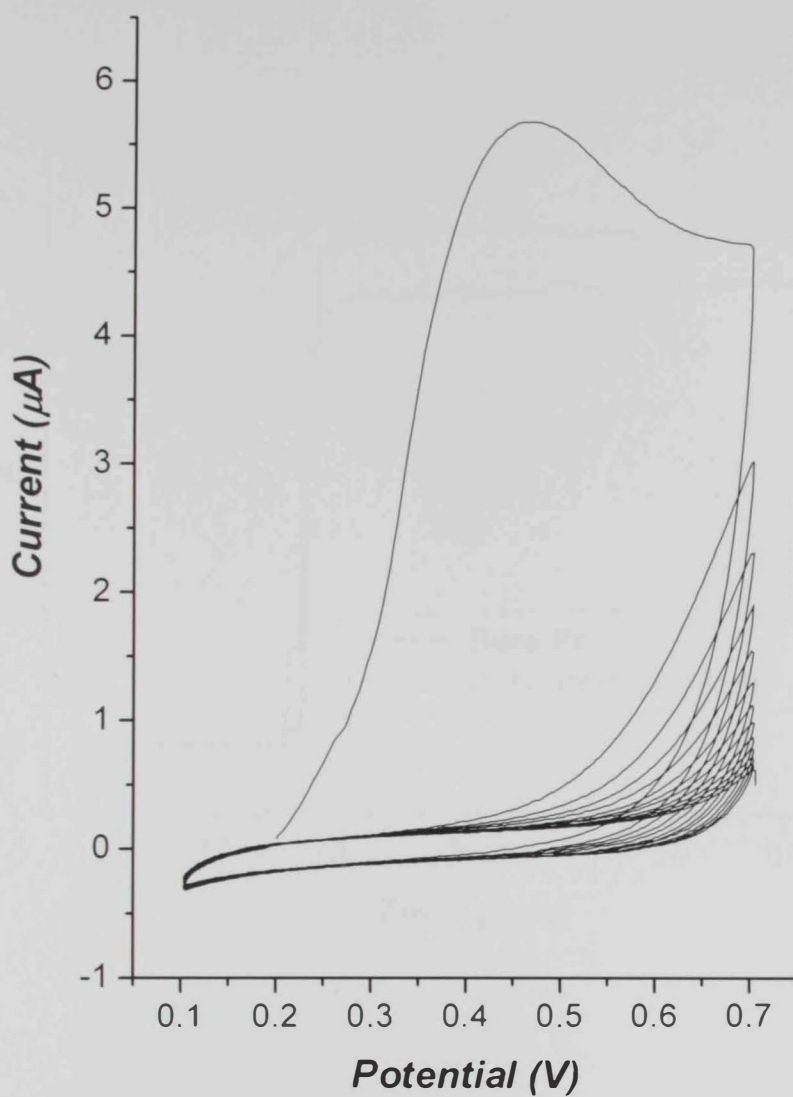


Figure 3.32: Cyclic voltammogram of the *m*-PDA on Pt electrode. The film growth was indicated by the progressive decay of the peak current.

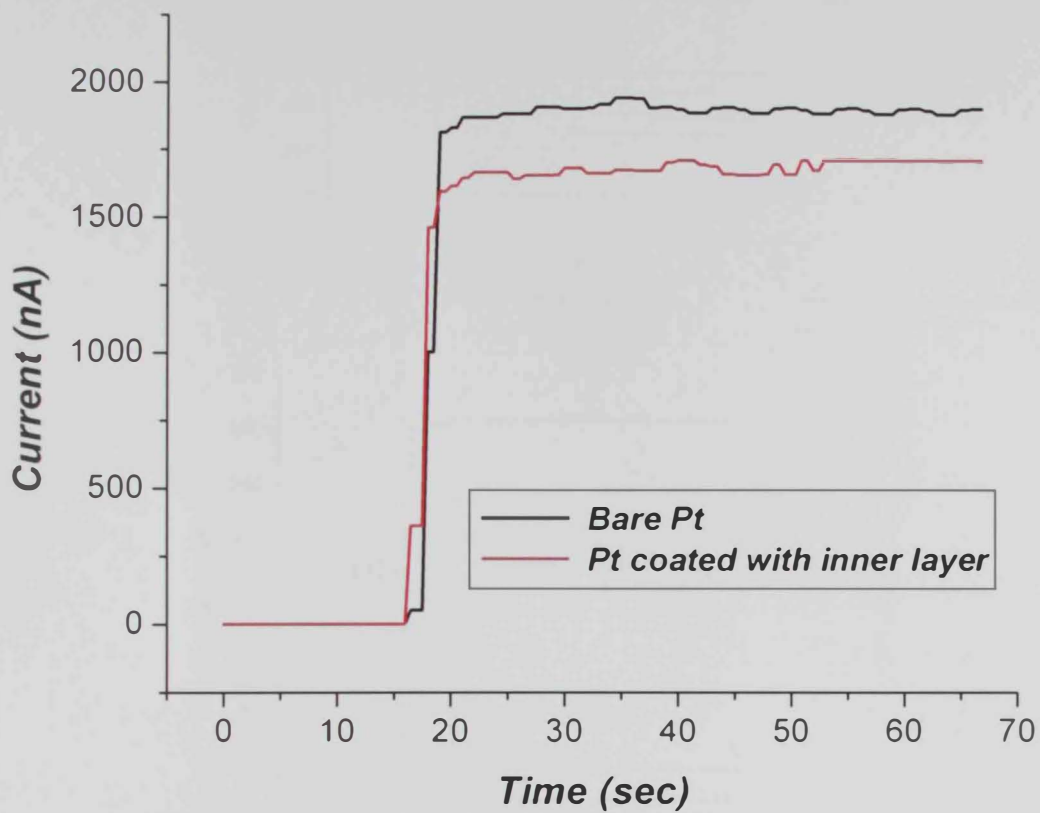


Figure 3.33: The amperometric response of bare and coated Pt electrode with Poly(m-PDA) inner layer to 0.2 mM hydrogen peroxide.

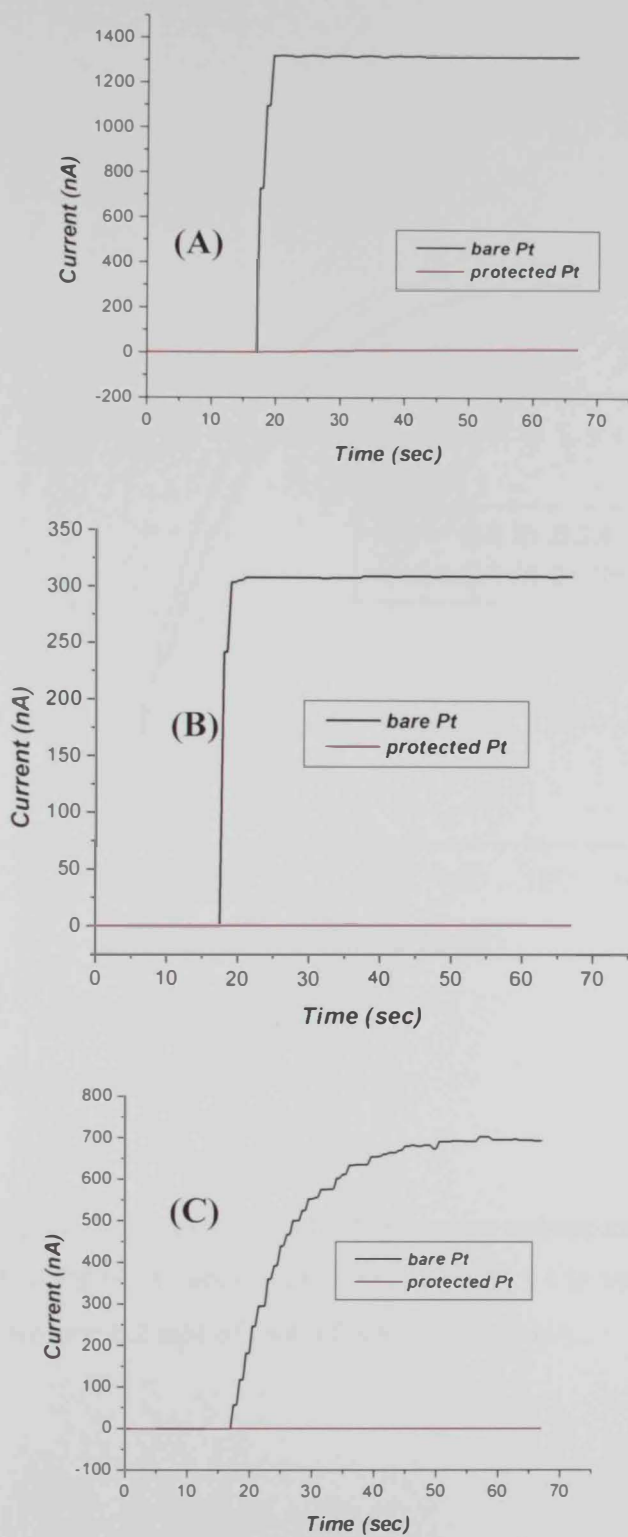


Figure 3.34: Rejection properties of the poly(*m*-PDA) layer. The black and red traces in A, B and C correspond to 0.2 mM of AA, AAP, and UA at bare and protected Pt electrode with Poly(*m*-PDA) layer, respectively.

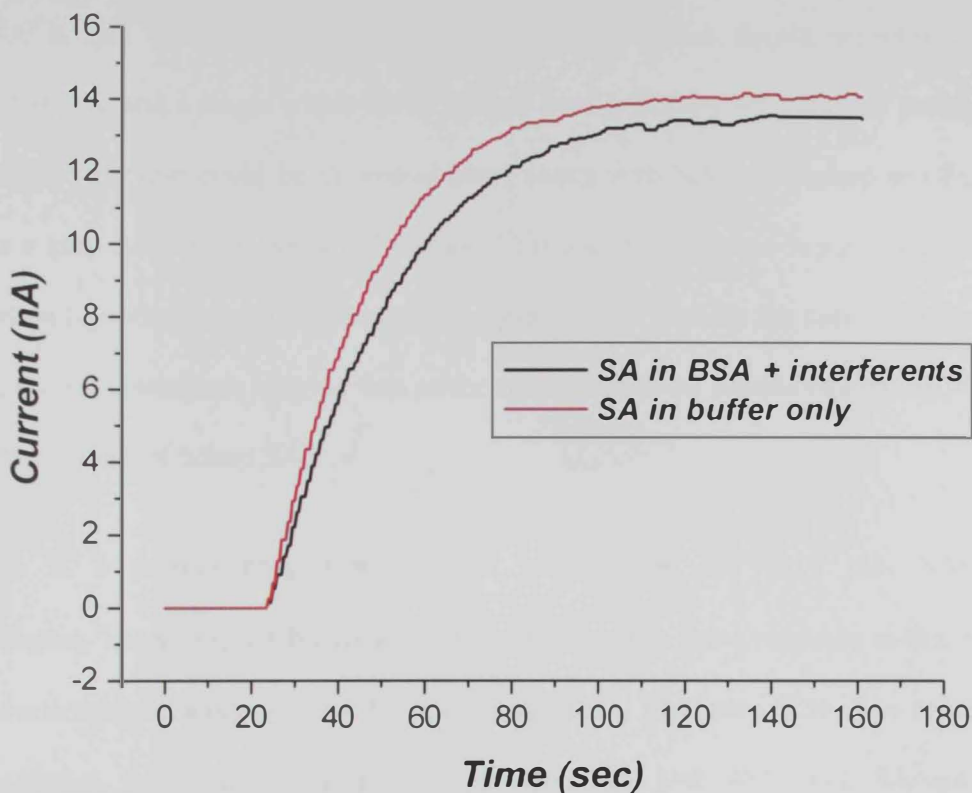


Figure 3.35: The amperometric responses of SA biosensor correspond to the addition of 0.5 mL of 2 mM SA in PB (Red trace) and 0.5 mL of 2 mM SA in bicarbonate buffer pH 7.4 containing 5% BSA and 0.2 mM of each of AA, AAP, and UA.

3.4.6 Application of SA biosensor to real biological samples

Finally, the reliability of the developed SA biosensor for measuring both free and bound SA in real biological samples was assessed using two Epotin samples, from different batches, and a single whole blood sample from a healthy volunteer. In principle, neuraminidase enzyme could be co-immobilized along with NANA-aldolase and PO to construct a total SA (free + bound) biosensor. This suggests a future separate extensive investigation to optimize such three-enzyme sequence biosensor. In the current assays of total SA, the neuraminidase enzyme was added to the sample as soluble enzyme in PB to catalyze the release of bound SA.

Epotin is a protein drug that contains only bound SA (≥ 10 mol SA/mol erythropoietin). Therefore, SA biosensor was not expected to show response to this drug unless neuraminidase was added to the sample as shown in **Figure 3.36**. The assay of Epotin samples from two different batches gave 15 and 40.7 mol SA/mol of erythropoietin. Analysis of the same batches by the pharmacopoeia method^[25, 120] gave 13 and 37 mol SA/mol of erythropoietin, respectively which agreed very well with the results obtained with the SA biosensor.

Figure 3.37 showed how free, and total SA could be determined using SA biosensor alone or and a combination of SA biosensor and soluble neuraminidase enzyme. Since pyruvate is a common substrate in human body fluids and can cause interference in this enzymatic assay, a biosensor for pyruvate was developed and used to measure pyruvate in real samples. This biosensor was prepared by replacing the NANA-aldolase in the sialic acid biosensor by BSA. The sensor showed excellent steady state response stability and linearity up to 0.6 mM (**figure 3.38**). The pyruvate biosensor was used as a blank in

measuring TSA in real samples. The values of the pyruvate and TSA in the blood sample of the healthy volunteer and the serum sample of the cancer patient is shown in **table 1** below.

Table 1: The values of pyruvate and TSA in blood and serum samples for a healthy volunteer and a cancer patient.

| <i>Samples</i> | <i>Pyruvate Conc (mM)</i> | <i>Total sialic acid (mM)</i> |
|--------------------------|---------------------------|-------------------------------|
| Healthy volunteer | 0.372 | 1.539 |
| Cancer patient | 0.327 | 2.114 |

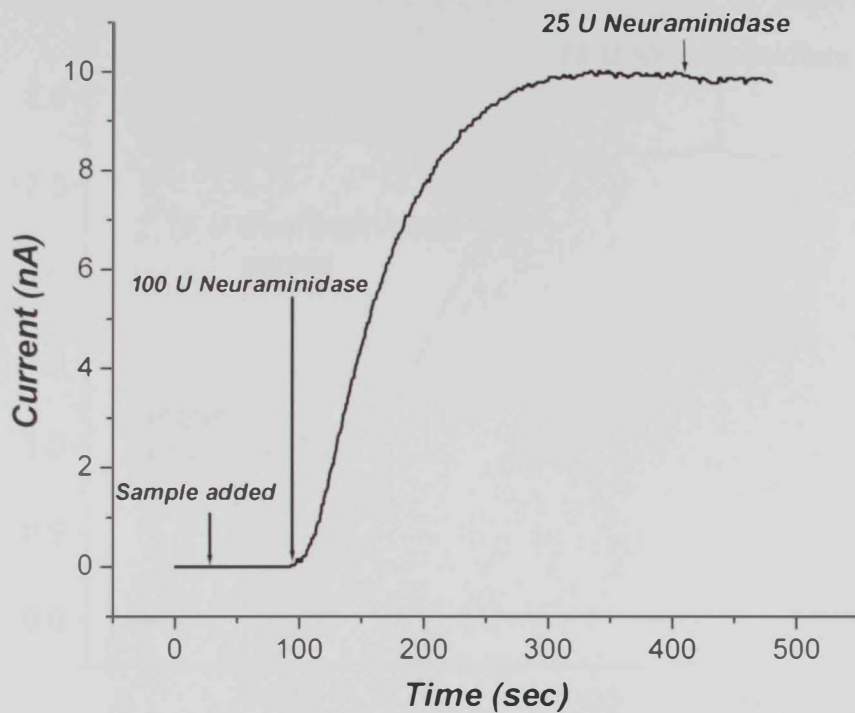


Figure 3.36: Assay of Epotin sample using SA biosensor and soluble neuraminidase enzyme. Additional 25 units of neuraminidase were added to check the completion of the release of SA from erythropoietin.

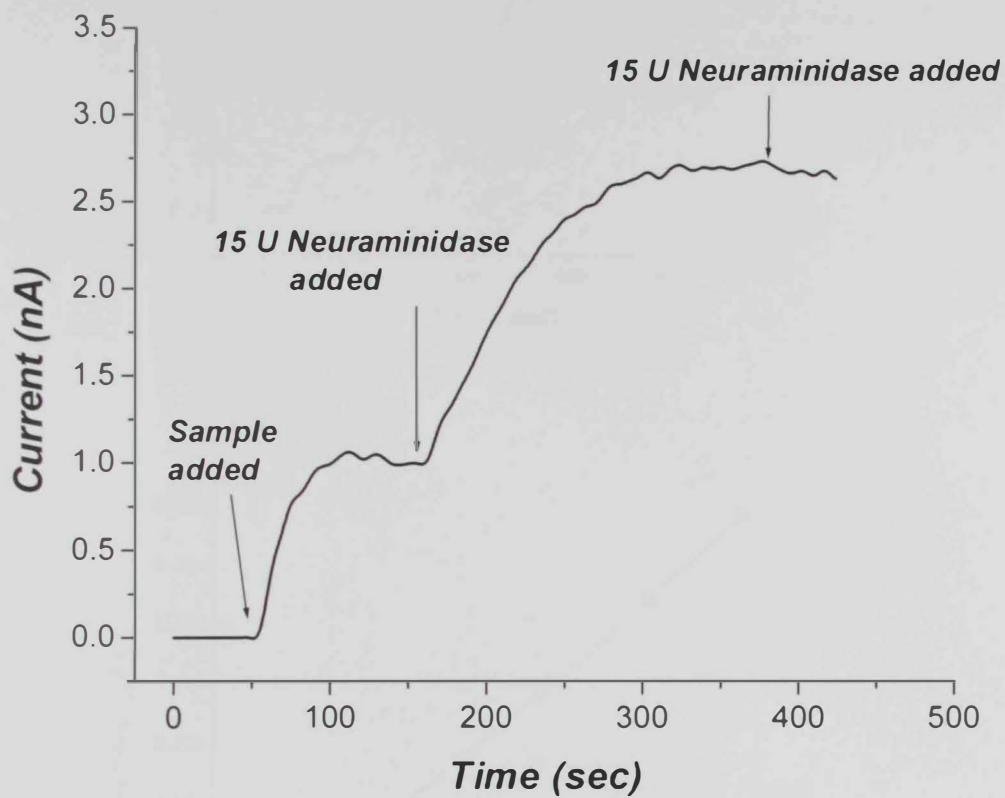


Figure 3.37: Assay of free and total SA in a whole blood sample from a healthy volunteer.

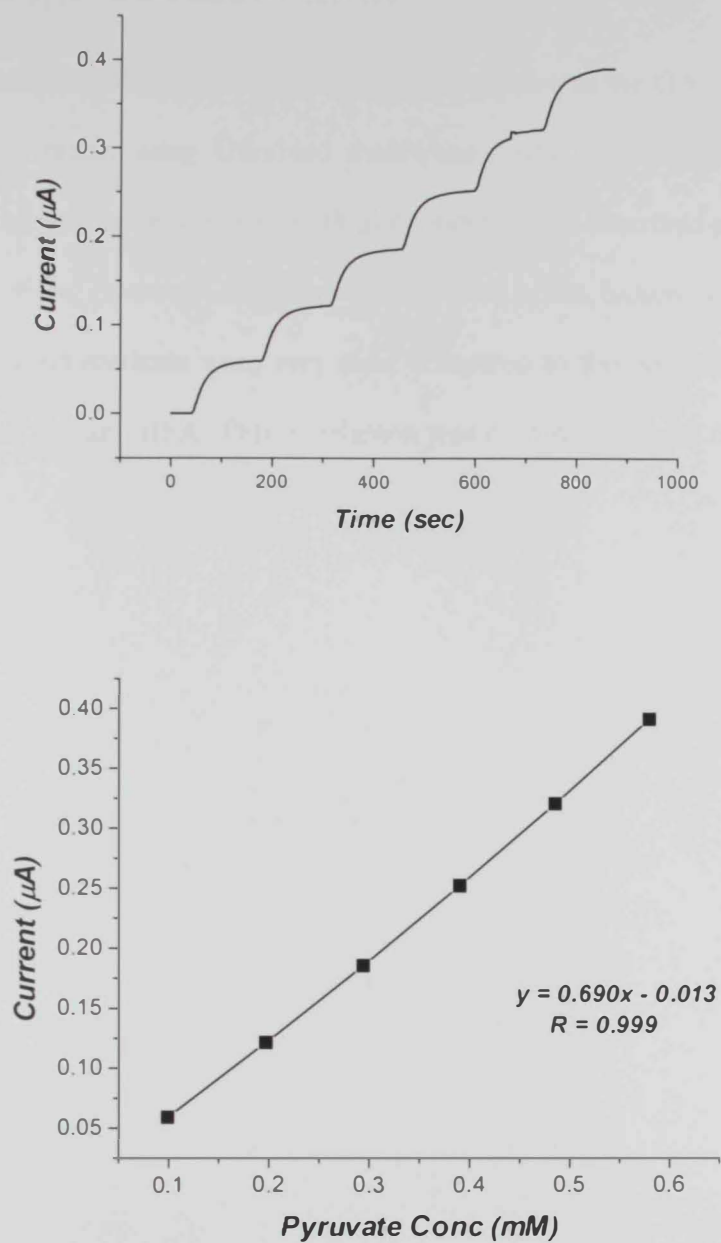


Figure 3.38: Multi-point calibration of Pyruvate biosensor in the range of 0-0.6 mM. (A) amperometric $I-t$ plot; (B) calibration plot based on the steady state current values obtained from (A). Each addition corresponds to 0.1 mM increment in SA concentration.

3.4.7 Additional approaches used for enzyme immobilization

Two other immobilization methods were tested parallel to the GA crosslinking, i.e., covalent immobilization using Ultrabind membranes, which already contain aldehyde groups, and a chitosan layer activated with glutaraldehyde as described previously in the experimental section.. However, the obtained responses of SA biosensors prepared using these immobilization methods were very poor compared to the response obtained with crosslinking with GA and BSA. This conclusion was confirmed by the data presented in **Figure 3.39**.



Figure 3.39. Comparison of the response of SA biosensors prepared using different immobilization methods. The biosensors were prepared using GA crosslinking with BSA, Ultrabind membranes, and a chitosan layer activated with glutaraldehyde. The response of the biosensors was measured in current (nA) versus glucose concentration (mM).

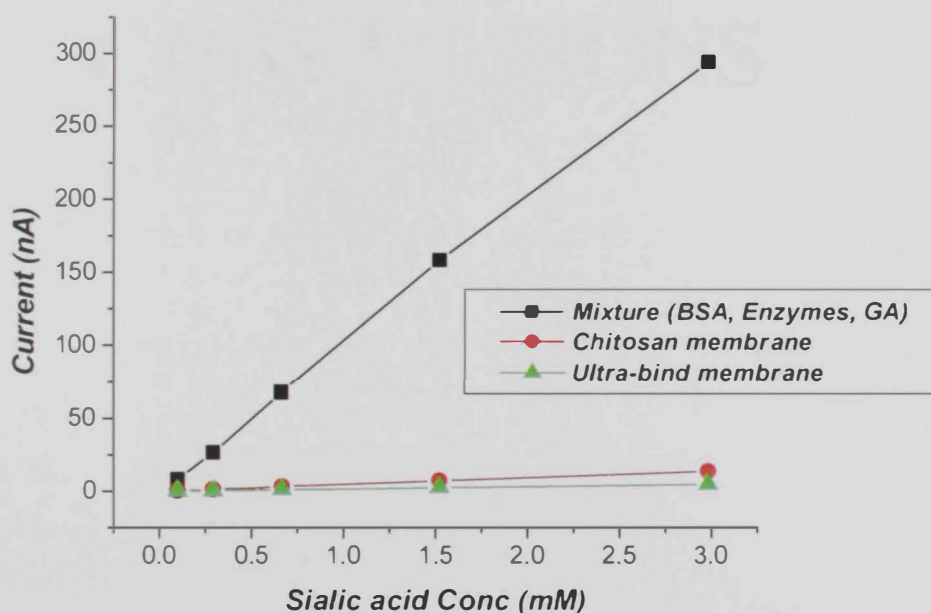
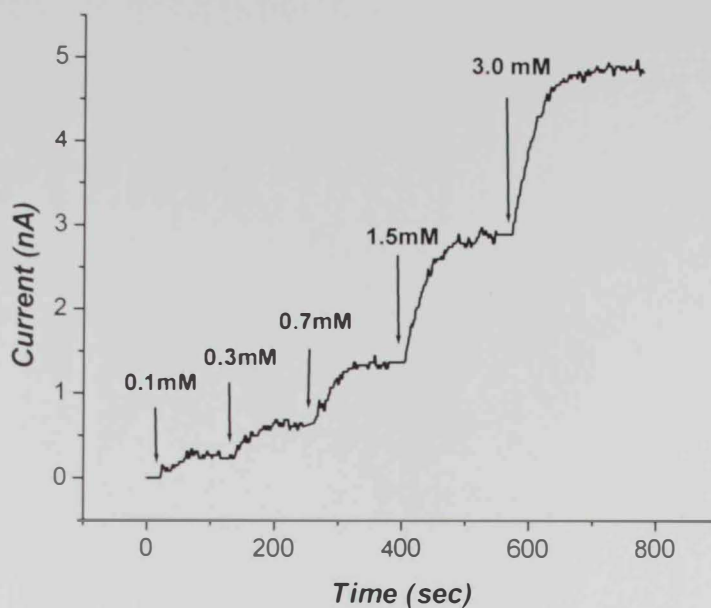


Figure 3.39: (A) Amperometric response of SA biosensor prepared with enzymes immobilized on Ultrabind membrane. (B) Calibration plots for SA obtained with GA-BSA, chitosan and Ultrabind methods showing the relative sensitivity obtained in each case.

CHAPTER IV

CONCLUSIONS

4. Conclusions

Several conclusions could be drawn from the presented work are as follow:

(i) The dual enzyme system (NANA-aldolase-PO) could be coupled successfully with the amperometric transduction of hydrogen peroxide to develop novel electrochemical methods for the assay of sialic acid.

(ii) The developed flow injection system allowed for simple determination of sialic acid with adequate sensitivity for direct determination of SA in real samples.

(iii) Preparation, characterization and application of the first biosensor for sialic acid was presented. The sensor represented a reproducible, fast, simple, and inexpensive way for sialic acid determination.

(iv) The advantages of the presented sialic acid biosensor suggest its wide use as a screening tool for quantification of blood SA and to monitor tumor therapy.

(v) Assay of sialic acid in more blood samples will be carried out to further demonstrate the reliability of the presented sialic acid biosensor.

REFERENCES

References

- [1] Wang B. and Bran-Miller J. The role and potential of sialic acid in human nutrition. *Eur J Clin Nutr* 2003; 57: 1351-1369.
- [2] Lamari FN. and Karamanos NK. Separation methods for sialic acids and critical evaluation of their biologic relevance. *J Chrom B* 2002; 781: 3-19.
- [3] Chou HH, Hayakawa T, Diaz S, Krings M, Indriat E, Leakey M, Paabo SYS, Takahata N, Varki A. Inactivation of CMP-N-acetylneuraminic hydroxylase occurred prior to brain expansion during human evolution. *Proceedings of the National Academy of Science of the United States of America* 2002; 99:11736-11741.
- [4] Traving C, Schauer R. Structure, function and metabolism of sialic acids. *Cellular and Molecular Life Sciences* 1998; 54: 1330-1349.
- [5] Sillanaukee P, Pönniö M, Jääskeläinen IP. Occurrence of sialic acids in healthy humans and different disorders. *Eur J Clin Invest* 1999; 29: 413-425.
- [6] Siskos PA, Spyridaki ME. Determination of sialic acids in biological fluids using reversed phase ion-pair high performance liquid chromatography. *J Chrom. B* 1999; 724: 205-212.
- [7] Spyridaki ME, Siskos PA. Development of a new direct reversed-phase ion-pair high-performance liquid chromatographic method for the separation and determination of sialic acids. *J Chrom A* 1999; 831: 179-189.
- [8] Millar J. The Asialylation of plasma lipoproteins. *Atherosclerosis* 2001; 154: 1-13.
- [9] Spyridaki ME, Siskos PA. An improved spectrophotometric method for the determination of free, bound and total N-acetylneuraminic acid in biological fluids. *Anal Chim Acta* 1996; 327: 277-285.

- [10] Rutishauser U. Polysialic acid at the cell surface: Biophysics in service of cell interactions and tissue plasticity. *J Cell Biochem* 1998; 70: 304-312.
- [11] Pönniö M, Alho H, Nikkari ST, Olsson U, Rydberg U, Sillanaukee P. Serum sialic acid in a random sample of the general population. *Clin Chem* 1999; 45: 1842-1849.
- [12] Crook M. The determination of plasma or serum sialic acid. *Clin Biochem* 1993; 26: 31-38.
- [13] Huggett RJ. *Biomarkers, Biochemical, Physiological and Histological Markers of Anthropogenic stress*. Lewis Publishers. London. UK 1992.
- [14] Tadmouri G, Al-Sharhan M. Cancer in the United Arab Emirates. Genetic Disorders in the Arab World: United Arab Emirates 2002.
- [15] El-Hayek M, Trad O, Donner M, Hardy D. Pediatric Oncology in the United Arab Emirates: The Twam Hospital Experience. *Med Pediatr Oncol* 2003; 41: 486-487.
- [16] Paszkowska A, Berbee H, Semczuk A and Cybulski M. Sialic acid concentration in serum and tissue of endometrial cancer patients. *Eur J Obstet Gynecol Reprod Biol* 1998; 76: 211-215.
- [17] Wongkham S, Bhudhiswasdi V, Chau-in S, Boonla C, Muisuk K, Kongkham S, Wongkham C, Boonsiri, Thuwajit P. Clinical significance of serum total sialic acid in cholangiocarcinoma. *Clin Chim Acta* 2003; 327: 139-147.
- [18] Diamantopoulou S, Stagiannis KD, Vasilopoulos K, Barlas P, Tsegenidis T, Karamanos K. Importance of high-performance liquid chromatographic analysis of serum *N*-acetylneuraminic acids in evaluating surgical treatment in patients with early endometrial cancer. *J Chrom. B: Biomed Sci and Appl* 1999; 732: 375-381.
- [19] Chien CH, Wei YH, Shaw JF. Immobilized enzyme system for determination of

- sialic acid in serum or urine. *Enzyme Microb Technol* 1991; 13: 45-52.
- [20] Paszkowska A, Cybulski M, Smeczuk A, Postawski K, Berbec H. Total sialic acid content in endometrial cancer tissue in relation to normal and hyperplastic human endometrium. *Cancer Detect. & Prevent.* 2000; 24: 459-463.
- [21] Lahdenne P, and Heikinheimo M. Clinical use of tumor markers in childhood malignancies. *Ann Med* 2002; 34: 316-323.
- [22] Kimura Y, Fujieda S, Takabayashi T, Tanaka T, Sugimoto C, Saito H. Conventional tumor markers are prognostic indicators in patients with head and neck carcinoma. *Cancer letters* 2000; 155(2): 163-168.
- [23] Wongkham S, Boonla C, Kongkham S, Wongkham C, Bhudhiswasdi V, Sripan B. Serum total sialic acid in cholangiocarcinoma patients: an ROC curve analysis. *Clin Biochem* 2001; 34: 537-541.
- [24] Shaw CJ., Chao H, Xiao B. Determination of sialic acids by liquid chromatography-mass spectrometry. *J Chrom A* 2001; 913: 365-370.
- [25] Lappin T. The Cellular Biology of Erythropoietin Receptors. *The Oncologist* 2003; 8: 15-18.
- [26] Skibeli V, Nissen-Lie G, and Torjesen P. Sugar profiling human serum erythropoietin differs from recombinant human erythropoietin. *Blood* 2001; 98: 3626-3634.
- [27] Egrie JC, Dwyer E, Browne JK, Hitz A, Lykos MA. Darbepoetin alfa has a longer circulating half-life and greater in vivo potency than recombinant human erythropoietin. *Exp Hematol* 2003; 31: 290-299.
- [28] Tsuda E, Kawanishi G, Ueda M, Masuda S, Sasaki R. The role of carbohydrate in recombinant human erythropoietin. *Eur J Biochem* 1990; 188: 405-441.
- [29] Seibert FB, Pfaff ML, Seibert MV. A tryptophane-perchloric acid method to

- measure sialic acid. *Arch Biochem Biophys* 1948; 18: 279-295.
- [30] Folch J, Arsove S, Meath JA. Isolation of brain strandin, new type of large molecule tissue component. *J Biol Chem* 1951; 191: 819-831.
- [31] Ayala W, Moore LV, Hess EL. Purple colour reaction given by diphenylamine reagent with normal and rheumatic fever sera. *J Clin Invest* 1951; 30: 781-785.
- [32] Hess EL, Coburn AF, Bates RC, Murphy P. A new method for measuring sialic acid levels in serum and its application to rheumatic fever. *J Clin Invest* 1957; 36: 449-455.
- [33] Klenk E, Langerbieins H. Orcinol method for measuring sialic acid. *Hoppe Seyler's Z Physiol Chem* 1941; 270: 185-193.
- [34] Svennerholm L. Quantitative estimation of sialic acids. *Biochim Biophys Acta* 1957; 24: 604-611.
- [35] Jourdian GW, Dean L, Roseman S. A periodate-resorcinol method for the quantitative estimation of free sialic acids and their glycosides. *J Biol Chem* 1971; 246: 430-435.
- [36] Veer PB, Mostafa S. Adaptation of the Periodate-resorcinol method for the determination of sialic acids to a microassay using microtiter plate reader. *Anal Biochem* 1993; 213: 438-440.
- [37] Damratsamon S, Peraohan , Maitree S, Prachya K. A Periodate-resorcinol microassay of total sialic acid in human serum. *Chiang Mai Med. Bull* 2001; 40: 111-118.
- [38] Aminoff D. Methods for the quantitative estimation of *N*-acetylneuraminic acid and their application to hydrolysates of sialomucoids. *Biochem J* 1961; 81: 384-392.
- [39] Warren L. Assay of sialic acids. *Methods Enzymol* 1963; 6: 463-465.

- [40] Skoza L, Mohos S. Stable thiobarbituric acid chromophore with dimethyl sulphoxide in the assay for *N*-acetyl-neuraminic acid. *Biochem J* 1976; 159: 457-462.
- [41] Mandic R, Opper C, Kappe J, Wesemann W. Platelet sialic acid as a potential pathogenic factor in coronary heart disease. *Thromb. Res* 2002; 106: 137-141.
- [42] Kalyan G, Dalavaikodihalli NN, Bidhan CK, Zachariah B, Sanat KS. Oxidative changes and desialylation of serum proteins in hyperthyroidism. *Clin Chim Acta* 2003; 337: 163-168.
- [43] Ozlem OS, Refiye Y, Hacı O, Ozgey Y, Aysen Y, Tugba T. Effects of Parsley (*Petroselinum crispum*) extract versus glibornuride on the liver of Streptozotocin-induced diabetic rats. *J Ethnopharmacol* 2006; 104: 175-181.
- [44] Massamiri Y, Beljean M, Durand G, Feger J, Agneray J. Determination of erythrocyte surface sialic acid residues by a new colorimetric method. *Anal Biochem* 1979; 91: 618-625.
- [45] Kenzaburoh Y, Toshihiko U, Noriyoshi M, Masahiro K, Takahiro I. Direct determination of bound sialic acids in sialoglycoproteins by acidic ninhydrin reaction. *Anal Biochem* 1989; 179: 332-335.
- [46] Hess HH, Relde E. Fluorometric assay of sialic acids in brain gangliosides. *J Biol Chem* 1964; 239: 3215-3220.
- [47] Hammond KS, Papermaster DS. Fluorometric assay of sialic acid in the picomole range. *Anal Biochem* 1976; 74: 292-297.
- [48] Murayama JI, Tomita M, Tsuji A, Hamada A. Fluorometric assay of sialic acid. *Anal Biochem* 1976; 73: 535-538.
- [49] Masaki I, Kiyoshi I, Yuki S, Kiyoshi T, and Megumi S. An improved fluorometric high-performance liquid chromatography method for sialic acid determination: an

- internal standard method and its application to sialic acid analysis of human apolipoprotein E. *Anal Biochem* 2002; 300: 260-266.
- [50] Teshima S, Tamai K, Hayashi Y, Emi S. New enzymatic determination of sialic acid in serum. *Clin Chem* 1988; 34: 2291-2294.
- [51] Brunetti P, Jourdan GW, Roseman S. The sialic acids. III. distribution and properties of animal *N*-acetylneuraminic adolase. *J Biol Chem* 1962; 237: 2447-2453.
- [52] Sugahara K, Sugimoto K, Nomura O, Usai T. Enzymatic assay of serum sialic acid. *Clin Chim Acta* 1980; 108: 493-498.
- [53] Kolisis FN. An immobilized bienzyme system for assay of sialic acids. *Biotechnol Appl Biochem* 1986; 8:148-152.
- [54] Anumula KR. High-Sensitivity and High-Resolution Methods for Glycoprotein Analysis. *Anal Biochem* 2000; 283: 17-26.
- [55] Rohrer JS. Analyzing sialic acid using high-performance anion-exchange chromatography with pulsed amperometric detection. *Anal Biochem* 2000; 283: 3-9.
- [56] Dong X, Xu X, Han F, Ping X, Yuang X, Lin B. Determination of sialic acids in the serum of cancer patients by capillary electrophoresis. *Electrophoresis* 2001; 22: 2231-2235.
- [57] Makatsori E, Karamanos NK, Anastassiou ED, Hjepe A, Tsegenidis T. Determination of glucoseamine in nutritional supplements by reversed-phase ion paring HPLC. *J Liq Chrom Related Technol* 1998; 21: 3031-3045.
- [58] Hara S, Takemori Y, Yamaguichi M, Nakamura M, Ohkura Y. Fluorometric high-performance liquid chromatography of *N*-acetyl- and *N*-glycolylneuraminic acids and its application to their microdetermination in human and animal sera.

glycoproteins, and glycolipids. *Anal Biochem* 1987; 164:138-145.

- [59] Guttman, A. Analysis of monosaccharide composition by capillary electrophoresis. *J. Chromatogr A* 1997; 763: 271-277.
- [60] Mechref Y, Ostrander, GK, El Rassi Z. Capillary electrophoresis of carboxylated carbohydrates. *J Chromatogr A* 1997; 792: 75-82.
- [61] Honda S, Okeda J, Iwanaga H, Kawakami S, Taga A, Suzuki S, Imai K. Ultramicroanalysis of reducing carbohydrates by capillary electrophoresis with laser-induced fluorescence detection as 7-nitro-2,1,3-benzoxadiazole-tagged *N*-methylglycamine derivatives. *Anal Biochem* 2000; 286: 99-111.
- [62] Stroussopoulou K, Militsopoulou M, Stagiannis K, Lamari FN, Karamanos NK. A capillary zone electrophoresis method for determining *N*-acetylneuraminic acid in glycoproteins and blood sera. *Biomed Chromatogr* 2002; 16: 146-150.
- [63] Bohin A, Bouchart F, Richet C, Kol O, Leroy Y, Timmerman P, Huet G, Bohin J, Zanetta, J. GC/MS identification and quantification of constituents of bacterial lipids and glycoconjugates obtained after methanolysis as heptafluorobutyrate derivatives. *Anal Biochem* 2005; 340: 231-244.
- [64] Shaw C, Chao H, Xiao B. Determination of sialic acid by liquid chromatography-mass spectrometry. *J Chromatogr A* 2001; 913: 365-370.
- [65] Kawabata A, Morimoto N, Oda Y, Kinoshita M, Kuroda R, Kakehi K. determination of mucin in salivary glands using sialic acids as the marker by high-performance liquid chromatography with fluorometric detection. *Anal Biochem* 2000; 283: 119-121.
- [66] Kugimiya A, Yoneyama H, Takeuchi T. Sialic acid imprinted polymer-coated quartz crystal microbalance. *Electroanal* 2000; 12: 1322-1326.
- [67] Kugimiya A, Takeuchi T. Surface plasmon resonance sensor using molecularly

- imprinted polymer for detection of sialic acid. *Biosens & Bioelect* 2001; 6: 1059-1062.
- [68] Aubeck R, Eppelsheim C, Brauchle C, Hampp N. Potentiometric thick-film sensor for the determination of the tumor marker bound sialic acid. *Analyst* 1993; 118: 1389-1392.
- [69] Thevenot DR, Toth K, Durst RA, Wilson GS. Electrochemical biosensors: recommended definitions and classification. *Biosens & Bioelect* 2001; 16: 121-131.
- [70] Wilson GS, Gifford R. Biosensors for real time in vivo measurements. *Biosens & Bioelect* 2005; 20: 2388-2403.
- [71] Mello LD, Kubota LT. Review of the use of biosensors as analytical tools in the food and drink industries. *Food Chemistry* 2002; 77: 237-256.
- [72] Wang J. Electrochemical biosensors: Towards point-of-care cancer diagnostics. *Biosens & Bioelect* 2006; 21: 1887-1892.
- [73] Patel PD. Biosensors for measurements of analytes implicated in food safety: a review. *Trends Anal Chem* 2002; 21: 96-115.
- [74] Velasco-Garcia MN, Mottram T. Biosensor technology addressing agricultural problems. *Biosystems Eng* 2003; 84: 1-12.
- [75] Lee WY, Kim SR, Kim TH, Lee KS, Shin MC, Park JK. Sol-gel derived thick film conductometric biosensor for urea determination in serum. *Anal Chim Acta* 2000; 404: 195-203.
- [76] Scheller F, Schubert F. *Biosensors*. Elsevier. Amsterdam; 1992. 361p.
- [77] Karakus E, Pekyardımcı SS, Kılıç E. Potentiometric bienzymatic biosensor based on PVC membrane containing palmitic acid for determination of creatine. *Process Biochem* 2006; 41: 1371-1377.

- [78] Gerard M, Chaubey A, Malhotra BD. Application of conducting polymers to biosensors. *Biosens & Bioelect* . 2002; 17: 345-359.
- [79] Tymecki L, Knocki R. Thick-film potentiometric biosensor for bloodless monitoring of hemodialysis. *Sens Actuators B* 2006; 113: 782-786.
- [80] Torbiéro HB, Assié-Souleille S, Colin R, Dollat X, Franc B, Martinez A, Temple-Boyer P. Development of pNH_4^+ -ISFETs microsensors for water analysis. *Microelect J* 2006; 37: 475-479.
- [81] Hai A, Ben-Haim D, Korbakov N, Cohen A, Shappir J, Oren R, Spira ME, Yetzchik S. Acetylcholinesterase-ISFET based system for the detection of acetylcholine and acetylcholinesterase inhibitors. *Biosens & Bioelect* 2006; in Press.
- [82] Wang J. Electrochemical detection for microscale analytical systems; a review. *Talanta* 2002; 56: 223-2231.
- [83] Amine A, Mohammadi H, Bourais I, Pallesschi G. Enzyme inhibition-based biosensors for food safety and environmental monitoring. *Biosens & Bioelect* 2006; in Press.
- [84] Leonard P, Hearty S, Brennan J, Dunne L, Quinn J, Chakraborty T, Kennedy R. Advances in biosensors for detection of pathogens in food and water. *Enzyme Microb Technol* 2003; 32: 3-13.
- [85] Karube I, Nomura Y. Enzyme sensors for environmental analysis. *Journal of Molecular Catalysis B: Enzymatic* 2000; 10: 177-1781.
- [86] Velasco-Garcia M., and Mottram T. Biosensor technology addressing agricultural problems. *Biosystems Eng* 2003; 84: 1-12.
- [87] Mulchandani A, Chen W, Mulchandani P, Wang J, Rogers KR. Biosensors for direct determination of organophosphate pesticides. *Biosens & Bioelect* 2001; 16:

225-230.

- [88] Kim J, Grate JW, Wang P. Nanostructures for enzyme stabilization. *Chem Eng Sci* 2006; 61: 1017-1026.
- [89] Krajewska B. Application of Chitin- and chitosan- based materials for enzyme immobilizations: a review. *Enz Microb Technol* 2004; 35: 126-139.
- [90] Mulchandani A, Bassi AS, Nguyen A. Tetrathiafulvalene-mediated Biosensor for L-lactate in Dairy Products. *J Food Sci* 1995; 60: 74-78.
- [91] Campás M, Szydłowska D, Trojanowicz M, Marty J. Towards the protein phosphatase-based biosensor for microcystin detection. *Biosens & Bioelect* 2005; 20: 1520-1530.
- [92] Lenigk R, Lan E, Lai A, Wang H, Han Y, Carlier P, Renneberg R. Enzyme biosensor for studying therapeutics of Alzheimer's disease. *Biosens & Bioelect* 2000; 15: 541-547.
- [93] Sun Y, Yan F, Yang W, Sun C. Multi-layered construction of glucose oxidase and silica nanoparticles on Au electrodes based on layer-by-layer covalent attachment. *Biomaterials* 2006; 27: 4042-4049.
- [94] Rosane I, de Oliveira WZ, Fernandes SC, Vieira. Development of a biosensor based on guilo peroxidase immobilized on chitosan chemically crosslinked with epichlorohydrin for determination of rutin. *J Pharm Biomed Anal* 2006; 41: 366-372.
- [95] Marrakchi M, Dzyadevych SV, Biloivan OA, Martelet C, Temple P, Jaffrezic-Renault N. Development of trypsin biosensor based on ion sensitive field-effect transistors for protein determination. *Mat Sci Eng C* 2006; 26: 369-373.
- [96] Yao T, Kobayashi N, Wasa T. Flow-injection analysis for L-glutamate using immobilized L-glutamate oxidase: comparison of an enzyme reactor and enzyme

electrode. *Anal Chim Acta* 1990; 231: 121-124.

- [97] Mak WC, Ng YM, Chan C, Kwong WK, Renneberg R. Novel biosensors for quantitative phytic acid and phytase measurement. *Biosens & Bioelect* . 2004; 19: 1029-1035.
- [98] Matsumato K, Tsukatani T. Simultaneous quantitation of citrate and isocitrate in citrus juice by a flow-injection method based on the use of enzyme reactors. *Anal Chim. Acta* 1996; 321: 157-164.
- [99] Sato N, Usui K, Okuma H. Development of a bienzyme reactor sensor system for the determination of ornithine. *Anal Chim Acta* 2002; 456: 219-226.
- [100] Kwan RCH, Hon PYT, Renneberg R. Amperometric biosensor for rapid determination of alanine. *Anal Chim Acta* 2004; 523: 81-88.
- [101] Inaba Y, Hamada-Sato N, Kobayashi T, Imada C, Watanabe E. Determination of D- and L-alanine concentrations using a pyruvic acid sensor. *Biosens & Bioelect* 2003; 18: 963-971.
- [102] Shin SJ, Yamanaka H, Endo H, Watanabe, E. Development of an octopine biosensor and its application to the estimation of scallop freshness. *Enzyme Microb Technol* 1998; 23: 10 - 13.
- [103] Chein CH, Wei YH, Shaw JF. Immobilized enzyme system for determination of sialic acid in serum or urine. *Enz Microb Technol* 1991; 13: 45-52.
- [104] Chein CH, Wei YH, Yeh S, Li C. An immobilized-system for the determination of sialic acid using cloned neuraminidase from clostridium perfringens. *Biotechnol Appl Biochem* 1994; 19: 51-60.
- [105] Ruzicka J., Hansen E., Flow Injection Analysis. 2nd ed. John Wiley & Sons, NY. 1988.
- [106] Marzouk SAM, Sayour HEM., Ragab AM., Cascio WE, Hassan SSM, A simple

- FIA-system for simultaneous measurements of glucose and lactate with amperometric detection. *Electroanal* 2000; 12: 1304-1311.
- [107] Saurina J, Hernandez-Cassou S. Quantitative determination in conventional flow injection analysis based on different chemometric calibration Strategies: a review. *Anal Chim Acta* 2001; 438: 335-352.
- [108] Samcová E, Marhol P, Opekar F, Langmaier J. Determination of urinary 8-hydroxy-2'-deoxyguanosine in obese patients by HPLC with electrochemical detection. *Anal Chim Acta* 2004; 516: 107-110.
- [109] Li T, Coufal P, Opekar F, Štulík K, Wang E. An amperometric detector with a tubular electrode deposited on the capillary for capillary liquid chromatography. *Anal Chim Acta* 1998; 360: 53-59.
- [110] Marzouk SA. Improved electrodeposited iridium oxide pH sensor fabricated on etched titanium substrates. *Anal Chem* 2003; 75: 1258-1266.
- [111] Bard AJ, Faulkner LR. *Electroanalytical Methods: Fundamentals and Applications*. 2nd ed. John Wiley & Sons. NY. 2001.
- [112] Cardosi MF. Hydrogen peroxide-sensitive electrode based on horseradish peroxidase-modified platinized carbon. *Electroanal* 1994; 6: 89-96.
- [113] De Benedetto GE, Palmisano F, Zambonin PG. One-step fabrication of a bienzyme glucose sensor based on glucose oxidase and peroxidase immobilized onto a poly(pyrrole) modified glassy carbon electrode. *Biosens & Bioelect* 1996; 11: 1001-1008.
- [114] Nakabayahi Y, Yoshikawa H. Amperometric biosensors for sensing of hydrogen peroxide based on electron transfer between horseradish peroxidase and ferrocene as a mediator. *Anal Sci* 2000; 16: 609-613.
- [115] Liu S, Dai Z, Chen H, Ju H. Immobilization of hemoglobin on zirconium dioxide

- nanoparticles for preparation of a novel hydrogen peroxide biosensor. *Biosens & Bioelect* 2004; 19: 963-969.
- [116] Ricci F, Palleschi G. Sensor and biosensor preparation, optimization and applications of prussian blue modified electrodes. *Biosens & Bioelect* 2005; 21: 389-407.
- [117] Garjonyte R, Malinauskas A. Operational stability of amperometric hydrogen peroxide sensors, based on ferrous and copper hexacyanoferrates. *Sens Actuators B* 1999; 56: 93-97.
- [118] Marzouk SAM, Cosofret VV, Buck RP, Yang HH, Cascio WE, Hassan SSM. Amperometric monitoring of lactate accumulation in rabbit ischemic myocardium. *Talanta* 1997 44: 1527-1541.
- [119] Malinauskas A, Garjonytė R, Mažeikienė R, Jurevičiūtė I. Electrochemical response of ascorbic acid at conducting and electrogenerated polymer modified electrodes for electroanalytical applications: a review. *Talanta* 2004; 64: 121-129.
- [120] British Pharmacopoeia 2005, Volume 1. Monographs: Medical and Pharmaceutical substances. Erythropoietin Concentrated Solution.

إن كفاءة الطرق الكهروكيميائية المبتكرة وفعاليتها جعلت من السهل استخدامها لقياس حمض السياليك في العديد من التطبيقات الطبية، و بالخصوص كمؤشر غير محدد للسرطان وكذلك إمكانية استخدامها في متابعة علاج السرطان.

ودرجة حرارة 37°م وباستخدام كلا الإنزيمين (NANA-aldolase/PO) بنسبة 1.5 و استخدام العامل المساعد الثيامين بيروفوسفات بتركيزات ما بين 0.5-2.0 ميلي عياري.

المرحلة الثانية من هذا البحث هدفت إلى تصميم واستخدام نظام حقن مستمر مستند على مفاعل إنزيمي (IER) و كاشف سريان أمبيرومترى لقياس فوق أكسيد الهيدروجين. وقد تم تحضير المفاعل الإنزيمي بواسطة تثبيت كلا الإنزيمين على حبيبات زجاجية منظمة المسامات، و التي قد عُبئت في أبوية زجاجية يتراوح طولها ما بين 3-5 سم و نشطت باستخدام الجلوترالدهيد. و قد اقترح استخدام كاشف بلايتين أنبوبي الشكل والذي من ميزاته كبر مساحة السطح، و قد أثبت استخدامه زيادة حساسية التقدير تحت الظروف الملائمة و التي قد تم الحصول عليها من الدراسة الأولية، حيث أن من السهل تحسين المدى الخطي وتقليل وقت التحليل وزيادة الحساسية بحيث تتوافق مع خصائص الأداء المطلوبة، و ذلك بالسيطرة على سرعة تدفق المحلول الناقل و حجم العينة الذي يتم حقنه. كما تم استخدام نظام الحقن المستمر الذي تم توصيفه لقياس حمض السياليك في عينات حقيقية.

أما المرحلة الثالثة من هذا البحث فقد كانت الجزء الأكثر تحدياً، حيث كانت تهدف إلى تصميم وتوصيف أول مجس الحيوي لحمض السياليك و الذي يتطلب لتثبيت الإنزيمين بشكل متكامل و قريب من سطح قطب البلايتين. على الرغم من استخدام ثلاث طرق مختلفة لتثبيت الإنزيمات؛ إلا أن الطريقة التي تم فيها استخدام الجلوترالدهيد كعامل مثبت مع الـBSA كانت الأكثر فعالية. وكطريقة مبتكرة، فقد استخدم غشاء بولي إستر دقيق المسامات كركيزة لطبقة الإنزيمات مما جعل التصاق الطبقة أفضل و قلل من التفاوت المحتمل حدوثه عند تكرار تحضير هذه الطبقة.

عند دراسة تأثير الـ pH على الإنزيمات المثبتة، قد وجد أن قيمة الـ pH المثلى زادت بمقدار وحدة pH واحدة (تقريباً 7.3) عن تلك في التحفيز المتجانس. وقد تم دراسة خصائص طبقة الإنزيمات المثبتة وذلك للحصول على أفضل تكوين للطبقة و أفضل سمك مما ينتج عنه استجابة سريعة و مستقرة. وقد أمكن قياس حمض السياليك بتركيزات ميكرونية تصل إلى 10 ميكرو عياري.

و لزيادة اختيارية المجس الحيوي لحمض السياليك و منع التداخل من المركبات الأخرى القابلة للأكسدة مثل حمض الأسكوربيك، حمض اليوريك و الأستامينوفين؛ فقد تم ترسيب طبقة بوليمر داخلية كهروكيميائياً. ونتيجة لكفاءة المجس الحيوي فقد تم استخدامه بنجاح لقياس حمض السياليك في عينات حيوية حقيقية.

الملخص

يطلق مصطلح "حمض السialogic" على عائلة مكونة من 43 مركب مشتق من حمض النيورامينيك ويعتبر حمض N-أسيتايل نيورامينيك (NANA) أكثر مركبات هذه العائلة شيوعاً. ويكتسب قياس مستوى تركيز حمض السialogic في الإنسان أهمية كبرى وذلك لأن التفاوت في مستوى تركيز هذا الحمض يرتبط بعدة ظروف صحية وعدة أمراض بشكل عام، و ببعض أنواع السرطان بشكل خاص حيث وجد أن مستوى حمض السialogic مرتفع نسبياً في مصل الدم. يدخل حمض السialogic كذلك في التركيب البنائي لهرمون هام يدعى الإريثروبويتين الذي يحفز إنتاج كريات الدم الحمراء و الذي يستخدم في علاج فقر الدم (الأنيميا).

وعلى الرغم من الأهمية الفسيولوجية البالغة لحمض السialogic والمميزات الجذابة للطرق التحليلية الكهروكيميائية، فقد لوحظ عدم وجود أي تقارير منشورة لتوصيف التقدير الكمي لحمض السialogic بالطرق الكهروكيميائية، مما حث إجراء هذا البحث لاستحداث وتقويم أول طريقة تقدير لحمض السialogic بواسطة تقنية الحقن المستمر معتمدة على استخدام كاشف سريان أمبيرومترى وكذلك استحداث أول مجس حيوي (biosensor) المعتمد على التوصيل الأمبيرومترى، وذلك للحصول على طرق سهلة وسريعة ومباشرة للتقدير الكمي لحمض السialogic في التطبيقات الطبية والحيوية.

يعتمد مبدأ قياس حمض السialogic في هذا البحث على تأثير إنزيمين وهما N-acetylneuraminic acid aldolase (NANA-aldolase) و Pyruvate oxidase (PO) ويعمل الإنزيم الأول على تحفيز تحليل حمض السialogic لإنتاج حمض البيروفيك ويعمل الإنزيم الثاني على تحفيز أكسدة حمض البيروفيك، في وجود الأوكسيجين المذاب، لإنتاج فوق أكسيد الهيدروجين والذي يمكن أكسدته على سطح قطب بلاتين مستقطب عند جهد 0.6 فولت نسبة إلى جهد القطب الكهربي المرجعي Ag/AgCl ويمثل التيار الكهربي الأتودي المتولد نتيجة لعملية الأكسدة هذه الإشارة المستخدمة في التقدير الكمي لحمض السialogic.

في المرحلة الأولى من هذا البحث تم تقويم تأثير المتغيرات التجريبية المختلفة على إنتاج مركب فوق أكسيد الهيدروجين باستخدام كلا الإنزيمين، وقد أجريت هذه الدراسة الابتدائية باستخدام كلا الإنزيمين في الحالة الذائبة (التحفيز الإنزيمي المتجانس). وكنتيجه لهذه الدراسة فقد وجد أنه يمكن الحصول على أعلى إشارة تيار كهربي مكافئة لتركيز ما من حمض السialogic باستخدام محلول الفوسفات المنظم والذي تركيزه 0.1 عياري عند pH 6.3



جامعة الإمارات العربية المتحدة
عمادة الدراسات العليا
برنامج ماجستير علوم البيئة

استحداث طرق تحليلية كهروكيميائية لتقدير حمض السيليك

كأحد مؤشرات السرطان

رسالة مقدمة من/

خولة علي راشد الطياري

مقدمة إلى/

جامعة الإمارات العربية المتحدة

استكمالاً لمتطلبات الحصول على درجة الماجستير في علوم البيئة

2006-2005